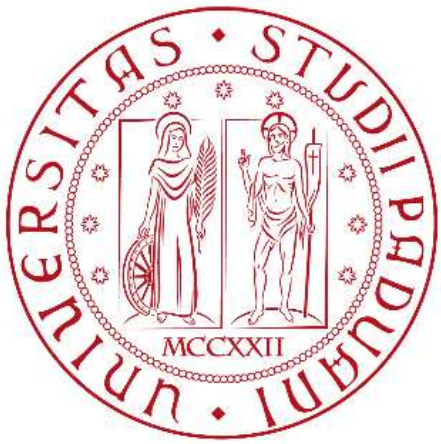

Università degli Studi di Padova

Dipartimento di Fisica e Astronomia "Galileo Galilei"

Corso di Dottorato di Ricerca in

Astronomia

The role of binaries in the structural evolution of star clusters and dwarf galaxies

Supervisor: Giovanni Carraro
Co-supervisor: Roberto Capuzzo-Dolcetta

Ph.D. student: Camilla Pianta

"Ma che dolce delirio è il loro, allorché si fabbricano mondi senza fine, allorché misurano come con il pollice e con il filo, sole, luna, stelle, sfere."

Erasmo da Rotterdam, Elogio della follia

Contents

List of tables

List of figures

Chapter I

Introduction

Galileo Galilei said that things are connected by invisible links, so that a flower cannot be picked without perturbing a star. Albert Einstein advised to look at the stars, each one following its orbit without making a sound, in eternal memory of Newton's reason, and learn from them. Stephen Hawking stated that his purpose was a complete knowledge of the universe, its being as it is and its very existence.
These are the founding concepts of Newtonian theory of gravity and of stellar dynamics: stars must be regarded not as mere isolated objects walking along their own evolutionary path, but as active participants to their parental systems' life journey across space and time via their mutual gravitational interactions. Enviable would be the external observer watching the spectacular scene of a universe progressively shaped and changed by such an interplay, holding all the answers in his hands, a "master of everything" who would hence exhort to pay attention and analyze carefully, because the way for understanding the universe is paved by stars.
According to Plato, astronomy urges the soul to see past the human world and reach the other: thus it is not surprising that the interest in the study of stars originated with the man in response to his natural need to make sense of the physical phenomena he was surrounded by. However, it took a long time before the discovery of stellar duplicity, the detection of the first binary stars dating back to the latter part of the 17^{th} century; even so, the effort in the physical characterization of binaries has grown stronger from that point onward due to the recognition of their impact on both stellar evolution and dynamics. This has led to the present-day ascertainment that the vast majority of stars is actually part of binary systems.

The first, straightforward manner of binary classification rests upon observational features (Podsiadlowski, 2014 [75]). Such a differentiation consists in:

- visual binaries, where the periodic motion of both the components is visible (binaries are called astrometric if only one component's motion is);
- spectroscopic binaries, where the Doppler shift owing to the components' orbital motion appears evident in spectral lines. In particular, a further distinction is made between single-lined and double-lined systems, depending on whether the Doppler shift is measured for one or both the components;
- photometric binaries, where a periodic variation of the photometric properties is noticed;
- eclipsing binaries, where one star eclipses the other during part of its orbit.

Binaries can be also labeled on the basis of their interaction with the companion, though, by accounting for the occurrence of Roche lobe overflow (RLOF) phenomenon. In fact, within the context of the restricted three-body problem, which follows a mass-less test particle's motion inside the gravitational field of two orbiting masses, the definition of an effective potential in a corotating frame allows to introduce the concept of Roche lobe. The effective potential, composed by the gravitational potential of the two massive objects and the centrifugal force acting on the test particle, possesses five critical points, i.e., the Lagrangian points, wherein its gradient becomes null: amid the three most important ones, which lie along the line joining the two stars, the inner one (L_1) sets the bordering equipotential surface between their respective spheres of influence. Now, this equipotential surface is commonly referred to as the critical Roche lobe potential, and its part engulfing the star as the Roche lobe: simply put, the Roche lobe is the equipotential surface, connected to the inner Lagrangian point L_1, which determines the maximum size of a star in a close binary.
If one star starts to fill its Roche lobe, then matter can flow into the Roche lobe of the companion through the Lagrangian point L_1, initiating a mass transfer process going exactly under the name of RLOF. This implies the division of binary systems in three broad categories:

- detached binaries, where both stars underfill their Roche lobe, so that RLOF cannot take place;
- semi-detached binaries, where only one star fills its Roche lobe, making mass transfer via RLOF possible;

- contact binaries, where both stars either fill or overfill their Roche lobes. In this case, RLOF mass transfer leads to the formation of a common envelope surrounding the two stars and, eventually, of a circumbinary disk if it reaches the other two above-mentioned Lagrangian points (L_2 and L_3), which are located outside the orbit.

Finally, binaries can be considered soft when their binding energy is lower than their mean kinetic energy, and hard when it is higher (Heggie, 1975 [32]). This notion, tightly related to the topic of stellar dynamics, will be deepen in the next chapter.

Chapter II

Stellar dynamics

2.1 Fundamentals

As highlighted by King (1974) [46], an effective description of stellar dynamics comes naturally from the comparison to other fundamental physical theories, i.e., celestial and statistical mechanics, and plasma theory.
Firstly, a loose link exists between stellar dynamics and celestial mechanics, since dealing with individual orbits and motions is not profitable in the case of large star numbers. On the contrary, the similarity to statistical mechanics is more solid, given the use of distribution functions to make theoretical models and predictions, even though the requirement of equilibrium conditions is not always satisfied when talking about stellar systems. Finally, stellar dynamics presents some analogies with plasma theory, where forces between particles are electrostatic, and hence inverse squared as well as in the gravitational instance. But if, on the one hand, electrostatic forces are both attractive and repulsive, on the other hand gravitational ones are not: as a consequence, in a plasma excesses of either charge tend to be leveled out by particles of the opposite charge (polarization or Debye shielding), whereas, in a stellar system, particle over-densities grow by collecting more density (Jeans gravitational instability).
So, stellar dynamics can be defined as a N-body problem, i.e., the study of a number of bodies interacting with each other only via their mutual gravitational forces, whose complexity is reduced by recognizing that not all such interactions are actually important. In fact, to a large extent, each body is assumed to move in the smoothed-out field of all the others because strong forces between neighboring objects rarely arise.

Since gravity is the sole meaningful force in this context, the Newtonian approximation is typically adopted: a stellar system is thus treated like a self-gravitating gas of stars, these ones represented by mass points flowing in an incompressible way according to Liouville's theorem. From the mathematical perspective, this corresponds to a six-dimensional phase space obtained by conjoining the position and velocity space, and fully described by a quasi-stationary, evolving density distribution function $f(\vec{r}, \vec{v}, t)$ through the Boltzmann equation, generally approximated by either the Vlasov or the Fokker-Planck equation. However, most often three out of six variables, i.e., two position components and the radial velocity component, of $f(\vec{r}, \vec{v}, t)$ are observed: unfortunately, just on occasion the other two velocity components from proper motions and hardly ever the third position component can be measured, indeed. Also, a further limitation derives from the allowance of only phase space regions where the integrals of motion, namely the energy and the angular momentum, are conserved. According to Jeans' theorem, $f(\vec{r}, \vec{v}, t)$ and the velocity distribution $f(\vec{v}, t)$, assumed to be Maxwellian, must be mutually consistent; in particular, a stellar system with such a velocity distribution is space-limited, its boundary being set by the Milky Way (MW) tidal force. To properly address this issue, though, the concept of relaxation (theory of stellar encounters) must be introduced.

2.2 Dynamical relaxation

2.2.1 Stellar encounters

When two stars pass so close to each other that the gravitational force between them becomes temporarily greater than the one exerted on them, individually, by the rest of the system, they form a two-body problem characterized by a hyperbolic motion around the center of mass of the pair: since, in a fixed coordinate system, there is no energy exchange, this phenomenon goes under name of stellar encounter (King, 1974 [46]).
Stellar encounters can be either strong or weak. The former cause stellar orbits to be modified by changing the involved stars' velocity of a quantity $\Delta\vec{v} \sim \vec{v}$ and are more relevant for low velocities, being the characteristic timescale for strong encounters directly proportional to the mean stellar velocity

$$t_s = \frac{\langle v \rangle^3}{4\pi G \langle m \rangle^2 n} \,, \tag{2.1}$$

where G is the gravitational constant, m the mean stellar mass and n the typical number density of stars. The latter, instead, produce only a small angular deflection of stars from their original orbit, but their cumulative effect may be actually non-negligible. Therefore, stars are accelerated (i.e., deflected) by the encounters with other stars or the collective gravitational field of the system they belong to, and experience either large or small velocity fluctuations, respectively. Nonetheless, since gravity is a long-range force, the influence of distant bodies proves relevant in changing the dynamical state of a stellar system towards equilibrium: this is the most general definition of relaxation process. Specifically, two-body relaxation is deemed as a "thermalization" process due to its modifying the stellar velocity distribution to a Maxwellian shape, the one expected from an equilibrium condition.
If two-body encounters are relevant in driving the dynamical evolution of a stellar system, then this is called collisional, whereas collisionless if they are not: in other words, collisionless systems, such as galaxies and open clusters (OCs), present a smooth dynamics, while collisional systems, such as globular clusters (GCs), a turbulent one.
Such a difference is formally encoded in the definition of two-body relaxation timescale (Spitzer, 1987 [98]), i.e., the timescale over which stars lose memory of their initial kinematics owing to the repeated, long-distance two-body interactions that make them slowly exchange energy or, equivalently, the time needed to significantly alter the velocity of a star through these very interactions:

$$t_{relax} = \frac{\langle v^2 \rangle^{\frac{3}{2}}}{4\pi G^2 \langle m \rangle \rho \ln(\Lambda)} , \tag{2.2}$$

with $\ln(\Lambda) \simeq 0.11$. A more general formulation of the relaxation timescale results from the crossing time, i.e. the time it takes for a star to cross its parental system (Heggie, 1988 [33]):

$$t_{relax} = n_{cross} t_{cross} = \frac{N}{6 \ln(N)} \frac{R}{\langle v \rangle} , \tag{2.3}$$

where n_{cross} provides the number of crossings for the cumulative gravitational perturbation from all members to change the star's energy by roughly its orbital energy and R represents the characteristic radius of the system. This expression points out that a star may be dramatically perturbed in a time dependent only on the number of stars N. *Ergo*, in collisionless systems, which host a small number of stars and have lifetime shorter than

t_{relax}, contrary to collisional ones, two-body relaxation is not efficient in redistributing energy between particles.

2.2.2 Energy equipartition: evaporation, mass segregation and gravothermal instability

The direct consequences of two-body relation are evaporation, mass segregation and core collapse, intrinsically linked to the concept of energy equipartition.
Since, according to the virial theorem in the assumption of equilibrium

$$2E_k + U = 0 \,, \tag{2.4}$$

where E_k is the kinetic energy and U the gravitational potential energy (Dolcetta, 2019 [17]), the rms velocity of stars is about a half the rms escape velocity, i.e.,

$$\langle v_{esc}^2 \rangle \simeq 4 \langle v^2 \rangle \,, \tag{2.5}$$

and since the stellar energy exchange tends to establish a Maxwellian velocity distribution in order to maintain such a condition, it follows that any particle in the Maxwellian tail, having a velocity more than twice the rms value, will escape from the system.
The escaping rate is determined by the time required for the energy exchange to be comparable with E_k: this is exactly the relaxation time. In practice, consisting two-body relaxation in the stellar energy re-distribution through gravitational encounters, with the subsequent onset of a Maxwellian velocity distribution at each system's point on a t_{relax}, every t_{relax} a constant fraction of stars acquires energy above v_{esc} and is inevitably lost.
So, if the fraction of escaping stars is f_{esc}, replenished by the very same relaxation process every t_{relax}, then the time over which a system dissolves by evaporation is

$$t_{ev} = \frac{t_{relax}}{f_{esc}} \,, \tag{2.6}$$

where t_{relax} is independent of the number of stars as expressed in Eq. 2.2; from Eq. 2.5, Spitzer (1971) [97] estimated that, in the case of dense, spherical stellar systems, $\sim 1\%$ of stars escape during a relaxation time, which yields $t_{dis} \sim 100\ t_{relax}$.

However, it must be noted that stars are likely to gain appreciable energy only if their orbit passes through the dense core of the system, where the rate of encounters and energy interchange is greatest: as a consequence, they will move in more and more elongated orbits rarely crossing the central regions, which implies that, when a star approaches the zero total energy needed for escape, its relaxation time increases steadily, and so does the system's dissolution time. More precisely, in $\sim 100\ t_{relax}$ a substantial number of core stars gain sufficient energy to make their orbits markedly elongated and accumulate in the outskirts, thus forming an extended halo of ejected objects.
Therefore, evaporation causes a stellar system to expand and transfer energy from the inner to the outer regions: this produces a contraction of the core and gives rise to a gravothermal instability possibly culminating in core collapse, whose reason resides in the negative heat capacity of every gravitational system. Assuming Eq. 2.4 and expressing E_k as for a gas, namely

$$E_k = \frac{3}{2} N k_B T \ , \tag{2.7}$$

with $k_B = 1.380649 \times 10^{-23}\ \mathrm{JK}^{-1}$ Boltzmann constant and T thermodynamic temperature, it follows that

$$E = -E_k = -\frac{3}{2} N k_B T \implies C = \frac{dE}{dT} = -\frac{3}{2} N k_B \ . \tag{2.8}$$

So, if the total energy is negative, the heat capacity C is too, which simply means that a gas reacts by getting hotter in response to a energy loss: transposed into a gravitational system, where T is represented by the velocity dispersion, "getting hotter" is equivalent to "increasing its velocity dispersion", a condition attainable only through the contraction of the core. Thereby, a circular process in which the subsequent escape of more particles, carrying energy away and contributing to the system's cooling, are counteracted by a further core contraction, is established.
This overall behavior can be understood in terms of tendency to energy equipartition. The equipartition theorem, which traces its roots back to statistical mechanics, states that particles in a system act for always having the same kinetic energy.
Consider a system formed by two populations of stars with mass m_1 and m_2, respectively, such that $m_2 \gg m_1$: then, energy equipartition leads to

$$E_{k,1} = E_{k,2} \Longleftrightarrow m_1\langle v_1^2\rangle = m_2\langle v_2^2\rangle \ , \tag{2.9}$$

which implies that

$$\langle v_1^2\rangle > \langle v_2^2\rangle \ , \tag{2.10}$$

i.e., that heavier stars will have, on average, lower velocity than lighter ones. While losing energy, heavier stars slow down and sink towards the system's center, hence creating a concentration better known as mass segregation. The process is driven by dynamical friction, a drag force transferring energy and momentum from more massive bodies to the field of lighter particles they are moving in: the motion of a massive objects induces an acceleration on the surrounding particles towards it and determines a local density enhancement, which translates into a stronger gravitational attraction slowing the object down.
The timescale for mass segregation is, once more, the relaxation time, also related to the dynamical friction timescale by the formula

$$t_{df} = \frac{\langle m\rangle}{m_{max}} t_{relax} \ , \tag{2.11}$$

where $\langle m\rangle$ is the average mass of light stars and m_{max} the mass of the moving heavy star, so that t_{df} configures as the timescale over which a system segregates up to a mass m_{max}. Clearly, the more massive the heavy star, the shorter the time it needs to reach the center. And yet, is equipartition always allowed? If, as said, $m_2 \gg m_1$ and heavier stars are segregated at the center of the system, then their total mass M_2 cannot exceed the critical value

$$M_{2,crit} = 0.16\left(\frac{m_1}{m_2}\right)^{\frac{3}{2}} M_1 \tag{2.12}$$

for energy equipartition with lighter stars to be possible, because the required value of $\langle v_2\rangle$ would be too large. This can happen either when $M_2 > M_1$ due to the overly high number of heavier stars, or when $M_2 < M_1$, but the density of such objects outweights that of the less massive population: in both cases, the concentration of heavy stars continues to

contract, originating, within the system's core, a dense nucleus which keeps transferring kinetic energy to the light stars, so that equipartition is never achieved.
In particular, this phenomenon, called Spitzer's (or gravothermal) instability (Spitzer, 1969 [95]), suggests that equipartition is initially impossible for all young systems, given their leaning to develop a contracting nucleus of heavy stars at their center. Still, the outcome of this process depends on stellar evolution, since such stars have a limited life and are likely to lose mass either by a gradual mass ejection or by a supernova (SN) explosion. For instance, as far as GCs are concerned, the ejected stellar mass will presumably escape entirely, with the resulting transformation of the nucleus in a collection of dead, compact stars; contrariwise, in OCs the relatively small number of heavy stars involved facilitates the contraction to terminate with the formation of a stable central binary.

2.2.3 Core collapse and binary heating

Core collapse, triggered by the combined effect of evaporation and mass segregation, is a runaway process that can be halted only by the addition of an extra energy source, typically provided by binary stars which formed in the high-density environment of the collapsing core.
In fact, binaries are central in governing the long-term dynamical evolution of stellar systems, for they can strongly affect both the final stages of core collapse and the post-collapse phase (McMillan, 1991 [64]). Such objects can form either via conservative three-body encounters, as long as a third star transports enough kinetic energy to leave the other two bound, or via dissipative two-body encounters, if two stars pass close to each other. In order of importance, dynamical binaries can be divided in a number of categories:

- three-body binaries, generated in three-body encounters occurring when the number of stars in the collapsing core becomes significantly low ($N \sim 30$), are likely to contain heavier-than-average cluster stars due to the fact that the binary formation probability is an increasing function of mass, and that lighter stars tend to be ejected during a triple interaction;
- tidal capture binaries, originated in consequence to the kinetic energy dissipation of two strongly, tidally interacting stars, are generally close and tight, owing to the induced circularization of their orbit;
- runaway mergers, namely a merger product of two colliding stars sinking to the cluster's center. In particular, this mechanism is expected to be efficient in dense

stellar cores, being the collision cross section small.

That said, binary heating is strictly connected to the energetics of stellar encounters. Given the expression for binary binding energy

$$E_b = -G\frac{m_1 m_2}{2a} \,, \tag{2.13}$$

where a is the orbital semi-major axis, during a triple interaction E_b can either increase when the third stars transfers kinetic energy to the binary, making it less bound, or decrease when the opposite is true, so that the binary becomes more bound. Therefore, in the former case the kinetic energy of the cluster diminishes because the binary absorbs it, whereas in the latter it is enhanced due to the energy loss from the binary. By implication, then, hard binaries possess the right features to be responsible for the halting of core collapse.
As explained by Kroupa (2001) [52], such an energy transfer may be easily comprehended with the equipartition argument, remembering the distinction between soft and hard binaries introduced in Sect. I: during stellar encounters, soft binaries tend to loosen up whenever receiving a further energy input, since their orbital velocity grows as well as their orbital separation, while hard binaries tend to tighten after releasing energy, which determines the shrink of their semi-major axes. This is the so called Heggie-Hills law for stimulated evolution: in a cluster, soft binaries becomes softer, whereas hard binaries harder (Heggie, 1975 [32]).
Fregeau, Ivanova, and Rasio (2009) [24] studied the change of the overall binary fraction in GCs, disentangling the contribution of hard from that of soft binaries, and found that it remains almost constant in time because the preferential stripping of single stars roughly compensates the destruction of core binaries owing to mass segregation and stellar encounters. Into specifics, they accounted for the importance of soft binaries, which, as an energy sink, boost core contraction: this speeds up binary disruption by producing a much earlier onset of the related burning phase, potentially affecting the system's evolution in a dramatic fashion. The core hard binary fraction, instead, tends to increase with time over a range of initial central densities for similar high values of f_b.
Interestingly, according to McMillan (1991) [64], the way a binary heats its parent cluster depends on the degree of consideration of its components as point masses. In this sense, two main mechanisms are worth mentioning:

- three-body binary heating, in which the point-mass approximation holds, being the separation between three-body binaries' components sufficiently wide. Dur-

ing interactions with other cluster members, the Heggie-Hills law can be applied: hard binaries liberate kinetic energy, thus heating the cluster, and soft binaries are commonly destroyed. Most notably, N-body simulations show that a hard binary formed near core collapse may rapidly dominate the dynamics of the system by coming to contain the bulk of its binding energy. Even so, this process appears to be self-limiting: since binary encounters get more violent at increasing binding energy, they would ultimately lead to the ejection of all the involved stars from the clusters;

- tidal binary heating happens through mass loss, because tidal binaries are extremely hard: as such, their treatment at a level with point masses in stellar encounters, although not fully correct, would produce their immediate ejection, followed by a net heating effect, just like in the case of mass loss. Despite the much lower efficiency compared to the three-body mechanism, the heating process is considerably faster, so that tidal binaries might reverse core collapse well before the three-body binary stage is reached.

Besides, another impactful phenomenon on close binary evolution may be magnetic braking (Verbunt and Hut, 1983 [103]). Magnetic braking, i.e., the loss of a star's angular momentum due to its magnetic field, can be ideally described as operating in two stages:

- the rotation of the secondary is slowed down by effect of stellar wind, which carries away angular momentum. Indeed, the moderate mass loss would imply a relatively high angular momentum one, provided that the wind is forced to corotate with the star out of large distances by the magnetic field lines;
- the primary tries to spin the secondary up to corotation using orbital revolution, to which the angular momentum loss is transferred from the secondary's rotation.

Both stages may lead to a large energy dissipation, comparable to the nuclear energy production of the secondary, and give rise to tidal interactions that get the components closer in the attempt of restoring corotation.
A special space deserve primordial binaries, originated along with the cluster they are hosted by. From the dynamical point of view, such objects are wide enough to behave like three-body binaries, but close enough to have a non-negligible influence on cluster evolution: in fact, if a cluster is rich in primordial binaries, then these ones might be able to terminate core collapse even in the absence of both tidal and three-body binaries, hence serving as an active energy source. Their subsequent fate would be quite miserable, though, since they are expected to be slowly disrupted amidst cluster evolution; actually, a few real star clusters may have come to the end of this fossil burning phase.

2.2.4 A battle: evaporation versus hard binaries

Hills (1975) [36] realized an analytic model for computing the evolution of a cluster core due to the simultaneous presence of stellar evaporation, which causes the core to contract, and hard binaries, which fuel its expansion by progressively enhancing its kinetic energy or, equivalently, by reducing its binding energy.
Starting from the fact that a well-defined central core can be treated as an independent stellar system having its own radius $R = R_c$, velocity $v = v_c$, number density $n = n_c$ and number of stars $N = N_c$, each one characterized by a binding energy $E_b = E_{b,c}$ (here binaries are regarded as single objects with mass equal to the sum of the components' masses, so that $E_{b,c}$ does not include the components' binding energies), the following equations can be derived.
Core stars evaporate into the halo at a rate

$$\frac{1}{N_c}\frac{dN_c}{dt} = \frac{1}{88 t_{relax}} \,, \tag{2.14}$$

and have $E \simeq 0$, so that $E_{b,c}$ remains almost constant; on the other hand, when binaries feed kinetic energy into the core, they entail the decrease of $E_{b,c}$ at a rate

$$\frac{1}{E_{b,c}}\frac{dE_{b,c}}{dt} = -\left(\frac{f_b}{A_0 \ln\left(N_c/2\right)}\right)\frac{1}{t_{relax}} \,, \tag{2.15}$$

where $A_0 = 1.3$ and f_b is the system's binary fraction.
Dividing Eq. 2.15 by Eq. 2.14 returns

$$\frac{N_c}{E_{b,c}}\frac{dE_{b,c}}{dN_c} = \frac{88 f_b}{A_0 \ln\left(N_c/2\right)} \,, \tag{2.16}$$

which can be integrated, after variable separation, to obtain some meaningful relations:

- $E_{b,c}$ in units of E_0:

$$\frac{E_f}{E_0} = \left(\frac{ln(N_f/2)}{ln(N_0/2)}\right)^{\frac{88 f_b}{A_0}} \,; \tag{2.17}$$

- R_c in units of R_0:

$$\frac{R_f}{R_0} = \frac{E_f}{E_0}\left(\frac{N_f}{N_0}\right)^2 ; \tag{2.18}$$

- n_c in units of n_0:

$$\frac{n_f}{n_0} = \left(\frac{E_f}{E_0}\right)^3\left(\frac{N_0}{N_f}\right)^5 ; \tag{2.19}$$

- v_c in units of v_0:

$$\frac{v_f}{v_0} = \sqrt{\frac{E_f}{E_0}\frac{N_0}{N_f}} . \tag{2.20}$$

where the suffixes 0 and f refer, respectively, to the initial and final values of the examined quantities.
These equations have been used by Hills (1975) [32] to assess changes in the main properties of the system as a function of N_c, finding that at large values of N_c its dynamical evolution is ruled by evaporation, while at small values of N_c by binaries. But if, on the one hand, evaporation triggers a net contraction of the core, on the other hand binaries make it expand monotonically: contrary to evaporation, driven by distant encounters, binaries give rise to a relevant energy exchange only in close encounters with field stars. Thereby, the predominance of evaporation when N_c is sufficiently large is due to the fact that, for a fixed value of f_b, the frequency of distant encounters increments their effectiveness by a factor $\ln(N_c/2)$ at increasing N_c. As the decline of N_c proceeds along with core contraction, then, binaries begin to supersede evaporation, slowing its rate down until they prevail.
An application to real star clusters pointed out that dense central cores cannot develop by evaporation in systems where f_b is high (i.e., old OCs), since binaries dominate from the beginning, but that they are normally observed when f_b is low and evaporation is able to overcome the action of binaries (i.e., GCs).

2.2.5 Post-collapse evolution

Baumgardt, Hut, and Heggie (2002) [5] report results of N-body simulations of isolated star clusters, performed up to the point of their nearly complete dissolution, since they are an ideal environment to test many, actually present dynamical aspects.
As already discussed, in the absence of a external energy source such as binary hardening,

star clusters undergo core contraction in consequence to heat transfer from this region to the halo, until they centrally collapse after a significant number of relaxation times. When this happens, their structure becomes almost independent of both the initial density and particle number. Encounters between single stars inside the system half-mass radius constitute the dominant escape mechanism and are responsible for the build-up of a radial anisotropic velocity distribution in the halo: specifically, the anisotropy extends from the outer parts down into the core at the onset of core collapse, to finally increase towards the halo during the post-collapse phase. Moreover, it seems conceivable that isolated star clusters become vulnerable to radial orbit instabilities for large enough particle number, which anisotropy is directly proportional to; however, no indication for the onset of such instabilities was seen in the runs.

By contrast, encounters with binaries take place near the cluster center, being such objects strongly concentrated towards the core, and account for $\sim 15\%$ of the ejected stars. Most notably, Baumgardt, Hut, and Heggie (2002) [5] estimated that only a few binaries are necessary to drive the post-collapse expansion, for their number drops with particle number according to the law $N_b \sim N^{0.3}$, but that in models experiencing core oscillations they are effective merely when the center is in a contracted condition.

Chapter III

The fate of star clusters: violent relaxation, stellar evolution and effects of the Galactic tidal field

3.1 Dissolution processes in star clusters

Two-body relaxation is not the only form of relaxation that can take place in a stellar system: when stars move in a non-stationary potential, a process called violent relaxation can be started due to the change of the potential with time. But, while being exclusively possible in collisionless systems, it precedes two-body relaxation in collisional ones and plays a crucial role in the very early dynamical stages of clusters' lifetime, when virial equilibrium does not subsist (is violated). Intuitively, then, violent relaxation possesses a direct link to the efficiency of star formation (SF) process (Shukirgaliyev et al., 2017 [88]). SF takes place in collapsed, cold, dense gas clumps inside molecular clouds and, once thermonuclear reactions start in newborn stellar cores, they heat, ionize and drive the residual gas out of star forming regions: in particular, the most massive objects are able to blow it up in a few Myr via their strong winds, radiation pressure and eventual explosion as SNe Ib,c or II. The collective stellar feedback from all stars can terminate SF and totally remove the residual gas from the newly formed star cluster.
Now, as stated by Gieles (2010) [28], the life of star clusters can be broadly divided into three time-spans, according to the dominant, ongoing disruption mechanism affecting the system long-term survival chances.

The first few Myr are exactly characterized by the residual gas expulsion from the SF process, which determines the cluster expansion or even complete dissolution. The importance of such a phase depends on a number of factors: the initial cluster density and virial state, the timescale for gas expulsion and the star formation efficiency (SFE), defined as the mass fraction of gas effectively converted into stars. For instance, in case of subvirial initial conditions, a SFE of ~ 0.125 is sufficient to expel all the residual gas, contrary to the analytic estimate of 0.5 for virialized, embedded star clusters under the assumption that the timescale for gas expulsion is much lower than the crossing time. In this approximation, the slow gas removal may result in a bound system for a SFE of ~ 0.1 (Baumgardt and Kroupa, 2007 [4]). Yet, since the percentage of gas gone into stars is usually $< 30\%$ in star forming regions of the solar vicinity, it follows that $> 70\%$ escapes, thus weakening the cluster's gravitational potential: such a phenomenon, caused by residual gas expulsion, drives the system out of virial equilibrium. The subsequent evolution through a new equilibrium state is called violent relaxation, and may be interrupted by the star clusters "infant mortality", i.e., their eventual dissolution due to the loss of stars before achieving a new equilibrium condition. When the most massive stars explode as SNe, then, the resulting shocks eject much of the gas and clearly part of the cluster mass, making the system unbound.
By following Hills (1980) [37], the simpler problem of sudden mass loss from a cluster in equilibrium, where the mass is ejected in less than the dynamical timescale

$$t_{dyn} = (G\rho)^{-\frac{1}{2}} \, , \tag{3.1}$$

is taken as a starting point for analyzing the early unbinding of newborn stellar systems. As an example, mass expulsion that arises precisely at the formation of a star cluster from an interstellar cloud is referenced: if the conversion of gas into stars is not complete, the remaining embryonic gas may be driven out of the system as an expanding H II region produced by the UV flux from young, massive upper-main-sequence stars. Indeed, since the typical sound speed of 12 kms^{-1}in an H II region is an order of magnitude greater than the escape velocity from an OC, such gas can easily leave the cluster within a dynamical timescale. Given that impulsive mass loss does not affect stellar velocities, the virial theorem applies and the initial velocity dispersion takes the expression of

$$v_0^2 = \frac{GM_0}{2R_0} \, , \tag{3.2}$$

where M_0 and R_0 are, respectively, the initial mass and radius of the cluster. Immediately after the gas is sent off the system, then, the stars preserve their velocities, but the total mass of the cluster is reduced to M. The cluster will be out of equilibrium, and have energy

$$E = \frac{1}{2}\left(Mv_0^2 - \frac{GM^2}{R_0}\right) . \tag{3.3}$$

Once virial equilibrium is restored, the cluster energy will remain the same despite a change of its radius, i.e.,

$$E = -\frac{GM}{4R} . \tag{3.4}$$

This translates into the initial-final radius relationship for the cluster

$$\frac{R}{R_0} = \frac{M_0 - \Delta M}{M_0 - 2\Delta M} , \tag{3.5}$$

which diverges if half the cluster mass is removed: thus, in a virialized system half the mass needs to be lost in order to unbind it.
Hills (1980) [37] next briefly discussed the case of adiabatic mass loss, occurring whenever the mass loss rate is small on the dynamical timescale: by implication, virial equilibrium is preserved, as demonstrated by the modified initial-final radius relationship

$$\frac{R}{R_0} = \frac{M_0}{M_0 - \Delta M} , \tag{3.6}$$

divergent only if $\Delta M = M_0$. In other terms, the cluster is destined to stay bound independently of the strength of mass removal.
Still, a real OC is unlikely virialized by the time SNe from massive stars go off and drive gas out: in fact, it would collapse from an initial radius R_0 to a new radius R_1, and possibly come into virial equilibrium again with some final radius R, such that the total energy is half the potential energy

$$E = -\frac{3GM^2}{10R} \,, \tag{3.7}$$

and that the initial-final radius relationship results

$$\frac{R}{R_0} = \frac{1}{2}\left(\frac{M_0 - \Delta M}{M_0 - \Delta M(R_0/R_1)}\right) . \tag{3.8}$$

In order for the system to become unbound, then, the condition $R \to \infty$ must be satisfied by setting the denominator of Eq. 3.8 equal to zero, i.e.,

$$\frac{\Delta M}{M_0} = \frac{R_1}{R_0} \,. \tag{3.9}$$

In particular, since calculations based on the SF process in molecular clouds show that a typical proto-cluster would probably have $R_1/R_0 \sim 10$ or more, it follows that unbinding a cluster would require only 10% of its mass.
The reason for the need of so little mass loss can be retrieved in the virialization process. Consider a cluster of stars, all stationary and at a large distance: due to their mutual gravitational attraction, they begin to fall to the center of the cluster, picking up speed and experiencing strong interactions with each other. In this way, energy is transferred among them, and their trajectories are redirected and randomized, so that, over a long enough time, the system will enter a virial state.
Now, an eventual mass loss at the very beginning of the cluster lifetime will not affect the virialization process, because of its taking also gravitational potential energy away: stars will approach each other and reach the cluster center with lower speed, but qualitatively nothing else will change. On the contrary, if a fraction of mass is lost when stars are passing through the central regions, the associated gravitational potential energy will be transferred to the remaining mass in form of kinetic energy, with a consequent speed gain, such that the closer the stars are to the center of the cluster when this happens, the more remaining mass necessitates to keep the system bound. Thereby, given that the cluster collapses by quite a bit after the explosion of the first SNe, it would be easily disrupted even in the event of a modest mass loss.
As a closing note, Hills (1980) [37] highlighted that, when the proto-cluster gas contains an appreciable magnetic field, its compression in the collapsing cloud is such to drain off

some of the gravitational energy that otherwise would go into the kinetic energy: this drives up the minimum mass loss required for the system dissociation, which remains still very small, though.
Studies on the effects of instantaneous residual gas expulsion on model star clusters pointed out that the minimum SFE for a system to overcome such a critical process is 15%, and that the violent relaxation phase lasts no longer than 20 Myr, regardless of the SFE and the initial stellar mass. On the contrary, the dissolution timescale seems to be related to the cluster bound mass at the end of violent relaxation, with systems characterized by high SFE following a much tighter mass-dependent relation with respect to low-SFE ones, which constitute the vast majority and disappear within 1 Gyr. Also, the combination of high-SFE and low-SFE clusters, with domination of the latter, yields a dissolution timescale for the solar neighborhood in agreement with that inferred from observations, without the need of additional disrupting processes such as encounters with giant molecular clouds.
Notably, according to the star cluster age distribution in the solar neighborhood, infant mortality is high: by implication, the presently observed MW star clusters must be those who survived both the gas expulsion and the violent relaxation phase, and hence became gravitationally bound systems.
Clusters able to avoid infant mortality continue to lose mass through the evolution of their stars during the subsequent 500 Myr. Given that the timescale for stellar evolution is considerably longer than the crossing time, the global reaction will be an adiabatic expansion, particularly severe in the event of a primordially mass segregated cluster (Vesperini, McMillan, and Portegies Zwart, 2009 [105]): indeed, a preferential mass stripping from the central regions, where massive stars tend to concentrate, implies a major expansion. Moreover, since the early generation of mass segregation is disfavored in initially clumpy stellar systems (Lynden-Bell, 1967 [56]), which are likely to undergo a rapid phase of violent relaxation such to erase any substructures, and the clump-merging timescale is typically shorter than that for gas expulsion, the cluster survivability may be enhanced (Fellhauer, Wilkinson, and Kroupa, 2009 [21]).
Nevertheless, bound star clusters are deemed to dissolve with time as well, especially in consequence of the tidal stripping process they are subject to while orbiting inside the Galaxy. As a result, the star cluster lifetime depends not only on its mass density and hosted number of stars, but also on the strength of the external tidal field.
In fact, up to about 1 Gyr, external disruptive factors like encounters with giant molecular clouds (GMCs) and two-body relaxation in the tidal field of the host galaxy become relevant. The impact of the tidal field on a cluster is typically quantified by the ratio

between the half-mass radius and the Jacobi radius R_{hm}/R_J, so that the lower its value, the longer the system's lifetime (Shukirgaliyev et al., 2019 [87]). Specifically, R_{hm}/R_J diminishes in two different cases: the former at increasing Galactocentric distance, for fixed cluster mass and size (i.e., with constant R_{hm}), and the latter at decreasing cluster size, for fixed cluster mass and Galactocentric distance (i.e., with constant R_J). Therefore, to boost the survival chances of a star cluster after the end of violent relaxation, one should either place it at larger distances from the Galactic center, where the tidal field is weaker, or make it more compact by reducing its size.

3.2 Dynamical evolution of globular clusters

The dynamical evolution of GCs is dominated by two-body relaxation and gravitational shocks, which can be broadly divided into tidal and compressive (Ostriker, Spitzer, and Chevalier, 1972 [71]): the former occur in OCs in consequence of the interactions with interstellar clouds and can be defined as such because the duration of the perturbing tidal force is much shorter than the star cluster period, while the latter affect GCs whenever they pass through the Galactic plane by compressing them along the z direction due to the variation with height of the perpendicular component of the gravitational acceleration $g(z)$, with a resulting increase of the cluster's kinetic energy. On this matter, Ostriker, Spitzer, and Chevalier (1972) [71] underlined that the cluster lifetime due to GMC heating is inversely proportional to the volume density of the molecular gas, but directly proportional to the density of the cluster itself: this incidentally explains why this dissolution mechanism is most effective in spiral galaxies, characterized by high gas density, indeed.
According to observational data, these two combined processes are responsible for the escape of the bulk of low-mass stars, typically located in the GCs' outskirts. Also, gravitational shocks tend to reduce the time for core collapse in such systems, thus suggesting that both the number of faintest stars and the mass-to-light ratio should be enhanced at a major distance from the Galactic center, especially when the cluster relaxation timescale is large.
In connection with this, Spitzer and Schwarzschild (1951) [96] noted that understanding whether stars in the MW continue to follow their original orbits or perturbing processes have been effective in changing them is fundamental to interpret the observed stellar motions: in the former case, the current σ_{obs} would be completely determined by events at the time the MW settled to its present state, whereas in the latter some of the velocity

features might come from perturbation processes continuously happening during the stars' life. Beyond stellar encounters, such perturbations are typically encounters of different nature, namely between stars and GMCs, because the uneven distribution of interstellar matter, concentrated into clouds, tends to deviate stellar orbits. Since clouds possess much larger masses than stars, encounters involving these types of objects are characterized by considerably shorter relaxation times. Even if they result always comparable to the age of the Galaxy, so that energy equipartition has not been established yet, star-clouds encounters may have already produced noticeable effects on stellar velocities: stars are generally speeded up in order for relaxation time to be diminished and energy equipartition to be reached. Clearly, this phenomenon is much more prominent at increasing age of the involved stars: hence, red giant branch (RGB) and main sequence (MS) stars would suffer more from a velocity enhancement with respect to OB stars.
However, gravitational shocks and encounters with interstellar clouds are not the sole type of perturbation affecting the pre-collapse phases of Galactic GCs.
Heggie (1975) [32] designed N-body calculations to investigate the survival of star clusters with large membership against two important disruptive processes, i.e., the mass loss resulting from stellar evolution and the tidal stripping due to the gravitational field of the parent galaxy, provided that relaxation effects are negligible over time-scales equivalent to the duration of the simulations and that the galactic tide does not show any time dependence.
Since each star loses a certain mass fraction near the end of its own evolution, the total mass of the cluster is decreased: therefore, the cluster potential weakens and the system expands with the consequent outflow of part of its stars across the tidal radius, so that further mass is removed. Such an outcome is far more severe if the cluster initially contains a considerable number of massive stars. On the contrary, the additional input of evaporation caused by two-body encounters produces a minor effect compared to the aforementioned processes. Although their simultaneous occurrence, as the cluster loses mass the action of the steady tidal field starts to prevail, until the system's virial state is irreversibly perturbed.
By expressing virial equilibrium as

$$\frac{R_t(4E + V_s)}{2GM^2} = -\frac{\mu}{(R_{hm}/R_t)} - \frac{4\nu}{3}\left(\frac{R_{hm}}{R_t}\right)^2, \tag{3.10}$$

where V_s is a rotational term, while R_{hm} and R_t are the half-mass and the tidal radius, and μ and ν dimensionless constants, the following points can be put forward. When R_{hm}/R_t

is small, the right-hand side of equation 3.10 is dominated by the first term, which comes from the self- potential of the cluster, whereas when R_{hm}/R_t is large it is dominated by the second term, which is due to the potential of the galaxy and the centrifugal force: hereby, if regarded as a function of R_{hm}/R_t, the right-hand side of equation 3.10 must have a maximum value at a particular point. Initially, R_{hm}/R_t is below the maximum, and so is the value of the function on the left-hand side of equation 3.10, but afterwards both these quantities rapidly rise as a result of stellar evolution mass loss, so that, once the function on the left-hand side of equation 3.10 exceeds the maximum, the cluster gets out of equilibrium and disrupts. In fact, the cluster expansion causes R_{hm} to increase and R_t to decrease in proportion to $M^{\frac{1}{3}}$ at the same time, given that stars moving beyond the tidal radius cease to be members. This means that the mass loss rate from stellar evolution must be low in order for the cluster to avoid early dissolution and eventually head towards core collapse.

In addition to this, Spitzer (1958) [94] claimed that the presence of a tidal field introduces a new timescale for star cluster evolution: this is the dissolution timescale t_{dis}, i.e., the time for the system to lose $\sim 98\%$ of the initial mass due to the escape of stars across the tidal boundary, which is worth comparing to the binary burning timescale t_{bb}, i.e., the time needed to deplete $\sim 80\%$ of the initial binary fraction. Since the mass loss rate associated to the action of the tidal field is almost independent of the central cluster regions' properties, where binaries tend to accumulate and act as an energy source against core collapse, by implication $t_{dis} < t_{bb}$: tidal dissolution can happen so fast to be unable to fully suppress the primordial binary population. In the presence of a tidal field, then, star clusters evolve towards similar conditions to those they would have if they were isolated, because, after a few relaxation times, the ratio R_c/R_{hm}, where R_c is the cluster core radius, gets to attain almost the same value as isolated Plummer models with comparable initial binary fraction at the end of the core collapse phase.

It follows naturally that binaries play a non-negligible role in the dynamics of star clusters embedded in an external field. To this regard, Trenti, Heggie, and Hut (2007) [101] took into consideration the evolution of King models with different number of stars and primordial binary fraction immersed in the Galactic tidal field, and compared the results of their N-body simulations to those of both Fregeau et al. (2003) [22] and Fregeau (2004) [23], who performed Monte Carlo simulations of both isolated and tidally truncated star clusters having particle number $N = 3 \times 10^5$ and primordial binaries in fraction $f_b = 2 - 20\%$. Indeed, they discovered not only that the core radius of tidally limited clusters may undergo an initial expansion when a significant primordial binary population is present, but also that this one may be able to delay the core collapse phase, leading to

an eventual dissolution before its onset.
Also McMillan (1991) [64] addressed the topic of primordial binaries in GCs surrounded by the Galactic tidal field, and highlighted that they may come to rapidly dominate the overall system evolution and remain in control until complete ejection or unbinding. Interestingly, because of the competition between tidal stripping and binary destruction, the initial binary fraction may either be depleted prior to the cluster evaporation, or fall to a minimum value and grow back again at late times: the critical value for any of the two scenarios to take place is $f_{b,crit} \sim 10\%$ for the parameters of a typical MW GC.

3.3 Old open clusters, a family in between

Owing to their characteristic physical properties, old OCs may be viewed in the manner of a bridge between common OCs and GCs.
As reported by von Hippel (2005) [106], the total number of OCs in the MW is $\sim 10^5$, i.e., three order of magnitude larger than the predicted number of GCs, and, while these ones are distributed in a mostly spherical configuration in both the MW halo and disk, OCs occupy only the disk, with the older ones populating mainly its thick part and the younger ones its thin part at a scale height of $50 - 300$ pc. The age distribution of OCs spans from few hundreds Myr to few Gyr, with an average of ~ 300 Myr: this significant age spread indicates that OCs are continuously forming in the MW. From early statistics (Oort, 1958) [70], old OCs (age ≥ 1 Gyr) resulted very scarce compared to the expected number, obtained by extrapolating the population of young OCs and assuming a uniform SFR over the Galactic disk's lifetime: such an under-abundance is reasonably explained as the result of the concurrent infant mortality phenomenon and disruptive effects of encounters with GMCs in the thin disk (Spitzer, 1958 [94]), which could easily destroy a typical open-cluster-like system, depending on its mass and core radius. Therefore, the currently observed old OCs have likely survived thanks to their larger masses, higher central concentrations and orbits that allow them not to come into contact with GMCs in the thin disk, a scenario validated by their preferential location at a distance from the Galactic plane. On the subject, Janes and Phelps (1994) [43] demonstrated that old OCs are completely absent inside a radius of ~ 7.5 kpc from the Galactic center, where their spatial distribution drops off rapidly, and that they can reach a scale height of ~ 375 pc throughout the thick disk.
Due to their major richness and compactness with respect to young OCs, which appear sparsely distributed, loosely concentrated and composed by a few tens or hundreds of

stars, old OCs must have undergone significant dynamical evolution on a par with GCs (Friel, 1993 [25]). Not by accident, indeed, King (1962) [45] pointed out that M67, NGC 188 and NGC 7789 followed the same surface density profiles as isothermal spheres modified by tidal forces, and successfully described them through models with small R_t/R_c ratios (i.e., $R_t \sim 10-25$ pc, $R_c \sim 1-2$ pc). Being dynamically relaxed, then, old OCs show signatures of both mass segregation, such as the concentration of massive stars and the flattening of the luminosity function (LF) in the central regions, and evaporation, such as the presence of a considerable amount of low-mass stars well outside the tidal radius. Thus, OCs look particularly vulnerable to the Galactic tidal field action.
In addition to this, Janes and Phelps (1994) [43] investigated the cumulative age distribution of Galactic OCs, claiming that it could be fit by a combination of two exponentials in cluster age, with a corresponding lifetime of ~ 200 Myr and ~ 4 Gyr. They hence argued that the former component should represent the bulk of OCs, whereas the latter only a tiny part.
Always in this sense, Spitzer (1958) [94] evaluated the magnitude of the interaction with GMCs based on the impulsive approximation, namely on the assumption, adequate if the cluster gravitational potential is taken to vary as the squared distance from the Galactic center, that member stars do not move appreciably from their original position during the cloud passage. Such an approximation has been used to determine the disruption timescale t_{dis} of different density MW OCs: the Hyades ($\rho \simeq 0.3$ $M_\odot/pc^3$), the Pleiades ($\rho \simeq 6$ $M_\odot/pc^3$) and M67 ($\rho \simeq 70$ $M_\odot/pc^3$). Given that $t_{dis} = 1.9 \times 10^8 \rho$ yr, only relatively dense clusters, such as M67, are able to survive dissolution for a long time: in fact, $t_{dis} = 5 \simeq 10^9$ yr for M67, but $t_{dis} = \simeq 10^7$ yr and $t_{dis} \simeq 10^9$ yr for the Hyades and the Pleiades, respectively. Thereby, this analysis has led to the conclusion that all Galactic OCs having mean density $\bar{\rho} \in [0.5, 5]$ $M_\odot/pc^3$ will probably dissolve after repeated tidal disturbances in $\sim 10^8 - 10^9$ yr, which may account for the scarcity of observed clusters with age $> 10^9$ yr.
As a closing note, OCs lose members steadily, and most eventually dissolve into the Galactic field star population, despite the very low dispersions (i.e., $\sigma_{int} \sim 1-3$ kms^{-1}), which translates into a wide stellar mass range, i.e., $10^2 - 10^3$ $M_\odot$, with a present-day average of ~ 700 $M_\odot$ instead of the initially estimated value of ~ 4500 $M_\odot$ (von Hippel, 2005 [106]): this mass gap seems to represent a further confirmation of the dissolution process such systems experienced in the past or are still undergoing. Not by chance, then, almost all stars form in clusters with mass function of the form $N(m) \propto m^{-2}$ (Goodwin and Bastian, 2006 [31]).

3.3.1 The most famous: M67 and NGC 188

The interest in old OC like M67 lies in their offering the chance to investigate the effects of stellar interactions and cluster evolution, being them dynamically well evolved. Hurley et al. (2005) [40] discussed the results from a direct N-body model of M67 in comparison with the related observational data, looking at the overall structural properties of the cluster and at the nature of its stellar population.
The initial conditions for the model comprehend a total mass $M \simeq 14400$ $M_\odot$, with single stellar masses extracted from a Kroupa initial mass function (IMF) in the interval [0.1,50] $M_\odot$, and a binary population in fraction $f_b = 0.5$, characterized by a logarithmic semi-major axis distribution ($a \in [0, 50]$ AU) and a thermal eccentricity distribution ($e \in [0, 1]$). Besides this, the cluster has been described by a Plummer model with radius $R = 3$ pc and solar metallicity, embedded in the MW tidal field, and assigned an age of 4 Gyr.
The simulations' outcomes provides a good match with observations and can be summarized as follows:

- f_b remains almost constant due to the balance between the destruction of soft binaries in two-body interactions and of hard binaries through dynamical hardening and binary evolution, and to the preferential escape of low-mass single stars via tidal stripping, which makes encounters with binaries less probable;
- the large f_b contributes to maintain the cluster evolution relatively regular;
- since M reduces to ~ 2000 $M_\odot$ at 4 Gyr and 13 relaxation times have elapsed in reaching such an age, M67 may clearly be considered a dynamically relaxed system with no information about its original IMF left.

Instead, observations of the 7-Gyr-old OC NGC 188 revealed the existence of a rich binary population and a wide variety of its dynamical interactions products, such as blue stragglers (BSs) and X-ray binaries (Geller and Mathieu, 2012 [27]). In this respect, field binaries represent a fundamental benchmark for OC binaries, since they are unlikely to endure dynamical encounters, given the low stellar density of the Galactic field.
In studying NGC 188, 85 binaries out of a complete sample of 129 detected binary members have been used to determine both the associated fraction and the orbital parameter distributions, which have been compared first to the tabulated data of R10, i.e., the most important catalog of field stars by Raghavan et al. (2010) [79], and then to N-body simulations of the 3-Gyr-old OC M67 by Hurley et al. (2005) [40] in order to assess the impact of stellar dynamics on shaping the cluster binary population and creating exotic stars. Specifically, accepted binaries are almost all hard, as characterized by orbital

periods ranging from a few days to 10^4 days, and, among them, MS ones show period and eccentricity distributions compatible with those of field binaries in R10 (i.e., $\sim 29\%$ contrary to $\sim 19\%$), even if present in a higher percentage (i.e., $\sim 29\%$ contrary to $\sim 19\%$): such signatures, expected from dynamical relaxation processes, are in full agreement with the results of Hurley et al. (2005) [40].

3.4 Evolution of the binary fraction in star clusters

Li and Mao (2018) [55] stressed that the binary fraction is a key parameter in stellar population studies. Even so, unfortunately, its value remains unclear for most star clusters and galaxies, the MW included: indeed, for the Galaxy only a lower limit of about 50% has been set. Moreover, its sensitivity not only to some observational features, such as the spectral type, but also to several determination techniques reduces the accuracy of related physical analyses.
Notably, contradictory outputs arise from different attempts to constrain the binary fraction of star clusters. For example, Ivanova et al. (2005) [42] addressed the evolution of the binary fraction in GCs via the Monte Carlo approach, combining a population synthesis code and a simple treatment of dynamical interactions, and Sollima (2008) [91] revisited their research through a full analytical computation: in both cases, a rapid depletion of binaries in the cluster core was found.
In particular, as highlighted by Ivanova et al. (2005) [42], any strong interaction with another passing star can easily destroy soft binaries, whose orbital speeds are lower than the cluster velocity dispersion, while resonant binary–binary encounters, which typically eject two single stars, leaving only one binary (Mikkola, 1983 [65]), or produce physical stellar collisions and mergers, affect hard binaries. Additionally, many binary stellar evolution processes lead to disruptions (e.g., in consequence of the SN explosion of one component) or mergers (e.g., following a common envelope phase). These evolutionary destruction processes can also be enhanced by dynamics: for instance, more common envelope systems form in response to exchange interactions (Rappaport et al., 2001 [80]), whereas the orbital shrinkage and the development of high eccentricities through hardening encounters may cause the coalescence of binary components (Hills, 1984 [35]; Hurley et al., 2003 [38]). It is therefore natural to ask whether the small binary fractions currently detected in GCs' cores, compared to the solar neighborhood, result from these many disruptive processes, and what the initial binary fraction must have been in order to explain the present numbers. Although, of course, direct measurements of the primordial binary fraction are unfeasible, neither observational nor theoretical arguments seem to suggest

that the formation of binaries and hierarchical multiples in dense stellar systems should be quite dissimilar from other environments like OCs, the Galactic field, or star-forming regions. In fact, for the range of separations between 120 and 1800 AU, their binary fraction is akin to that of MS stars in the solar neighborhood, while at shorter periods it is higher.

By performing calculations in line with the "binary population synthesis with dynamics" approach, then, Ivanova et al. (2005) [42] found confirmation that the initial period distribution, assumed to be uniform in log$P$ over the range $P = 0.1 - 10^7$ d, is devoid above the boundary between hard and soft binaries through dynamical interactions. Indeed, in loose models the distribution remains much flatter, with more and more hard binaries disappearing at increasing density because stellar evolution is expected to suppress a fraction of them, especially at very short periods, and dynamical encounters should further phase out some of the wider remaining ones. Therefore, the binary period distribution evolves with the density from flat in log$P$ toward a sharply peaked functional form, even when adopting identical hard-soft binary boundaries.

But, most importantly, the authors estimated an actual binary fraction of $5 - 10\%$ in cluster cores owing not only to close encounters, but also to stellar evolution, which is the dominant disruption mechanism for hard binaries, and concluded that extremely high (i.e., near 100%) primordial binary fractions are likely.

On the other hand, Hurley, Aarseth, and Shara (2007) [39] realized N-body models reproducing both an old OC like M67 and GCs with different stellar densities in order to investigate the evolution of the core binary fraction, and in so doing they paid special attention to primordial binaries' orbital parameters due to their major influence. Specifically, the M67 model was tailored in accordance with the previous work by Hurley et al. (2005) [40], hence having 24000 stars at birth and an initial binary frequency of 50%. Considering that the cluster is subject to a standard Galactic tidal field (i.e., it describes a circular orbit in the solar neighborhood) and that stars are removed from the simulation when their distance from the density center exceeds twice that of the cluster tidal radius, a half-life of ~ 2 Gyr is obtained and, after 4 Gyr, only 2000 members are counted.

The effect of a substantial primordial binary population on evolving OCs is twofold: firstly, it renders the core-collapse phase less dramatic, and secondly it lowers the cluster lifetime. However, at late times the M67 model seems to have lost more than 90% of its original mass and to approach dissolution because, from 2 Gyr onward, evolution processes such to destroy binaries (i.e., dynamical encounters and mass transfer-induced mergers, enhanced by mass segregation) only partially offset the dominant escape rate of single stars from the cluster core: as a result, the number of binaries in the core decreases

with time, even though the binary fraction increases. In particular, mass loss from stellar evolution is significantly reduced at this stage compared to earlier ones (especially during the first 100 Myr), when more massive stars are present. Also, the characteristics of the binary content change markedly in time, with hard binaries obviously favored as the system ages. So Hurley, Aarseth, and Shara (2007) [39] inferred that, except for the advanced evolutionary phases, the overall binary fraction remains almost always close to the initial value outside the cluster central regions, irrespective of the simulation type. Finally, they suggested that, being the primordial binary frequency well preserved beyond the cluster half-mass radius, the currently observed binary fraction in these regions may constitute a good indicator of the primordial value, unlike the core binary fraction, which provides an upper limit. However, contrary to Hurley, Aarseth, and Shara (2007) [39], Fregeau, Ivanova, and Rasio (2009) [24] derived an increasing trend for the core binary fraction from an improved Monte Carlo evolution code.
Given this "colorful" scenario, Li and Mao (2018) [55] explored how the binary fraction changes with time owing to stellar evolution, and made clear the correlations between previous estimates. To this aim, they considered only optical binaries, which can always be observed and plotted onto the Hertzsprung Russel (HRD) or the Color Magnitude (CMD) Diagram, hence ruling out components such as neutron stars (NSs) and black holes (BHs). In this way, they witnessed a decrease of the optical binary fraction from 1 to about 0.81 or 0.85 in stellar populations described by the Salpeter and Kroupa IMF, respectively, on a timescale of 15 Gyr, this outcome depending on their age and metallicity. Such a behavior looks compatible with the predictions by Ivanova et al. (2005) [42] and Sollima (2008) [91] for the core binary fraction in GCs, whose reduction rate is inversely proportional to the central number density, but not entirely, since the optical binary fraction exhibits a slower decline due to both the larger orbital separations of binary pairs and the lack of dynamical processes. By contrast, the results of Hurley, Aarseth, and Shara (2007) [39] and Fregeau, Ivanova, and Rasio (2009) [24], who claimed the binary fraction to up in dense cluster cores, cannot be reproduced: this means that a reliable picture for the change of the binary fraction over time, such to take into account the effects of stellar evolution and dynamics, is not available yet. Nonetheless, the work of Li and Mao (2018) [55] may still be helpful for estimating the global optical binary fraction of star clusters or galaxies from a specific sample, recovering the primordial binary fraction of sparse stellar systems from the present observations, and supplying a certain answer for its future characteristics in response to stellar evolution.

3.5 Binaries and star clusters' dynamical mass estimates

Even though observations have shown that the majority of field stars are part of binary systems (Duquennoy and Mayor, 1991 [19]), binaries are not often properly taken into account when analyzing spectral line data of young stellar systems.
The dynamical mass of a star cluster

$$M_{dyn} = \eta \frac{R_{hm}\sigma_{los}^2}{G} \ , \tag{3.11}$$

where R_{hm} is the projected half-mass radius, σ_{los} the observed velocity dispersion and $\eta = 9.75$, is determined by using its integrated light and assuming virial equilibrium (Spitzer, 1987 [98]). The validity of this condition can be verified through a comparison between M_{dyn} and the photometric mass M_{phot}, derived from the cluster's total luminosity and age. Now, the fact that $M_{dyn} \sim M_{phot}$ for systems older than $50 - 100$ Myr, but $M_{dyn} >> M_{phot}$ for many younger ones, has been interpreted by Goodwin and Bastian (2006) [31] as a signature of gas expulsion and, consequently, of the infant mortality scenario, which would indicate the superviriality of such clusters. Still, according to theoretical predictions, after instantaneous gas removal about ten crossing times would be necessary to either completely disrupt or expand the system to a new equilibrium state: hence, only if the crossing time amounted to a few Myr, corresponding to an initial density $\rho \sim 100$ $M_\odot/pc^3$, a cluster already broken apart at 10 Myr would be caught. So, given that the sample of Goodwin and Bastian (2006) [31] was characterized by $t_{cr} = 2.5$ Myr and $\rho \sim 10$ $M_\odot/pc^3$, and that the mean measured velocity was ~ 20 kms^{-1}, the hypothesis of superviriality does not stand: in fact, with such a velocity, an unbound cluster would dissolve in a few Myr, instead of evolving for at least $10 - 100 t_{cr}$. Otherwise, the possibility for stellar velocities to be dominated by the orbital motion of unresolved binaries may account for the too large values of the observed velocity dispersion, which would explain the discrepancy between M_{dyn} and M_{phot}. Since the inflation of M_{dyn} due to binaries results more severe in systems hosting a substantial number of massive stars (~ 15 $M_\odot$), for which stellar multiplicity is high, and both short periods and close-to-one mass ratios are common, the analyzed clusters may have survived gas expulsion and entered the stellar evolution phase.
By means of available velocity dispersion measurements, de Grijs et al. (2008) [16] derived the dynamical masses and mass-to-light ratios in the V band (M/L_V) for a sample of Galactic OCs older than 40 Myr (hence such to have re-virialized after gas expulsion) and

exploited a diagnostic age versus mass-to-light ratio diagram to identify any deviation from the trend of M/L_V expected for single stellar populations (SSPs) governed by either the Salpeter or the Kroupa IMF. Into specifics, clusters way below the SSP lines in the diagram are regarded as dynamically hot and fated to a rapid dissolution, while those above the SSP lines as dynamically cold and thus required to re-virialize over a few crossing times for nearing them.
Since most targets were found to be supervirial, de Grijs et al. (2008) [16] suggested that the presence of binaries may inflate their velocity dispersion and cause them to move under the SSP lines, outweighing the effect of equipartition, which tends to lower the cluster velocity dispersion through the preferential loss of low-mass stars: this would result in a "top-heavy" mass function (MF) and, therefore, in an underestimation of M/L_V with respect to the predicted photometric evolutionary sequences for standard SSP models. Nevertheless, the authors also emphasized that, for an OC to survive for any significant length of time and in the absence of significant external perturbations, it is necessary but not sufficient to lie close to or (in the event of a conspicuous binary population) somewhat below the SSP lines, although such a location may adequately reflect the overall cluster dynamics.
Kouwenhoven and de Grijs (2008) [49] argued that the importance of binaries in the dynamical mass determination depends not only on star cluster and binary population properties, but also on selection effects. In fact, systems with larger stellar density ($M \leq 10^5$ $M_\odot$, as reported by Kouwenhoven and de Grijs, 2008) [49] are least affected by unresolved binary orbital motion, and both the eccentricity and the mass ratio distribution have a smaller impact on the observed velocity dispersion, compared to the semi-major axis distribution and the binary fraction (i.e., the tighter a binary, the higher its orbital velocity). Moreover, σ_{los} is typically measured from spectral lines of red giants, which may not be representative of the cluster as a whole, and if observations are concentrated in its central regions, where massive stars sink, then the inflation of the dynamical mass may reach the 40%.

3.6 Simulations of Galactic open clusters with *PeTar*

To briefly recap the foremost arguments thus far covered, OCs, found primarily in the Galactic disk, appear as short-lived stellar systems, given their sparseness and young age (Bergond, Leon, and Guibert, 2001 [9]); although interactions with GMCs were at first regarded as the most plausible cause for the scarcity of old Galactic OCs (Gieles, 2010 [28]), several are, actually, the mechanisms favoring their early dissolution. In particular,

beyond residual gas expulsion from the SF process and mass loss due to stellar evolution, which act during the first few hundred Myr of a cluster's life (Spitzer, 1958 [94]), two-body relaxation in the tidal field of the host galaxy is of major importance on longer timescales. By letting stars exchange energy and momentum in an effort to reach energy equipartition, two-body encounters are responsible for the onset of dynamical friction, i.e., a drag force accelerating low-mass particles to the escape velocity in about a half-mass relaxation time, which they need to establish a Maxwellian velocity distribution (Spitzer, 1987 [98]). Therefore, stars in the outskirts of collisionless systems embedded in an external potential are more likely to be stripped from tidal forces, since they may easily exceed the local escape velocity, while massive stars tend to sink towards the central regions.
Mass segregation, together with energy equipartition and a high binary fraction, are fundamental both in driving the long-term evolution and in shaping the current properties of star clusters (Vesperini, 2010 [104]). Specifically, as highlighted by Kouwenhoven and de Grijs (2008) [49], their effect mostly concerns the system observed velocity dispersion and reflects upon the related dynamical mass estimate through the formula 3.11. Derived from the virial theorem under the implicit assumption of all stars being single, this expression is typically adopted to evaluate the total mass of unresolved clusters by neglecting the presence of binaries in line-of-sight velocity dispersion measurements, so that a systematic error is inevitably introduced. In fact, the non-removal of binary orbital motion from σ_{los}, which represents the individual stars' velocity dispersion, would result in a significant over-estimation of the dynamical mass. According to Kouwenhoven and de Grijs (2009) [48], the contribution of binaries is especially relevant when $\sigma_{los} \leq 1$ kms^{-1}, i.e., in the case of low-density stellar systems, such as OCs: this is indeed confirmed by the strong observational evidence of their hosting a sizable, primordial binary fraction (Portegies Zwart et al., 2001 [76]). Hence, contrary to mass segregation and energy equipartition, which tend to lower the dynamical mass of OCs (de Grijs et al., 2008 [16]), binary stars play a pivotal role in its inflation.
However, up to now models addressing this issue, despite providing a thorough treatment of the aforementioned phenomena, have not fully accounted for the existence of the Galactic tidal field, which is expected to have non-negligible importance, given the flattening of OCs haloes (Wielen, 1975 [108]), with the purpose of mitigating computational difficulties. Furthermore, the Galactic tidal field can be either static or time dependent, this one being originated by the periodic passage of OCs through the Galactic disk (Bergond, Leon, and Guibert, 2001 [9]): if the former moderately assists cluster dissolution, the latter, instead, notably speeds the process up owing to the repeated disk shocks.

In order to assess to which extent binary stars inflate the dynamical mass of OCs surrounded by the Galactic tidal field taken only in its static component, so that the effects of disk shocking can be ignored, an upgraded version of the work by Rastello, Carraro, and Capuzzo-Dolcetta (2020) [81] may arouse interest. The impact of a model binary population on the velocity dispersion and, therefore, the related dynamical mass of open-cluster-like stellar systems can be evaluated by using the state-of-the-art N-body code *PeTar* by Wang et al. (2020) [107], which can accurately handle an arbitrary fraction of multiple systems while keeping a high performance thanks to hybrid parallelization methods. Yet, most importantly, *PeTar* allows not only to follow in detail the long-term evolution of perturbed binaries by the implementation of sophisticated tools for handling mass loss, mass transfer and close encounters, but also to select an external tidal field from Galpy, a Python library for Galactic dynamics (Bovy, 2015 [12]). As a note, both the generation of initial conditions and the simulations' output data analysis are intended to be performed by means of a Python program expressly developed to be compatible with *PeTar*, which constitutes a novelty with respect to previous N-body codes.
Rastello, Carraro, and Capuzzo-Dolcetta (2020) [81] realized three open-cluster-like models (A, B, C) with the same physical features, except for the primordial binary fraction. The star density distribution is that of a Plummer sphere (Plummer, 1911 [74]) of scale radius $R = 1$ pc and total mass $M = 630$ $M_\odot$, and stellar masses are sampled from a Kroupa IMF (Kroupa, 2001 [52]) in the interval [0.1,100] $M_\odot$, such to yield the average stellar mass $\langle m \rangle = 0.63$ $M_\odot$. All clusters initially contain $N = 1000$ stars, a fraction $f_b = N_b/N$ of which is assumed to be in binary pairs; thereby, N_b is the number of binaries and $N_s = N - 2N_b$ that of single stars. In the specific, $f_b = 0.05, 0.15, 0.30$ for model A, B and C, respectively. Binary stars are coupled using the mass ratio distribution $f(q) \propto (m_1/m_2)^{-0.4}$, where m_1 represents the primary and m_2 the secondary component (Kouwenhoven et al., 2008 [50]), and the relative orbital parameters, i.e., the semi-major axis and the eccentricity, extracted accordingly from a logarithmic distribution $f(a) = 1/a$ (Kroupa, 1995 [53]) and a thermal distribution $f(e) = 2e$ in the range [0,1] (Jeans, 1919 [44]). Lastly, the metallicity is chosen to be solar ($Z_\odot = 0.2$), and stellar evolution is included in the calculations.
The so configured model clusters are virialized, located in the solar position and simulated up to ~ 1.5 Gyr: now, the addition of the MW potential, consisting of a power-law, exponentially cut-off spherical potential for the bulge, a Miyamoto-Nagai potential for the disk and a NFW potential for the halo (Bovy, 2015 [12]), is expected to alter their lifetime duration by accelerating their disruption. To avoid such a catastrophic outcome, the mock systems must be either made more compact and densely populated, or displaced far away

from the Galactic disk: wherefore, considering an old OC like M67, as reproduced by Hurley, Aarseth, and Shara (2007) [39], might offer a solution to the problem, without the need of moving the cluster barycenter.
Irrespective of the application of an external potential, the M67-like-cluster should present specific evolutionary features, such as a sharp drop of its total mass and binary fraction during the first 50 Myr due to both residual gas expulsion and the explosion of massive stars as SNe Ib,c or II, which rapidly reach their final life stages. The two processes combined together should trigger a sudden, global expansion causing a rise of the system kinetic energy and, in turn, of its velocity dispersion. Even so, this momentary departure from virial equilibrium should be effortlessly overcome by a natural physical readjustment, owing to the still large bound mass.
After this short time frame, the effects of dynamics should prevail over stellar evolution, with the progressive appearance of evaporation and mass segregation. In particular, the mass loss rate is expected to slow down and, given the preferential escape of low-mass stars and the hardening of close binaries already sunk toward the cluster core, the overall binary fraction to remain almost constant at a slightly lower value than the primordial one. Clearly, embedding the system in the Galactic field should bolster evaporation through the further stripping of stars outside the tidal radius, but the subsequent enhancement of the mass loss rate should not suffice for cluster dissolution.
On the other hand, the role of binaries in inflating the system dynamical mass is supposed to be important both in the absence and in the presence of the external potential due to the nearly total conservation of the binary fraction: thus, when passing from the particle-dominated to the binary-dominated case (Kouwenhoven and de Grijs, 2008 [49]), the boost of the measured velocity dispersion should become more evident at increasing binary fraction, no matter of the higher density of the M67 model compared to younger OCs like those examined by Rastello, Carraro, and Capuzzo-Dolcetta (2020) [81].

Chapter IV

Dwarf galaxies, relics of the early universe

4.1 Cosmological scenario

The ΛCDM model, also known as the Standard Model, is the current prevailing cosmological paradigm to explain the formation and evolution of the universe. According to this scenario, the universe is dominated at 70% by dark energy and at 25% by cold dark matter (CDM), with the adjective "cold" referring to the typical velocity of dark matter (DM) particles, which would have been non-relativistic when they decoupled from baryons in its early phases: this feature is most important, since it implies that structure formation is not suppressed on any relevant galactic scale. Also, the slower a particle, the higher its mass, so that to the estimated thermal velocity of CDM particles $v_{th}^{z=0}$, where $z = 0$ indicates the actual value of the cosmological redshift, corresponds the mass $m \sim 10^2$ GeV. Baryons, instead, contribute to the remaining 5% of the universe composition.
Finally, besides CDM, the Standard Model assumes the cosmological constant Λ, which accounts for the accelerated expansion rate of the universe without affecting the dynamics of the individual galaxies.
Uncovering the nature of DM is one of the most challenging open questions in astrophysics, for it could bring fundamental insights on the evolution of the universe as a whole: in this sense, dwarf galaxies are believed to contain the key answer. As suggested by Bullock and Boylan-Kolchin (Bullock and Boylan-Kolchin) [14], dwarf galaxies are identified as objects having stellar mass $M_{star} \leq 10^9$ $M_\odot$ and can be divided into three

main categories: bright dwarfs ($M_{star} \approx 10^{7-9}$ $M_\odot$), classical dwarfs ($M_{star} \approx 10^{5-7}$ $M_\odot$) and ultra-faint dwarfs (UFDs, $M_{star} \approx 10^{5-2}$ $M_\odot$). Yet, dwarf galaxies are more commonly classified as dwarf spheroidals (dSphs) compared to dwarf irregulars (dIrrs) due to their lack of gas, ongoing SF and satellite character of larger systems. But, before addressing the properties of dwarf galaxies in detail, it is of major importance to retrieve their origin inside the ΛCDM context, where the cosmic structure is seeded by primordial adiabatic fluctuations and grows by gravitational instability in an expanding background. Soon after overdense regions of the universe become non-linear, they stop expanding and collapse, converting potential energy into kinetic energy in the process: the result are gravitationally bound concentrations of DM called virialized halos, with masses

$$M_{vir} = \frac{4\pi}{3} r_{vir}^3 \Delta \rho m \ , \tag{4.1}$$

where R_{vir} is the virial radius and $\Delta \sim 300$ the overdensity parameter; from M_{vir}, the virial velocity is derived:

$$v_{vir} = \sqrt{\frac{GM_{vir}}{R_{vir}}} \ . \tag{4.2}$$

To first approximation, DM halo density profile is generally described by the Navarro Frank and White (NFW) functional form, nearly universal over all masses and characterized by a steep fall-off at large radii shifting to a mildly divergent cusp towards the center:

$$\rho(r) = \frac{4\rho_{-2}}{\left(\frac{r}{r_{-2}}\right)\left(1 + \frac{r}{r_{-2}}\right)} \ , \tag{4.3}$$

where r_{-2} represents the radius where the log-slope of the profile is -2, i.e., the transition value from the inner $1/r$ cusp to the outer $1/r^3$ curve, and $\rho_{-2} = \rho(r_{-2})$. Although only two parameters, namely r_{-2} and ρ_{-2}, are required to determine a NFW halo, for a fixed halo mass M_{vir}, r_{-2} is often expressed in terms of the concentration parameter

$$c = \frac{R_{vir}}{r_{-2}} \ , \tag{4.4}$$

so that the combination $M_{vir} - c$ completely specifies the profile. Given the steady density increase at small radii, it follows that, under the aforementioned condition, early-forming halos tend to be denser than later-forming ones.
Since the ΛCDM model states that low-mass halos collapse first in a hierarchical clustering fashion, their centers are expected to survive the assembling process and to become filled with substructures.
However, contrary to pure DM simulations, which have provided confirmation of this hypothesis, hydrodynamical simulations have shown that baryonic feedback can alter model predictions to various degrees.
The properties of DM halos control when dwarf galaxies form, their gas content and their resilience to heating by stellar feedback and reionization. The correspondence between galaxy stellar masses and DM halos is named stellar mass-halo mass (SMHM) relation (Simon, 2019 [89]), and consists in a power-law $M_{star} \propto M_{halo}^{\alpha}$ for M_{star} above the UFD regime, while its behavior is still a matter of debate for lower values of M_{star}.
Most galactic halos born before reionization had $M_{halo} < 1.2 \times 10^8$ $M_\odot$, and those able to survive the modern epoch and form stars would constitute a subpopulation of dwarf satellites orbiting larger halos. N-body simulations of CDM forecast a number of DM halos around the MW much greater than the number of observed luminous satellites, which points out that feedback processes must have been very efficient in suppressing SF in the first, small halos, hence remained mostly dark. In the pre-reionization era, the formation of the first dwarf galaxies is regulated by feedback effects acting on cosmological scales and having a non-negligible influence on both the number and the luminosity of these objects. Another obstacle to SF in the high-redshift universe is the lack of coolants such as carbon (C) and oxygen (O), essential for a gas of primordial composition (i.e., made of hydrogen) to cool down and initiate SF at $T \sim 10^4$ K, unless a sufficient amount of molecular hydrogen (H_2) is produced. In DM halos with mass $M_{halo} < 1.2 \times 10^8$ $M_\odot$, whose gas has circular velocity $v_c < 20$ kms^{-1}, though, H_2 is almost completely destroyed by the far-ultra-violet (FUV) radiation, otherwise called negative feedback, emitted by the first few Population III stars and such to prevent SF to start.
On the other hand, DM halos with mass $M_{halo} \geq 1.2 \times 10^8$ $M_\odot$ may experience a quenching of SF because of the action of ionizing radiation from massive stars, which can blow out most of the primordial gas even before the onset of SN-driven winds and reduce SF rates through the reionization of neutral atomic hydrogen (HI): this determines a temperature enhancement to $T \sim 2 \times 10^4$ K, with a subsequent clamping of gas condensation. As a result, Bovill and Ricotti (2009) [11], by setting the critical value of the circular velocity to $v_c^{crit} = 20$ kms^{-1}, equivalent to the critical halo mass $M_{halo}^{crit} = 1.2 \times 10^8$ $M_\odot$, for the

quenching of SF at the reionization epoch ($z = 6$), defined dwarfs galaxies conceived in DM halos with $v_c < v_c^{crit}$ prior to reionization as pre-reionization fossils, and with $v_c > v_c^{crit}$ prior and following reionization as non-fossils. Along the same line, Ricotti and Gnedin (2005) [83] reviewed this distinction in terms of star formation history (SFH) by claiming its diversity to be a relic feature of reionization: dwarfs whose SFH was sharply truncated in earlier epochs are true fossils, whereas those that continued to form stars are either polluted fossils or survivors.
Nonetheless, it must be noted that fossil galaxies might undergo a late phase of gas accretion and related SF well after reionization (i.e., at $z = 1 - 2$), hence not being real fossils anymore: for this reason, the definition of "fossil galaxy" should be carefully used. In this regard, Benıtez-Llambay et al. (2015) [8] argued that protracted SF and enrichment are not inconsistent with reionization, actually. In fact, reionization is likely to evaporate mainly low-density gas from dwarf galaxies' halos, but to have little effect on the gas that has already cooled to higher densities as immune to UV radiation, so that SF would proceed until either the gas is totally depleted, or the newborn stars have expelled it via feedback: as a consequence, reionization would cause a slow tapering, rather than an abrupt cessation, of the SF activity in dwarf galaxies.
The imprint of reionization on galaxy formation can be located not only in the number of predicted halos massive enough to harbor luminous galaxies exceeding by orders of magnitude that of observed dwarfs, but also in the type of hosted stars. Halos above the critical threshold, whose SFH is interrupted due to the loss of baryons induced by the combined effect of cosmic reionization and stellar feedback, end up to be emptied of gas once having successfully formed dwarf galaxies characterized by a single population of old stars; conversely, halos below the critical threshold suffer more from the impact of reionization, as they are subject either to a SF delay, which leads to systems with prominent young stellar components, or to its truncation, which results in systems doomed to stay dark.
Also Mashchenko, Wadsley, and Couchman (2008) [59] proposed energy feedback from SN explosions and stellar winds as a major mechanism shaping the evolution of dwarf galaxies, and included these phenomena, together with SF, in cosmological simulations run between $z = 150$ and $z = 5$ with the parallel tree code Gasoline, which portrays dark and stellar matter as a collection of particles and employs the smooth particle hydrodynamics formalism for the gas treatment. They found that the DM distribution develops the classic filamentary structure on large scales and that the most massive galaxies, originated around $z = 10$, are able to keep their SF activity during reionization, in spite of this one being responsible for the quick dispersion of many star clusters where

SF took place. Only past $z = 6$, when the galactic stellar mass reaches the value of $\sim 10^7$ $M_\odot$, surviving star clusters start to be seen: interestingly, these long-lived clusters have broadly the same size (~ 10 pc), mass ($\sim 10^5$ $M_\odot$) and heavy element abundance ($\sim 3\%$ of the solar one) as GCs detected in the local universe. Therefore, this agreement with observations suggests that Local Group dwarf galaxies with mass below 10^7 $M_\odot$ could not produce GCs, while more massive ones did.
Another validation of this theory comes from Simon (2019) [89], who focused his attention on UFDs due to their reputation of being the most DM-dominated systems known and of residing in the smallest DM halos yet found. In fact, he estimated that the vast majority of UFD stars had originated by the end of reionization, consistently with the idea of its associated gas heating to have contributed to the quenching of SF. So, since they underwent little to no further evolution after that time and have survived up to now as pristine relics of the early universe, UFDs are deemed to represent not only the extreme limit of the galaxy formation process, but also valuable laboratories to try and constrain the nature of DM. What is more, Simon (2019) [89] highlighted the importance of studying UFD chemical evolution and nucleosynthesis in this context; specifically, at low metallicities ([Fe/H]) UFDs show enhanced α-element ratios ([α/Fe]), while the opposite happens at high metallicities, a behavior resulting from the different chemical yields of SNe. Given that UFD small stellar masses imply that they hosted relatively few SN events, core-collapse SNe should have exploded quickly after the onset of SF, thus producing considerable amounts of α-elements, but been counterbalanced by the subsequent occurrence of type Ia SNe, which tend to release iron-peak elements and hence lower the α-element ratio.
Now, the transition between the two regimes is placed at the metallicity value [Fe/H] $= -2.3$: SF must have continued for more than ~ 100 Myr, in such a way that the most metal-poor (i.e., with [Fe/H] $= -3$) UFD stars were enriched by Pop III SNe, while those having [Fe/H] ≥ -3 by Pop II SNe.
Finally, one of the key properties of UFDs is their luminosity function (LF), since it provides the connection between the low-luminosity galaxy observed today and their progenitor systems at high z, which may have played a significant role in the universe reionization. Boylan-Kolchin et al. (2015) [13] quantified the correspondence between Local Group dwarf galaxies and faint galaxies at high z by using their SFHs to calculate their UV luminosities as a function of time. They found first that reionizing the universe requires a major contribution of UV photons from galaxies at least as faint as Fornax, and then that, if the currently measured faint-end slope of the UV LF (i.e., $\alpha \sim -2$) is extrapolated to the absolute magnitude $M_{UV} = -3$, UFDs would dominate the ionizing

photon production of the universe. This α value overpredicts the observed number of Local Group dwarf galaxies, though: indeed, when considering a shallower faint-end slope (i.e., $\alpha \sim -1.25$), as emerged from the Sloan Digital Sky Survey (SDSS) data, only bright dwarfs appear to contribute to reionization.

4.2 Problems within the ΛCDM model

Reionization and stellar feedback have been proved useful to find solutions of the three main problems within the ΛCDM model, which, in spite of guessing right the large-scale structure of the universe, still presents a few critical issues on smaller scales. These problems are known with the names of "core-cusp", "missing satellites" and "too-big-to-fail".

4.2.1 The core-cusp problem

The core-cusp problem can be labeled as the tendency of the central regions of DM-dominated galaxies to be less dense and cuspy than expected for standard ΛCDM halos: in fact, despite the DM density profile should diverge at small radii, observations of low-mass dwarf galaxies, such as UFDs, indicate near-constant density cores (Mashchenko, Wadsley, and Couchman, 2008 [13]).
Massive stars inject large amounts of energy into the surrounding medium via stellar winds and SN explosions: this originates a dramatic, large-scale perturbation of the interstellar gas, which is accelerated close to the sonic speed. Since this phenomenon is more severe in dwarf galaxies owing to their lower gas pressure and their observed irregular gas distribution, stellar feedback has been suggested as a possible explanation for the removal of the predicted central DM cusps and the consequent creation of kpc-size cores in all systems having stellar mass $M_{star} > 10^6$ $M_\odot$ (Madau, Shen, and Governato, 2014 [57]).
Notably, cosmological simulations of dwarf galaxy formation and evolution by Mashchenko, Wadsley, and Couchman (2008) [59] have shown that stellar feedback does not expel gas at high z; instead, SN explosions compress gas into large filaments confined to the galactic central regions and moving with speeds of $\sim 10 - 20$ kms^{-1}, which is exactly the gas motion resulting in the gravitational local DM heating to obtain the cusp flattening. Thus, stellar feedback is expected to play a pivotal role there because the baryon fraction may reach the 50%, and the gas mass dominates that of DM. Interestingly, resonant heating due to feedback-powered bulk gas motion, applied to the most massive dwarf generated

in the simulations, turns the cusp into a flat core with radius r $\simeq$ 400 pc and average density $\bar{\rho} \simeq 0.2$ $M_\odot pc^{-3}$, close to the parameters inferred for the dwarf galaxy Fornax, which presents the same core radius and very similar average density ($\bar{\rho} \simeq 0.1$ $M_\odot pc^{-3}$). Also, the same mechanism leads to a reduction of the dynamical friction efficiency in such regions, hence aiding to push potentially newborn GCs to orbits distant from the galaxy center until stars stop forming, as witnessed in the case of Fornax.
Additionally, Madau, Shen, and Governato (2014) [57] demonstrated that both the offset between the DM mass in the cored and cuspy models ΔM_{DM}, and the DM mass removal efficiency increases at decreasing halo mass, which implies that the smaller the host halo, the more rapid the flattening of the dwarf galaxy density profile. In particular, DM particles stripped from the central cusp are not lost, but end up to be part of the halo, in such a way that the near-constant density core can be constructed.
This phenomenon, called feedback induced core formation, actually depends on the galactic stellar mass and the number of generated stars:

- if enough stars formed, the released SN energy would be sufficient to redistribute DM and create significant cores;
- if too many stars formed, the excess central mass would compensate stellar feedback by dragging DM back in;
- if too few stars formed, there would not be enough SN energy to alter the halo density profile, which would consequently remain cuspy.

Fainter galaxies, such as UFDs, enters this last case. On top of that, according to Bullock and Boylan-Kolchin (2017) [14], feedback induced core formation peaks in efficiency at $M_{star}/M_{vir} \approx 5 \times 10^{-2}$, in the regime of the brightest dwarfs, while it becomes ineffective when $M_{star}/M_{vir} \leq 10^{-4}$, which corresponds to the regime of classical dwarfs and UFDs. Since these values are obtained by assuming the current virial mass $M_{vir}(z = 0) \simeq 10^{10}$ $M_\odot$, meaning that the peak core formation ratio involves a stellar mass $M_{star,peak} \simeq 10^8$ $M_\odot$.

4.2.2 The missing satellites problem

The missing satellites problem consists in a discrepancy between the number of observed galaxies and the number of predicted subhalos. In this respect, Simon and Geha (2007) [90] pointed out that, as foreseen by the ΛCDM model, large DM halos should be surrounded by a number of smaller halos able to support molecular cooling and initiate SF following

the mass function (MF)

$$\frac{dN}{dM_{star}} \propto M_{star}^{-1.9} \ , \tag{4.5}$$

contrary to observations, which revealed a number of MW satellites about an order of magnitude lower compared to theoretical expectations, in agreement with a flatter MF

$$\frac{dN}{dM_{star}} \propto M_{star}^{-1.5} \ . \tag{4.6}$$

Now, whilst one may argue that the solution to this problem lays with the observational search for dwarf galaxies, the most natural explanation is found in galaxy formation physics: by positing that galaxy formation becomes increasingly inefficient as the halo mass declines, the tiniest DM halos would have simply failed to form stars altogether. Thereby, if the known MW satellites are assigned to the largest DM halos and the missing ones to such subhalos, there would no longer be a number mismatch.

4.2.3 The too-big-to-fail problem

From the solution of the missing satellites problem comes the prediction that the inferred central masses of the MW satellites should be consistent with those of the largest subhalos in ΛCDM simulations. And yet, these very simulations suggest that such halos are actually too centrally concentrated to form galaxies, when they should be too big to fail at this, given that even lower-mass halos can host luminous stars.
Based on this evidence, Bullock and Boylan-Kolchin (2017) [14] argued that the too-big-to-fail problem might be partially solved by accounting for the action of stellar feedback in the generation of baryon-induced DM cores. Considering that the typical mass range of the problem is $M_{star,crit} \simeq 10^6$ $M_\odot$, associated to the critical ratio $M_{star}/M_{vir} \leq 10^{-4}$ at which stellar feedback becomes negligible, the existence of DM cores if $M_{star} > M_{star,crit}$ would explain why part of bright dwarfs are characterized by low observed densities, but not the fact that others not satisfying this condition have low densities too.
To reconcile ΛCDM hypotheses with the internal structure of low mass halos, tidal effects such as shocks and stripping have been hold to constitute an additional form of feedback able to reduce MW satellites' central densities due to their being embedded in the Galaxy potential. Still, the lack of a systematical difference between possibly interacting dwarf

and field galaxies has led to conclude that such mechanisms would not be crucial in modifying the DM density distribution.

4.3 Dynamical mass inflation in dwarf galaxies

Associating DM halos to galaxies is a difficult task because their mass do not scale linearly with galaxy mass: for this reason, a common approach consists in measuring this quantity directly and inferring the DM halo properties through stellar kinematics. Since bright dwarfs typically possess gas disks with ordered kinematics, rotation curves, which report the velocities of stars orbiting about the Galactic center as a function of the distance from this point, can be extracted even up the flat part of the profile. On the contrary, such a procedure is not feasible for both dSphs and UFDs as they appear as dispersion-supported, rather than rotationally-supported systems: thus, their masses must be probed via velocity dispersion measurements obtained either from integral field spectroscopy (dSph case) or star-by-star (UFD case). In fact, being almost completely deprived of gas from reionization and extremely faint, UFDs do not allow the use of integral field spectroscopy along the line-of-sight (los), so that any attempt to measure their observed velocity dispersion must involve individual stars.
The dwarf galaxy mass derived through the formula

$$M_{dyn} = \eta \frac{R_{hm}\sigma_{obs}^2}{G} \tag{4.7}$$

by using the observed velocity dispersion σ_{obs} is hence called dynamical mass and always estimated within a specific radial extent, i.e., the projected half-mass radius R_{hm}, under a number of specific assumptions: virial equilibrium, absence of unresolved binaries and utter stellar membership.
According to Simon (2019) [89], the virial equilibrium condition is quite delicate when it comes to dwarf galaxies, given that may have experienced recent disk shocks, which can modify the presently observed velocity dispersion; however, even if proper motion measurements show that many such systems are close to their orbital pericenters, the impact of pericentric passages is lessened by their typical occurrence at a distance of $\simeq 40$ kpc away from the Galactic disk. Also, tidally disturbed galaxies have been proven not to have a meaningfully altered observed velocity dispersion, thus implying that a temporary departure from virial equilibrium would not dramatically affect the estimate of the dynamical mass. More concerning is, instead, the hypothesis of all binaries to be

resolved in order for them not to inflate the observed velocity dispersion above its intrinsic value, since their fraction is expected to be high in low-metallicity environments such as UFDs. Notably, here the influence of binaries might be magnified by the limited available stellar sample, for which only single-epoch velocity measurements are most often possible. Finally, ruling out the contamination by foreground MW stars is critical too, because their velocities are very close to the systemic velocity of dwarf galaxies. A common approach to deal with this issue is based on the use of membership probabilities for each sampled star, which ordinarily works in the case of dSphs, where large memberships may be achieved, but not always in that of UFDs.
The interest in Local Group dwarf galaxies has been growing over the last decades due to their huge mass-to-light ratios, as obtained by analyzing their stellar kinematics (Amorisco and Evans, 2011 [2]).
Several studies conducted on dSphs in the MW halo (i.e., Fornax, Sculptor, Ursa Minor I, Draco, Leo I, Leo II, Sagittarius, Sextans and LGS 3) pointed out that the observed velocity dispersion is significantly inflated with respect to the intrinsic value, which would be of the order of $1-3$ kms^{-1}, if GCs' kinematic properties were scaled by the structural parameters of dSphs (Mateo, 1997 [61]). Additional research on eight dwarfs, including both dSphs and UFDs (i.e., Canes Venatici I and II, Ursa Minor I and II, Leo IV and T, Hercules, and Coma Berenices), corroborates this result through the detection of values between $3.3-7.6$ kms^{-1}for σ_{obs} (Simon and Geha, 2007 [90]), thus challenging the claim about the existence of systems having $\sigma_{obs} < 7$ kms^{-1}(Wyse and Gilmore, 2008 [111]). In fact, Simon and Geha (2007) [90] discovered an interesting correlation between the absolute magnitude in the V band and the velocity dispersion of their sampled galaxies: if $M_V \leq -6$, $\sigma_{obs} \simeq 7-8$ kms^{-1}, whereas if $M_V > -6$, $\sigma_{obs} \simeq 4-5$ kms^{-1}, meaning that more luminous objects, such as dSphs, have larger velocity dispersion compared to fainter ones, such as UFDs. Also McConnachie and Côté (2010) [63] found that the expected velocity dispersion of MW satellites with $M_V \geq -7$ should be $\simeq 0.2$ kms^{-1}, but values ≥ 3 kms^{-1}are actually measured.
Also, the application of the M_{dyn} relation to UFDs shows that $M_{dyn} \geq 10^5$ M$_\odot$ within R_{hm}, but that the luminosities are a factor of ~ 100 smaller: given the expected value of the mass ratio in the V band $(M/L)_V \simeq 2$ M$_{\odot,V}$/L$_{\odot,V}$, Simon (2019) [89] concluded that nearly all UFDs have masses dominated by something other than stars (Fig. 5.9).

Different scenarios to account for the notably large velocity dispersion of dwarf galaxies and, consequently, for the inflation of their dynamical mass have been proposed: the most

accredited one asserts the presence of a considerable amount of DM in such systems, while others suggest that they are either out of virial equilibrium because actually ongoing tidal disruption, or affected by the presence of a non-negligible number of unresolved binaries.

4.3.1 The dark matter and tidal stripping hypotheses

The high velocity dispersions detected among MW satellites have been frequently interpreted in terms of them being embedded in massive DM halos: to this end, theoretical models trying to link present-day dwarf galaxies to their alleged parental DM halo and to determine their mass in the absence of detailed photometric and kinematic data have been developed. For instance, Amorisco and Evans (2011) [2], instead of using Jeans equations to infer the observed velocity dispersion of dSphs once a parametric light profile (e.g., a King or a Plummer profile) for the stellar component and a NFW density law for the DM halo are assumed, proposed a phase space modeling approach to better describe the flat trend of σ_{obs}, which hints that the dSphs' inner parts may be nearly isothermal. Such a condition, due to tidal stirring rather than physical collisions, can be represented by means of lowered isothermal distribution functions nestled in DM halos; since they cause the stellar component to relax in the DM gravity field, a dependence of the half-light radius R_{hl} on the line-of-sight central velocity dispersion σ_0 can be predicted: provided that the DM halo potential is a power-law function of the radius, the relationship between R_{hl} and σ_0 takes the form $R_{hl} \propto \sigma_0^{\beta}$, with $\beta = 1, 2$ for a cored or a NFW halo, respectively. However this theoretical correlation is suitable only for central regions, as it dramatically steepens at larger half-light radii.
Moreover, the authors showed that different DM halo profiles, whether cored or cusped, lead to very similar mass estimates within one particular radius, i.e., $\approx 1.7\ R_{hl}$. The enclosed mass, given by the formula

$$M(< 1.7\ R_{hl}) = 5.8 \frac{\sigma_0 R_{hl}}{G}\ , \tag{4.8}$$

has been calculated for a sample of MW satellites characterized by a flat velocity dispersion profile, finding that the two most massive ones are also the most luminous, namely Sagittarius ($M(< 1.7\ R_{hl}) \sim 2.8 \times 10^8\ \mathrm{M}_\odot$) and Fornax ($M(< 1.7\ R_{hl}) \sim 1.3 \times 10^8\ \mathrm{M}_\odot$), while the least massive ones are Willman I ($M(< 1.7\ R_{hl}) \sim 4 \times 10^5\ \mathrm{M}_\odot$) and Segue 1 ($M(< 1.7\ R_{hl}) \sim 6 \times 10^5\ \mathrm{M}_\odot$).

Albeit several constraints in favor of DM coming from observations (Draco, UMi, Carina, Segue 1 and 2, and wide binaries), the possibility of Galactic tides to determine the progressive dissolution of dwarf satellites has been put forward.
An ideal target for indirect DM detection experiments, owing to its proximity and high mass-to-light ratio, is surely Segue 1. Discovered by Belokurov et al. (2007) [6] as an overdensity of resolved stars in imaging data from the SDSS, with absolute magnitude and half-light radius intermediate between dSphs and GCs, i.e., $M_V \approx -3$ and $R_{hl} \approx 30$ pc, Segue 1 was formerly identified as an extended GC associated with the Sagittarius stream. Such an interpretation of Segue 1 was afterwards contested by Geha et al. (2009) [26], who noted that this object was unusually faint for its size. Therefore, they measured the radial velocities of 24 stars in Segue 1 through Keck/DEIMOS spectroscopy, and derived a velocity dispersion of ~ 4.3 kms^{-1}: this led to claim that Segue 1 was an UFD rather than a GC. By allowing these stars to be gravitationally bound to Segue 1 and in dynamical equilibrium, the implied mass-to-light ratio resulted $M/L \sim 1200$, which would make Segue 1 the most DM-dominated galaxy ever detected. Yet, both assumptions might be questionable: in fact, if Segue 1 was a GC undergoing tidal disruption as stated by Belokurov et al. (2007) [6], then unbound stars would not be so easy to distinguish from actual members, and the hypothesis of dynamical equilibrium would be naturally refuted; more seriously, if Segue 1 was really immersed in the Sagittarius stream, then contamination by stream stars would be hard to avoid, thus inducing the artificial inflation of the observed velocity dispersion and casting doubt on the existence of a predominant DM content in the galaxy. The analysis performed by Geha et al. (2009) [26] seems not to support this scenario for a number of reasons, though: first the missing evidence of both kinematic outliers in the observed stellar sample and tidal tails, and second the central concentration of the luminosity profile.
A similar case is represented by Segue 2, classified as a likely DM-dominated UFD by Belokurov et al. (2009) [7] because of its observed velocity dispersion inflated value, $\sigma_{obs} \simeq 3.4$ kms^{-1}, compared to the expected one, $\sigma_{int} \simeq 0.5$ kms^{-1}. The successive detection of a group of stars sharing the same radial velocities as Segue 2 members, but presenting higher metallicities, was regarded as the signature of a larger galaxy being tidally disrupted: hereby, according to Belokurov et al. (2009) [7], Segue 2, together with the above-mentioned, anomalous stellar stream, would constitute its remnant. To test this theory, Kirby et al. (2013) [47] enlarged the initial spectroscopic sample, consisting of only 5 RGB stars, to 26 such objects, and used their radial velocities to recompute the observed velocity dispersion of the galaxy; by means of the Monte Carlo Markov Chain (MCMC) method, they estimated an upper limit of $\sigma_{obs} \leq 2.2$ kms^{-1}at 90% confidence level, well

below the value obtained by Belokurov et al. (2009) [7] through a maximum likelihood procedure based on the assumption that the stellar velocity distribution is approximately Gaussian, a feature expected in the event of virial equilibrium. The inferred limit on the mass within the half-light radius is $M < 1.5 \times 10^5$ $M_\odot$, clearly lower than $M < 5.5 \times 10^5$ $M_\odot$ coming from $\sigma_{obs} \simeq 3.4$ kms^{-1}. In addition to this, Kirby et al. (2013) [47] not only detected a dispersion in [Fe/H] and a decline of [α/Fe] as a function of [Fe/H], chemical properties establishing that Segue 2 probably retained SN ejecta and that SF lasted for several generations of SNe Ia (i.e., at least 100 Myr), but also derived an average metallicity $\langle$[Fe/H]$\rangle = -2.22 \pm 0.13$ (about the same as Ursa Minor, 330 times more luminous than Segue 2), placing the galaxy more metal-rich than the luminosity-metallicity relation defined by the brightest MW satellites.

Taken together, such dynamical and chemical properties hence point to two possible formation scenarios: Segue 2 may either be the barest remnant of a tidally stripped, Ursa Minor-sized galaxy, once hosted by a substantial dark matter halo, or have formed with its present stellar mass and metallicity. Overall, the tidal stripping hypothesis seems more plausible, especially for the fact that MW's tides would have whittled Segue 2 down to the least massive galaxy known.

So, it is hardly surprising that the role of Galactic tides has been investigated in Ursa Minor (UMi), one of the closest MW satellites to present tidal tales, lumpiness and an asymmetric stellar distribution along its major axis. Since the amount of stripped material correlates with the strength of the MW tidal force, Gómez-Flechoso and Martınez-Delgado (2003) [30] remarked that the mass density at the tidal radius, as well as that of tidal tails on its very edge, is proportional to the MW potential: by implication, determining the MW halo potential means being able to evaluate the mass density of both the galaxy at the tidal radius position and of its associated tidal tails, which allows the computation of the mass-to-light ratio. Once having fixed the parameters of the MW potential using the observational data of the Sagittarius dwarf galaxy in order to probe the MW halo and, consequently, the UMi tidal tails mass density, and having accounted for both the luminosity profiles and brightness variations of these ones, the authors concluded that $M/L \sim 12$. This estimate, compatible with the observed value $M/L \sim 16$, differs much from $M/L \sim 60$ expected in the assumption of virial equilibrium, which seems to validate the idea of UMi being a tidally dissolving MW satellite, and thus to explain the measured inflation of its velocity dispersion.

On the other hand, whilst mindful that postulating the ongoing tidal disruption of MW dSphs feels natural given the well-recognized effects of Galactic tides on the Sagittarius dwarf, Wu (2007) [110] brought out some critical points:

- Sagittarius is much closer to the MW center than other dSphs, which makes it more vulnerable to tidal stripping;
- tides should introduce a strong velocity shear, but in dSphs almost no rotation signature is actually detected;
- an universal mechanism to raise the observed velocity dispersion of dSphs by tides appears not to exist.

By combining a parametric model for the MW potential, assumed to be spherical and DM dominated, with non-parametric two-integral models for the stellar distribution function, taken to be axisymmetric, they derived the mass of three target dSphs, i.e., UMi, Draco and Fornax, finding that it was sufficiently high to reject the conjecture of MW tidal forces to affect the observed kinematics in any meaningful way. Thereby, they interpreted the "extra-tidal extensions" in UMi and Draco as an extended, axisymmetric, virialized envelope, rather than as the outcome of a tidal stripping process. Still, a possible limitation of this analysis lies in that calculations have been performed within $r < 3$ kpc, where tidal forces are unlikely to be most effective.

In summary, given that σ_{obs} is a good estimator of the mass of a galaxy only when this is in virial equilibrium, speculations about the tidal disruption of the closest MW satellites, in order to account for their dynamical mass inflation, have been made. However, by enlarging the sample of observed dwarfs, it became apparent that most of them, regardless of their proximity to the MW, exhibited large velocity dispersions without evidence for streaming motions. In addition to this, some simulations predicted that a perigalactic passage would leave behind a velocity gradient larger than the velocity dispersion (Piatek and Pryor, 1995 [73]; Pryor, 1996 [77]), a feature that is not seen in any of the above-mentioned targets. The lack of a general theory to fully expound the action of tides in boosting the observed velocity dispersion of dwarf galaxies, then, favors a scenario in which tidal stripping, even if affecting their past history, cannot be pinpointed as the primary cause of the process. Therefore, the DM hypothesis ultimately prevails.

4.3.2 Unresolved binaries as an alternative to the dark matter hypothesis

Alternatively to the DM hypothesis, a theory involving radial velocity components from binary stars as participating to the enhancement of the dynamical mass of dwarf galaxies has been developed and applied to MW satellites.

Draco and UMi are characterized by high observed velocity dispersions ($\sigma_{obs} \sim 10$ kms^{-1}) and mass-to-light ratios ($(M/L)_V \sim 50 - 90$): the artificial inflation by the orbital motion of undetected binaries has been suggested as a viable explanation for this phenomenon, which has been investigated through Monte Carlo simulations of velocities measured at random times for a stellar sample with given binary fraction and period, eccentricity and mass ratio distributions. The outcomes of this analysis are the following:

- σ_{obs} calculated using the standard deviation is much more affected by unresolved binaries than that obtained from the biweight;
- the large values of σ_{obs} of dSphs with small intrinsic velocity dispersion (i.e., $\sigma_{int} \sim 6$ kms^{-1}) may be partially covered either by high binary fractions or by short-period binaries;
- multi-epoch velocity measurements are desirable to identify and remove binaries with large velocity amplitudes;
- even though the choice of the period, eccentricity and mass ratio distributions are guided by the results pertaining to field binaries, the binary fraction remains a free parameter of non-negligible influence.

On such premises, Pryor, Olszewski, and Armandroff (1995) [78] exploited the reduction of unresolved binaries' effects on velocity dispersion estimates, thanks to precise radial velocity measurements from multi-epoch observations of stars in Draco and UMi, for deriving their binary content. They found a binary fraction f_b ranging from 0.17 to 0.68, and combined these values with a model binary population to simulate the impact of binaries in other dSphs, deducing that, in both cases, it was minimal: this led the authors to assert that binaries were not responsible for the huge mass-to-light ratios of Draco and UMi, based on the available stellar sample.
A Monte Carlo experiment was performed to reproduce also the binary content of Carina (Mateo et al., 1993 [62]); here binaries would significantly affect the observed velocity dispersion only if a rather large binary frequency among giant stars was present, and if they were restricted to a small period range skewed towards short periods. Since the velocity distribution of Carina members argues against the existence of a great amount of high-amplitude binaries, the DM hypothesis was conclusively endorsed, despite the binary contribution in inflating σ_{obs} could not be safely ruled out.
Minor et al. (2010) [67] gave serious consideration to the contamination from binary orbital motion, and outlined a procedure to correct the velocity dispersion of dwarf galaxies to within a few percent accuracy by using a parameter called the threshold fraction,

independent of the underlying binary fraction and distribution of orbital parameters. In particular, contrary to both the mass ratio and the eccentricity distribution, the choice of the period distribution is quite relevant for estimating σ_{obs}: in this respect, the authors adopted a log-normal period distribution $f(P)$ with $\mu_{log(P)} = 2.23$ and $\sigma_{log(P)} = 2.3$, as reported by Duquennoy and Mayor (1990) [18] relative to G-dwarf stars in the solar neighborhood. Such a similarity is motivated by the little modification binary orbital parameters undergo during simulations of the SF process, which always involves the turbulent fragmentation of a rotating gas cloud. That said, the threshold fraction is an observable quantity defined as the fraction F of stars in a sample exhibiting a change in radial velocity greater than a certain threshold Δv after a time Δt between measurements. The response of F at varying binary fraction f_b, time interval Δt and period distribution's parameters has been explored, revealing that:

- changing f_b has approximately the same effect as changing $f(P)$;
- multi-epoch observations of more than 10^3 stars would be required to break this degeneracy and constrain $f(P)$ independently of f_b;
- $\Delta t = 1 - 2$ yr is the optimal time interval to appraise F with a velocity error of the order of 1 kms^{-1}, since the fraction of stars with measurable Δv does not rise significantly when Δt is extended beyond 2 yr;
- σ_{obs} going from 4 to 10 kms^{-1}are unlikely to be inflated by more than 20% due to binary orbital motion in dSphs.

Despite the straightforward formulation, there are two main difficulties in extracting F from actual data sets: first, the non-existence of a common time interval Δt, typically replaced by several time intervals for various subsets of stars, and then the fact that different velocity estimates have their own associated errors.
All in all, the addition of more and better velocity measures from multi-epoch observations has mitigated the skepticism surrounding the large velocity dispersions of dSphs. As such, it is now widely accepted that these galaxies are some of the most DM-dominated objects in the universe. However, the question of unresolved binary contamination is still open ended for UFDs: subsequently, several efforts in this direction have been made.
Aware that the fraction of solar-type close binaries tends to be higher in low-metallicity environments (Badenes et al., 2018 [3]), Minor et al. (2019) [68] modeled the binary population of the UFD Reticulum II (Ret II) in order to evaluate the eventual inflation of its observed velocity dispersion owing to binary orbital motion. To this purpose, they applied a Bayesian method to inspect multi-epoch radial velocities of 26 stars and, assuming a

mean orbital period of ~ 27 yrs in accordance with Badenes et al. (2018) [3], estimated a binary fraction larger than 0.5 at the 90% confidence level albeit the small sample size. The best-fit intrinsic velocity dispersion, i.e., $\sigma_{int} \simeq 2.8$ kms^{-1}, results higher than the expected value $\sigma_{int} \simeq 0.21$ kms^{-1}if no DM were present, determined from the typical mass-to-light ratio $M/L \simeq 2$ M$_\odot$/L$_\odot$ of GCs. So, defining $\sigma_{int} \leq 0.21$ kms^{-1}as the "no DM regime", nearly all of Ret II's dispersion would be due to binaries. And yet, Badenes et al. (2018) [3]'s statistical analysis indicates that this is not the case, notwithstanding the apparently conspicuous binary content: indeed, the preference for a substantial number of short mean period binaries in Ret II, consistent with a similar outcome for the Segue 1 dSph (Martinez et al., 2011 [58]), is attributed to the aforementioned anti-correlation between close binary fraction and metallicity, which may be suitable for UFDs in that metal-poor stellar systems. By implication, Ret II was finally categorized as DM-dominated.
Other studies tried to leverage binary stars to probe the existence of DM, instead of refuting it, but obtained uncertain results.
By way of example, according to Peñarrubia et al. (2016) [72] wide binaries may offer a window onto DM on the smallest scales, and measuring their relative separation may constitute an alternative route to tie up the DM potential. The survival of wide binaries in the DM halo of UFDs has been explored through N-body simulations: in the subsequent mock data processing, the two-point correlation function (2PCF) of stellar pairs in these galaxies was denoted as a useful statistical tool to detect and characterize the semi-major distribution of wide binaries, and hence define the inner slope of the DM halo profile. This type of analysis requires deep photometric data with sub-arcsecond resolution, though, which makes it presently impracticable.
Besides this, some research addressed the relation between wide binaries and DM dynamical friction. If a massive body orbits within a DM halo, it will experience a net frictional drag which opposes to its motion: even if the timescales for dynamical friction in galactic systems are typically of Gyrs and there is no direct observation of orbital decay, this phenomenon has been studied to constrain the density profile of DM halos in dSphs. In particular, Hernandez and Lee (2008) [34] pointed out that dynamical friction will induce the progressive tightening of binary systems embedded in DM halos, leading to their components eventual merger in the absence of other concomitant effects, and estimated that the binary orbital decay should scale linearly with the DM density and the square root of the binary total mass ($\dot{a} \propto \rho_{DM} m_{cm}^{1/2}$). Hence, going to higher DM halo densities, such as those of dSphs, dynamical friction on binary stars might become relevant: in this context, wide binaries are doomed to decay in shorter timescales ($\tau < 10$ Gyr) compared to harder ones. Specifically, the initial binary orbital separation below which $\tau < 10$

Gyr turns out to be $\tilde{a}_0 = 0.067$ pc: since such a time corresponds approximately to the age of dSphs' stars, it follows that binaries born with $a_0 < \tilde{a}_0$ would suffer from the dynamical friction of DM halos because their decay time may grow shorter than their own lifetime. It is worth noting that an appreciable alteration of the initial distribution of binary separations in dSphs is very unlikely, for the collisional mechanism operating in GCs, liable to continuously replenish the wide binary population through the disruption of close binaries, is in this case not available. In fact, although the number of stars in a typical dSph is about 10 times larger than in a GC, the volume occupied by its stellar population is of the order of $(2\ \text{kpc})^3$ instead of $(20\ \text{pc})^3$, which makes collisions completely inefficient. So, if binaries with semi-major axis $a = a_0 < \tilde{a}_0$ were observed in dSphs, the existence of DM halos would be verified via the action of dynamical friction, but if, conversely, plenty of wide binaries were detected, then the DM hypothesis, which predicts their evolution into tighter systems, would be seriously challenged. However, since the presence of such binaries is currently unknown due to the impossibility of direct studies of MW satellites' binary semi-major axis distribution, no conclusion can be drawn.
Yet, above all, one major pitfall of measuring the velocity dispersion in UFDs is the need for multi-epoch observations, which are actually not possible for most of these galaxies, contrary to dSphs. To make matters worse, given the already small intrinsic velocity dispersions, also velocity errors of $\leq 1\ \text{kms}^{-1}$are needed.
So, *in interim*, Spencer et al. (2017) [92] proposed a different approach to provide a range of plausible σ_{int} values for UFDs based on the binary fractions in dSphs, with the aim of predicting how big of an effect binaries could have on UFDs. Taking as a target the Leo II dSph, they first generated a series of radial velocity Monte Carlo simulations characterized by the same velocity uncertainties and temporal observations as the real data, then used Bayesian analysis to compare these ones to simulations, and finally determined which binary fraction could best reproduce the observed velocities in Leo II.
To model the binary population of Leo II, a specific sample of stars was selected: all primary masses have been fixed to the typical RGB value $m_1 = 0.8\ \text{M}_\odot$, and secondary ones are such that $m_2 \leq m_1$ in order for the mass ratio $q = m_2/m_1$ to satisfy the condition $0.1 \leq q \leq 1$. This implies that secondaries must be neither remnants nor giants.
As far as the intrinsic binary orbital parameters P, q and e are concerned, the period distribution takes the log-normal form

$$\frac{dN}{d\log P} \propto \exp\left(-\frac{(\log P - \mu_{logP})^2}{2\sigma^2_{logP}}\right), \tag{4.9}$$

where $\mu_{logP} = 4.8$ and $\sigma_{logP} = 2.3$ for periods measured in days, while q and e have been extracted from two distributions each, in particular q from either a normal or a flat distribution, i.e.,

$$\frac{dN}{dq} \propto \exp\left(-\frac{(q-\mu_q)^2}{2\sigma_q^2}\right) \text{ and } \frac{dN}{dq} \propto const\ , \tag{4.10}$$

with $\mu_q = 0.23$ and $\sigma_q = 0.42$, and e from either a piece-wise distribution having a normal and a thermal component, i.e.,

$$\frac{dN}{de} \propto \begin{cases} \exp\left(-\frac{(e-\mu_e)^2}{2\sigma_e^2}\right) \text{ if } 1.08 < \log P < 3 \\ 2e \text{ if } \log P > 3 \end{cases} \tag{4.11}$$

with $\mu_e = 0.31$ and $\sigma_e = 0.17$, or a flat distribution:

$$\frac{dN}{de} \propto const \text{ if } \log P > 1.08\ . \tag{4.12}$$

Notably, considerations on these parameters yielded a minimum value $a_{min} = 0.21$ AU and a maximum value $a_{max} = 412$ AU for the semi-major axis.
Hence, four parameter combinations were obtained, the lowest binary fraction for Leo II $f_b = 0.30$ deriving from a flat $f(q)$ and flat $f(e)$, and the highest one $f_b = 0.34$ from a normal $f(q)$ and piece-wise $f(e)$.
Although the estimated binary fraction is larger than that assumed in previous kinematic studies of Leo II, the authors excluded a major impact of binaries on the intrinsic velocity dispersion owing to its already high value. Nevertheless, the very same binary fraction may have an effect in systems with smaller intrinsic velocity dispersion: to illustrate the severity of this issue, the observed velocity dispersion of six mock galaxies, having $\sigma_{int} = 0.5, 1, 2, 4, 8, 12$ kms^{-1}and containing 100 stars with single-epoch observations and velocity measurement errors of 1 kms^{-1}each, was computed through another set of Monte Carlo simulations. Following this exploration, dwarfs with $\sigma_{int} = 0.5 - 2$ kms^{-1}may show observed velocity dispersions $1.5 - 4$ times larger than in actuality, given a binary fraction of 0.3. This effect further magnifies due to the extreme faintness of UFDs and to the predominance in these galaxies of subgiants or MS stars, which allow tighter binary orbits

with shorter periods, rather than RGBs. Consequently, Spencer et al. (2017) [92] inferred that if the binary fraction of Leo II was present in UFDs, it would artificially inflate their velocity dispersion and make them appear more DM-rich.
To strengthen this conclusion, Spencer et al. (2018) [93] applied the very same procedure to Draco and UMi, finding a binary fraction $f_b \simeq 0.5$ for the former and $f_b \simeq 0.78$ for the latter if a log-normal period distribution (Eq. 4.9) and a normal mass ratio distribution (Eq. 4.10) are adopted. Interestingly, by testing other functional forms of $f(P)$ and $f(q)$, it turned out that the choice of the mass ratio distribution does not affect the evaluation of the binary fraction to a greater extent, in that it causes a change of $\sim 5 - 10\%$: as a result, more attention should be paid to the period distribution, being it most influential on the determination of f_b.
Secondly, the authors reanalyzed the binary fraction in Leo II ($f_b \simeq 0.36$), Carina ($f_b \simeq 0.2$), Fornax ($f_b \simeq 0.87$), Sculptor ($f_b \simeq 0.58$), and Sextans ($f_b \simeq 0.71$), and deduced that the probability for this quantity to be constant across all seven dwarfs is $< 1\%$, unless the period distribution varies greatly: this indicates that the binary populations in MW dSphs are not identical in regard to their binary fractions, period distributions, or both.
Now, properties of the binary populations in dSphs are intriguing in their own right, but they are also useful to establish how adversely binaries are impacting the velocity dispersions in UFDs: for this reason, the range of possible orbital parameters and binary fractions can be narrowed down by looking at the values occupied by dSphs. Thus, bearing in mind that, according to simulations, binaries are unlikely to boost the observed velocity dispersion of dwarfs with measured $\sigma_{obs} > 4$ kms^{-1}(i.e., dSphs) by more than 30% (Minor et al., 2010 [67]), but have up to a 40% chance of doing so in dwarfs with $\sigma_{int} \leq 4.5$ kms^{-1}(i.e., UFDs; Minor et al., 2010 [67]), the authors figured that providing better constraints over the binary fraction of dSphs may prove helpful to advance the research on UFDs.

As a conclusion, unresolved binary stars, independently of their fraction, are deemed not to play a pivotal role in inflating the observed velocity dispersion of dSphs, which are hereby regarded as DM-dominated systems, but to be important in the case of UFDs, i.e., the low-luminosity counterparts of dSphs. Notwithstanding that the sample of the examined UFDs has been moderately enlarged lately (Massari and Helmi, 2018 [60]), the small number statistics and the lack of appropriate multi-epoch observations remain a major problem in giving a safe estimate of their binary fraction and period distribution. So, unfortunately, only in quite a few instances the available spectroscopic data allow to constrain such quantities. Up to now, most models have been trying to reproduce

the observed velocity dispersion of dSphs by varying both the binary fraction and the binary orbital parameters, and have then compared the results to spectroscopic data in order to assess the significance of the binary contribution to σ_{obs} in UFDs (Spencer et al., 2017 [92]; Spencer et al., 2018 [93]). Still, the assumptions on the orbital parameter distributions, especially related to periods and semi-major axes, are an actual limitation in this context: hence the desire of a theoretical model to make as reliable and general as possible inferences about the binary population of these galaxies, with the ultimate purpose of challenging the DM hypothesis.

Chapter V

A parametric study of dwarf galaxies

In this chapter, a parametric study to explore the effects of the orbital parameters choice at varying binary fraction on the observed velocity dispersion of dSphs and UFDs will be presented. Such an investigation will, therefore, assess the impact of binary stars on the dynamical mass determination in the faintest MW satellites, in order to ascertain its being either complementary or alternative to the hypothesis of these galaxies to be DM-dominated.
Hence, a detailed description of the theoretical modelization, marking the differences with respect to past methods, will be given, followed first by a critical exposure, and then by a thorough discussion of this analysis' results. Finally, conclusions will be extracted and inserted in a more general cosmological context.

5.1 Methodology

5.1.1 Model settings

The parametric model has been built up by assuming as star density distribution that of a Plummer sphere of scale radius R and total mass M, according to the law

$$\rho(r) = \frac{3M}{4\pi R^3}\left[1+\left(\frac{r}{R}\right)^2\right]^{-\frac{5}{2}}, \tag{5.1}$$

and used to reproduce both a dSph galaxy with a scale radius $R = 3$ kpc, a total stellar mass $M = 10^7$ $M_\odot$ (Strigari et al., 2008 [99]) and an age of 13 Gyr, and an UFD of the same age, with a scale radius $R = 50$ pc and a total stellar mass $M = 5 \times 10^4$ $M_\odot$. Positions and velocities of both single stars and binary centers of mass are randomly sampled from this profile according to the algorithm proposed by Aarseth, Henon, and Wielen (1974) [1]. Radial positions are given by

$$r = \frac{R}{\sqrt{X_1^{-\frac{2}{3}} - 1}} \, , \tag{5.2}$$

and the corresponding position vector components are

$$\begin{aligned} x &= \sqrt{r^2 - z^2} \, \cos\left(2\pi X_3\right) \, , \\ y &= \sqrt{r^2 - z^2} \, \sin\left(2\pi X_3\right) \, , \\ z &= \left(1 - 2X_2\right) \, r \, , \end{aligned} \tag{5.3}$$

where X_1, X_2, X_3 are three random numbers in the interval [0,1]. The first N_s radial position vectors have been attributed to single stars ($\mathbf{r}_s$, with components $x_s,\ y_s,\ z_s$), and the remaining N_b ones to binary centers of mass ($\mathbf{r}_b$, with components $x_b,\ y_b, z_b$).
To obtain the components of the velocity vectors an accept-reject procedure has been employed, respecting the cut to the escape velocity at each position $\mathbf{r}$, i.e.,

$$v_{esc} = \sqrt{2U(r)} \, , \tag{5.4}$$

where $U(r)$ is the Plummer's potential at a distance r from the center. The velocity components are

$$\begin{aligned} v_x &= \left(1 - 2X_4\right) \, v \, , \\ v_y &= \sqrt{v^2 - v_x^2} \, \sin\left(2\pi X_5\right) \, , \\ v_z &= \sqrt{v^2 - v_x^2} \, \cos\left(2\pi X_5\right) \, , \end{aligned} \tag{5.5}$$

where X_4, X_5 are two random numbers in the interval [0,1]. Their units are, of course, those picked for the absolute value of the velocity v. Therefore, as in the case of positions,

the first N_s radial velocity vectors have been assigned to single stars ($\mathbf{v}_s$, with components $v_{x,s},\ v_{y,s},\ v_{z,s}$), and the other N_b ones to binary centers of mass ($\mathbf{v}_b$, with components $v_{x,b},\ v_{y,b},\ v_{z,b}$).
By definition, the Plummer model represents a system in virial equilibrium, as indicated by the virial ratio

$$Q = \frac{2T}{|U|} = \frac{2\left(\sum_{i=1}^{N_s} \frac{m_{s,i} v_{s,i}^2}{2} + \sum_{i=1}^{N_b} \frac{m_{b,i} v_{b,i}^2}{2} \right)}{\left| -G \sum_{i,j=0,\ i \neq j}^{N_s+N_b} \frac{m_i m_j}{|\mathbf{r}_i - \mathbf{r}_j|} \right|} = 1 \ . \tag{5.6}$$

The discrete stellar mass population is generated by sampling the Kroupa IMF (Kroupa, 2001 [52]) in the interval [0.1, 50] $M_\odot$, i.e.,

$$f(m) \propto m^{-\alpha}, \text{ with } \begin{cases} \alpha = 1.3, \text{ for } 0.1 \leq m/M_\odot < 0.5, \\ \alpha = 2.3, \text{ for } 0.5 \leq m/M_\odot \leq 50, \end{cases} \tag{5.7}$$

where the normalization constants are such to give a matching of the two power laws passing from a mass interval to the adjacent. The average star mass results $\langle m \rangle = 0.61$ $M_\odot$.
In the total number of stars in the system, N, the binary fraction is defined as $f_b = N_b/N$, where N_b is the number of stellar pairs (i.e., binaries). Consequently, $N = N_s + 2N_b$, where N_s is the number of single stars.
The overall star content has been set through a selection of N_s values from a given sample, and a random pairing of the other $2N_b$ ones, with the most massive member designated as the primary star (m_1) and the lightest as the secondary (m_2). Of course, $m_b = m_1 + m_2$ yields the mass of the binary. As an alternative to this method, a power-law mass ratio distribution $f(q) \propto q^{-0.4}$ (Kouwenhoven and de Grijs, 2008 [49]), where $q = m_2/m_1$, with extremes $q_{min} = 0.1$ and $q_{max} = 1$ (Rastello, Carraro, and Capuzzo-Dolcetta, 2020 [81]), has been adopted to couple binary components in the case of the UFD model.
Upon the assumptions made for the age of the system and its chemical composition ($X = 0.747$, $X = 0.252$, $Z = 0.001$), an evolutionary stage has been attached to each star for characterizing it as main sequence (MS), subgiant, red giant (RGB), asymptotic giant (AGB), horizontal branch (HB), all luminous objects, or as white dwarf (WD), neutron star (NS) or black hole (BH) dark remnant. Note that the baryonic dark stellar component

(WDs+NSs+BHs) comprises a fraction of about 54% of the total stellar mass.

The binary orbital parameters (Tab. 5.1), i.e., the semi-major axis a and the eccentricity e, have been determined in the following way.
The generic value of a has been extracted from a logarithmic semi-major axis distribution $g(a) \propto 1/a$ in the interval $a_{min} \leq a \leq a_{max}$ (Kroupa and Burkert, 2001 [51]), and thus obtained as

$$a = \exp\left(n_a X_a\right) + \ln\left(a_{min}\right) , \tag{5.8}$$

where X_a is random number in the interval [0,1] and

$$n_a = \ln\left(\frac{a_{max}}{a_{min}}\right) \tag{5.9}$$

the normalization factor. In particular, $g(a)$ corresponds (at fixed $m_1 + m_2$) to the period distribution

$$h(P) = \frac{g(a)}{\frac{dP}{da}} , \tag{5.10}$$

which, once a is expressed in terms of P through Kepler's third law, and in full respect of Öpik's law, gives

$$h(P) \propto \frac{1}{P} , \tag{5.11}$$

with $7 \times 10^{-2} \leq P\ (\text{days}) \leq 6 \times 10^{6}$, values in good agreement with Duquennoy and Mayor (1991) [19] and Kroupa and Burkert (2001) [54]. The eccentricity, instead, is taken from a thermal distribution $k(e) = 2e$ (Jeans, 1919 [44]), so that

$$e = \sqrt{n_e X_e + e_{min}^2} , \tag{5.12}$$

where, as above, X_e is a random number in the interval [0,1] and

$$n_e = e_{max}^2 - e_{min}^2 \tag{5.13}$$

the normalization factor.

Finally, both the positions and the velocities of the $2N_b$ binary components have been evaluated in the center of mass reference frame and by opting for a configuration in which the secondaries are at the apocenter of the orbit of the binary system they belong to, whereas the primaries are integral with their associated center of mass.
Thereby, given the apocenter radius and the orbital velocity moduli

$$\begin{aligned} r_{apo} &= a(1+e) \ , \\ v_{orb} &= \sqrt{\frac{Gm_b}{a}} \ , \end{aligned} \tag{5.14}$$

the components of the corresponding vectors have been calculated by means of a linear transformation to map random numbers from the interval [0,1] to the interval [-1,1]. In this way, the position and velocity vectors of primaries result

$$\begin{aligned} \mathbf{r}_1 &= \mathbf{r}_b + \frac{m_2}{m_b} \, \mathbf{r}_{apo} \ , \\ \mathbf{v}_1 &= \mathbf{v}_b + \frac{m_2}{m_b} \, \mathbf{v}_{orb} \ , \end{aligned} \tag{5.15}$$

whereas those of secondaries are

$$\begin{aligned} \mathbf{r}_2 &= \mathbf{r}_b - \frac{m_1}{m_b} \, \mathbf{r}_{apo} \ , \\ \mathbf{v}_2 &= \mathbf{v}_b - \frac{m_1}{m_b} \, \mathbf{v}_{orb} \ . \end{aligned} \tag{5.16}$$

As a closing note, the structural parameters R and M allowed the computation of the half-mass relaxation time

$$t_{rh} = \frac{\gamma N}{\ln \Lambda} \sqrt{\frac{R_{hm}^3}{GM}} \simeq \frac{\gamma N}{\ln(\lambda N)} \sqrt{\frac{(1.3\ R)^3}{GM}}\ , \tag{5.17}$$

with $\gamma = 0.138$, $\lambda \approx 0.11$, G gravitational constant, N total number of stars and $R_{hm} = 1.3\ R$ half-mass radius of the system.

Object	R (pc)	M ($M_\odot$)	t_{rh} (Gyr)	Age (Gyr)	L_{bol} ($L_\odot$)	L_V ($L_{V,\odot}$)	L_B ($L_{B,\odot}$)
dSph	3×10^3	10^7	1.79×10^5	13	1.35×10^8	1.38×10^7	1.67×10^7
UFD	50	5×10^4	43.07	13	6.72×10^5	6.88×10^4	8.37×10^4

Table 5.1: Structural parameters of the simulated galaxies.

Binary orbital parameters have been varied in order to test how much binary orbital motion affects the observed velocity dispersion: unsurprisingly, the semi-major axis distribution turns out to be the most relevant within this framework, since the shrinking of the distance between binary components has a major effect on the estimate of the velocity dispersion. Hence, first the upper boundary a_{max} has been selected in the range of values [50, 100, 200, 300, 400] AU while keeping fixed the lower one, a_{min}, at 0.2 AU, to do then the opposite, i.e., choosing the lower boundary in the interval [0.01, 0.02, 0.03, 0.05, 0.08, 0.1, 0.2, 0.4, 0.6, 1] AU and settling the upper one to 100 AU. Such a procedure has been repeated for different binary fractions, going from 0.05 to 0.4 in steps of 0.05, and a hundred simulations have been run for each one after the arrangement of the semi-major axis distribution's extremes; in the end, data from each set have been averaged in view of a more robust statistical significance of the output.

f_b	a_{min} (AU)	a_{max} (AU)	e
0.05–0.4	0.01–1	50–400	0–1

Table 5.2: Ranges of variation of parameters characterizing the binary populations.

5.1.2 Velocity dispersion

Following a scheme similar to that outlined in Rastello, Carraro, and Capuzzo-Dolcetta (2020) [81], various possible ways to evaluate the system velocity dispersion have been examined:

- by considering all the stars as if they were single, so that each binary component counts as one star:

$$\sigma_{tot} = \sqrt{\frac{\sum_{i=1}^{N} (\mathbf{v}_i - \langle v \rangle)^2}{N}} \,, \tag{5.18}$$

  where

$$\langle v \rangle = \frac{\sum_{i=1}^{N} \mathbf{v}_i}{N} \,; \tag{5.19}$$

- by distinguishing the contribution of single stars from that of binaries, which are represented by their own center of mass:

$$\sigma_{sb} = \sqrt{\frac{\sum_{i=1}^{N_s+N_b} (\mathbf{v}_i - \langle v \rangle)^2}{N_s + N_b}} \,, \tag{5.20}$$

  with

$$\langle v \rangle = \frac{\sum_{i=1}^{N_s+N_b} \mathbf{v}_i}{N_s + N_b} \,; \tag{5.21}$$

- by neglecting the presence of binary stars, thus accounting for the contribution of single stars only:

$$\sigma_s = \sqrt{\frac{\sum_{i=1}^{N_s} (\mathbf{v}_i - \langle v \rangle)^2}{N_s}} \,; \tag{5.22}$$

- By weighting the velocity of both single and binary components by their luminosity, according to the evolutionary type. Therefore, this way of estimating the velocity

dispersion differs from the first one only in the average of stellar velocities

$$\langle v \rangle = \frac{\sum_{i=1}^{N} L_i \mathbf{v}_i}{\sum_{i=1}^{N} L_i} , \tag{5.23}$$

so that

$$\sigma_{tot,lum} = \sqrt{\frac{\sum_{i=1}^{N} L_i (\mathbf{v}_i - \langle v \rangle)^2}{\sum_{i=1}^{N} L_i}} . \tag{5.24}$$

Specifically, the luminosity of both MS and RGB stars has been determined by fitting an isochrone of 13 Gyr from the Padua stellar and evolutionary tracks and isochrones database (Girardi et al., 2002 [29]);

- by weighting the velocity of single stars, only, by their luminosity according to the evolutionary type, i.e.,

$$\langle v \rangle = \frac{\sum_{i=1}^{N_s} L_i \mathbf{v}_i}{\sum_{i=1}^{N_s} L_i} , \tag{5.25}$$

which implies that

$$\sigma_{s,lum} = \sqrt{\frac{\sum_{i=1}^{N_s} L_i (\mathbf{v}_i - \langle v \rangle)^2}{\sum_{i=1}^{N_s} L_i}} . \tag{5.26}$$

In sum, the observed velocity dispersion has been computed by considering binaries as unresolved (Eq. 5.18, Eq. 5.24), while $\sigma_{s,b}$ (Eq. 5.20), σ_s (Eq. 5.22), and $\sigma_{s,lum}$ (Eq. 5.26) are not affected by binary orbital motion: as such, they do not depend on the variation of the binary semi-major axis and eccentricity, nor on the binary fraction. For this reason, $\sigma_s \equiv \sigma_0$ is let as identification of the intrinsic velocity dispersion, i.e., the velocity dispersion deriving from the structural parameters of the galaxy, defined in the assumption of global

virial equilibrium by the equation

$$\sigma_{int} = \sqrt{\frac{|U|}{M}} \,. \tag{5.27}$$

From this point forward, σ_{int} will be referred to as σ_0.

Notably, the model for the binary population corresponding to a random pairing of components' masses, a logarithmic semi-major axis distribution in the interval [0.2, 100] AU and a thermal eccentricity distribution has been chosen as a reference to compare the results of the parametric study, and σ_{tot} (Eq. 5.18) as the observed velocity dispersion to determine the virial mass of the mock galaxies.

5.1.3 Roche lobe overflow and luminosity cut-off

Besides the standard modelization, another set of simulations has been run for both galaxies to account for the possible occurrence of the RLOF phenomenon between close binary components.
As introduced in Chap. I, RLOF is a mass transfer process taking place when one of the stars in a binary (normally the primary, due to its higher mass and shorter nuclear timescale) fills its Roche lobe, for it encounters a "hole" in its equipotential surface near the Lagrangian point L_1: being hydrostatic equilibrium no longer attainable, matter flows into the Roche lobe of the companion. In particular, the mass-losing star is denoted as the donor, whereas the mass-receiving one as the accretor.
The mass transfer rate depends very sensitively on the fractional radius excess of the donor

$$\frac{\Delta R}{R} = \frac{R_D - R_L}{R_L} \,, \tag{5.28}$$

so that

$$\dot{m} = -A \frac{m_D}{P} \left(\frac{\Delta R}{R} \right)^3 \,, \tag{5.29}$$

where m_D and R_D represent, respectively, the mass and the radius of the donor, while R_L its Roche lobe radius, P the orbital period and $A \sim 10$ a constant. Note that the Roche lobe radius can be estimated by using the famous expression by Eggleton (1983) [20]

$$R_L = \frac{0.49 q^{\frac{2}{3}}}{0.6 q^{\frac{2}{3}} + \ln\left(1 + q^{\frac{1}{3}}\right)} a \ , \tag{5.30}$$

where $q = m_1/m_2$ as for the primary, and $q = m_2/m_1$ as for the secondary, and that it is approximated by a sphere of equivalent volume for a simplified computational treatment of binary stellar evolution in one dimension.
Hence, a modest radius excess leads to an enormous mass transfer rate, meaning that, in practice, for a relatively slow and steady mass transfer, the donor overfills its Roche lobe only by a small amount.
Given the binary orbital momentum

$$J = \sqrt{G \frac{m_D^2 m_A^2}{m_D + m_A} a(1 - e^2)} \ , \tag{5.31}$$

the mass transfer is conservative if $\dot{J} = 0$ and $\dot{m}_A = -\dot{m}_D$ (with m_A mass of the accretor), i.e., if both the orbital momentum and the total mass of the binary are conserved, and its stability is tied down to the response of the donor to the imposed mass loss and of the accretor to mass gain: indeed, whenever a star suddenly loses mass, it will depart from equilibrium and react by readjusting its structure in order to recover it. More precisely, the mass transfer results stable when most of the transferred material is accreted by the companion star, unstable otherwise.
In the model, all pairs whose components' stellar radii exceed the respective Roche lobe radii have been deemed as undergoing RLOF merger. Into specifics, the former have been calculated as the photospheric radii

$$R_{phot} = \sqrt{\frac{L}{4\pi\sigma T_{eff}^4}} \ , \tag{5.32}$$

where L represents the stellar luminosity, T_{eff} the effective temperature and

$$\sigma = \frac{\pi^2 k_B^4}{60\hbar^3 c^2} \tag{5.33}$$

the Stefan-Boltzmann constant, and the latter through the Eggleton's formula (Eq. 5.30) scaled by the pericenter distance $r_p = a(1-e)$ instead of the semi-major axis a, according to the prescription of Sepinsky, Willems, and Kalogera (2007) [86]. As a matter of fact, applications of the Roche model are built by surmising that the system's orbit is circular and that its components are rotating synchronously with the orbital motion; however, such assumptions cannot always be justified, neither on theoretical nor on observational grounds: both synchronization and circularization are driven by tidal interactions between binary components, but, since the former typically happens faster than the latter, they tend to become synchronized with the orbital motion near periastron before circularization is actually completed. A simple and accurate fitting formula for the Roche lobe radius of a star in a circular binary with synchronously rotating components is provided, as already mentioned, by Eq. 5.30, where the semi-major axis a corresponds to the radius of the circular orbit, and the shape and volume of the Roche lobe depend solely on the mass ratio of the system, although, for eccentric binaries with non-synchronous component stars, they also depend upon the eccentricity, the true anomaly, and the degree of asynchronism. For lack of a better treatment, Eq. 5.30 is therefore often extrapolated to eccentric binaries by introducing exactly the pericenter distance of their respective orbit.
Now, when including RLOF, a distinction between accepted and rejected binaries in computing the velocity dispersion must be made, since the former participate with their components' orbital motion, whereas the latter only with their center of mass velocity. Consequently, formula 5.18 becomes

$$\sigma_{tot} = \sqrt{\frac{\sum_{i=1}^{N_s}(\mathbf{v}_i - \langle v\rangle)^2 + \sum_{i=1}^{2N_{b,acc}}(\mathbf{v}_i - \langle v\rangle)^2 + \sum_{i=1}^{N_{b,rej}}(\mathbf{v}_i - \langle v\rangle)^2}{N_s + 2N_{b,acc} + N_{b,rej}}}\,, \tag{5.34}$$

where

$$\langle v\rangle = \frac{\sum_{i=1}^{N_s}\mathbf{v}_i + \sum_{i=1}^{2N_{b,acc}}\mathbf{v}_i + \sum_{i=1}^{N_{b,rej}}\mathbf{v}_i}{N}\,, \tag{5.35}$$

and formula 5.24 takes the form

$$\sigma_{tot,lum} = \sqrt{\frac{\sum_{i=1}^{N_s} L_i(\mathbf{v}_i - \langle v \rangle)^2 + \sum_{i=1}^{2N_{b,acc}} L_i(\mathbf{v}_i - \langle v \rangle)^2 + \sum_{i=1}^{N_{b,rej}} (L_{1,i} + L_{2,i})(\mathbf{v}_i - \langle v \rangle)^2}{\sum_{i=1}^{N_s} L_i + \sum_{i=1}^{2N_{b,acc}} L_i + \sum_{i=1}^{N_{b,rej}} (L_{1,i} + L_{2,i})}}, \quad (5.36)$$

with

$$\langle v \rangle = \frac{\sum_{i=1}^{N_s} L_i \mathbf{v}_i + \sum_{i=1}^{2N_{b,acc}} L_i \mathbf{v}_i + \sum_{i=1}^{N_{b,rej}} (L_{1,i} + L_{2,i}) \mathbf{v}_i}{\sum_{i=1}^{N_s} L_i + \sum_{i=1}^{2N_{b,acc}} L_i + \sum_{i=1}^{N_{b,rej}} (L_{1,i} + L_{2,i})}, \quad (5.37)$$

where the velocity of rejected binaries is weighted by the sum of their respective components' luminosities.
So, binaries experiencing RLOF in both their components are considered as single (merged) objects and contribute to the observed velocity dispersion with their center of mass velocity, whereas binaries characterized by only one component overfilling its Roche Lobe cannot be regarded as such because the outcome of the mass transfer is actually uncertain. Yet, a primary overflowing its Roche lobe triggers a sudden mass loss, which would elicit a rapid modification of the host binary structure, concerning mainly its luminosity and effective temperature: into specifics, the luminosity decline may be such prominent to make the binary slip out of a magnitude-limited stellar sample. *Ergo*, the assumption that a quick merger between binary components happens when their Roche lobes touch is not fully correct. On the basis of this knowledge, assigning to each merged binary a velocity equal to its previous center of mass one constitutes a conservative approach: indeed, the velocity dispersion in a state where only primaries undergo RLOF is a few kms^{-1}greater than in the event of RLOF of both the components, with such an enhancement becoming more evident at increasing binary fraction for both the simulated galaxies. This is due, intuitively, to the fact that a smaller number of binaries is rejected if one binary component is subject to RLOF instead of two.
Either way, this choice sounded appropriate because following the time evolution of the

simulated binary population, rather than examining its present configuration, would have not only introduced further complications and approximations in the analysis, but also rendered the results less accurate.
On top of that, a luminosity cut-off consisting in the removal of all stars with luminosity below the turn-off (TO) level, condition given by $L_1 + L_2 < L_{TO}$ as for binaries, has been performed with the aim of mimicking a realistic observational situation. Note that this operation is actually meaningful only for dSphs, whose velocity dispersion is typically derived from the fiber-fed multi-object spectroscopy of individual sources: therefore, only stars brighter than a certain threshold, to second of the instrumental set-up, can be fruitfully used. By contrast, in the case of an UFD the velocity dispersion is routinely obtained from integrated single slit spectroscopy, which collects all the underlying light. More trivially, the realization of a CMD to which applying a luminosity cut-off is possible only if a sufficient number of stars is detected, as it happens for dSphs, but not for UFDs.

5.2 Results and discussion

In this section a detailed look at the results of simulations will be provided, highlighting how the assumptions made on the binary population reflect upon the model galaxies' dynamical mass estimate.

5.2.1 Variation of binary orbital parameters

As a general, preliminary, consideration, it must be stressed that the observed velocity dispersion in a star system hosting a given set of binaries in fraction f_b can be represented as a linear combination of two (i.e., single star and unresolved binary) contributions:

$$\sigma^2_{obs} = (1 - f_b)\sigma^2_s + f_b\sigma^2_b \, . \tag{5.38}$$

Being $\sigma^2_s \propto |U|/M \propto M$ (Eq. 5.27), and σ^2_b independent of M, it is clear that, once a specific binary population is generated, the action of binaries is as more relevant as lighter the system is, even in the case of small binary fractions. So it is natural to expect a major enhancement of the output velocity dispersion in UFDs rather than in dSphs. This is indeed confirmed by a number of past studies on the binary content of dwarf galaxies (e.g., Simon and Geha, 2007 [90]; McConnachie and Côté, 2010 [63]; Spencer et al., 2018 [93]).

In the hypothesis of virialized (i.e., stationary) systems, the relative variation of the predicted virial mass with respect to the real one can be inferred from the relation

$$\frac{\Delta M}{M} = \frac{\sigma_{obs}^2 - \sigma_0^2}{\sigma_0^2} \ . \tag{5.39}$$

Obviously, an overestimate of the observed velocity dispersion immediately translates into an inflation of the dynamical mass of the system.
Given this, the main quantities to focus the attention on are the two expressions for the velocity dispersion σ_{tot} (Eq. 5.18) and the luminosity averaged $\sigma_{tot,lum}$ (Eq. 5.24), for they include the binary orbital motion, which becomes more and more important at increasing binary fraction and with the shrinking of the binary semi-major axis.
Fig. 5.1 shows, for the simulated UFD, the role of the variation of a_{max} in calculating σ_{tot} (Fig. 5.1, top-left panel) and $\sigma_{tot,lum}$ (Fig. 5.1, top-right panel), and the related effect on the $\Delta M/M$ evaluation (Fig. 5.1, bottom-left panel, and Fig. 5.1, bottom-right panel).
Note that $\sigma_{tot,lum}$ is systematically smaller than σ_{tot}, thus yielding a corresponding lower estimate for the virial mass. Since the difference between σ_{tot} and $\sigma_{tot,lum}$ reaches at most the 13% for a binary fraction $f_b = 0.4$ in the reference model case ($a_{max} = 100$ AU), it is deduced that the overall dependence of the observed velocity dispersion on a_{max} is not very relevant.
On the contrary, Fig. 5.2 clearly demonstrates that the lessening of a_{min} is much more important in inflating the velocity dispersion. In fact, when $a_{min} = 0.01$ AU, σ_{tot} results larger than 20 kms^{-1}even for $f_b = 0.05$, and then increases approximately as $\sqrt{f_b}$. This implies a huge enhancement of the predicted virial mass as opposed to the real mass of the system, which is evident from the bottom panels of Fig. 5.2.
Fig. 5.1 and Fig. 5.2 must be compared, respectively, to Fig. 5.3 and Fig. 5.4, which display the trend of σ_{tot} and $\sigma_{tot,lum}$, as well as that of the associated $\Delta M/M$, when adding RLOF. As expected, a modest, although global, decrease of the observed velocity dispersion can be immediately noticed; this is quite manifest especially in the luminosity averaged case, where the velocity of merging binaries is weighted by the sum of their components' luminosities (Eq. 5.36). Still, if binaries are assumed to drop out of the sample when RLOF befalls the primary star only, regardless of whether an actual merger occurs (Olszewski, Pryor, and Armandroff, 1996 [69]; Minor et al., 2010 [67]), the observed velocity dispersion increases again to almost recover its original value, owing to the smaller number of rejected pairs (Fig. 5.7).

With regards to the model dSph, the most meaningful results are reported in Fig. 5.5 and Fig. 5.6, which show, respectively, the dependence of σ and the related $\Delta M/M$ on the variation of a_{min} before and after imposing the aforementioned cuts. A straightforward comparison of Fig. 5.5 with Fig. 5.2, and of Fig. 5.6 with Fig. 5.4 corroborates the expectation that the boost of the global velocity dispersion caused by binaries is more prominent in lighter systems, like UFDs, than in dSphs. Note, *inter alia*, that the binary fraction slightly increases due to the luminosity cut-off, since it affects single stars more than binaries. In reference to Fig. 5.6, the new binary fraction, i.e., $f_b \in [0.09, 0.16, 0.23, 0.29, 0.33, 0.37, 0.41, 0.44]$, is indeed higher with respect to the original case.
Besides this, it is worth mentioning that, in line with the predictions by Rastello, Carraro, and Capuzzo-Dolcetta (2020) [81], although in the different context of open star clusters (OCs), the luminosity cut-off is not much impactful on the velocity dispersion estimate. In fact, the observed velocity dispersion is found to experience the most dramatic decline as a consequence of the RLOF rejection, not the luminosity cut-off, which provokes a further reduction of $\sim 1-5$ kms^{-1}with increased binary fraction. In particular, as for the reference model ($a_{min} = 0.2$ AU), the lessening of σ_{tot} goes from $\sim 25\%$ ($f_b = 0.4$) to $\sim 40\%$ ($f_b = 0.1$), whereas that of $\sigma_{tot,lum}$ from $\sim 20\%$ to $\sim 35\%$ for the same values of f_b.

5.2.2 Comparison between binary mass coupling methods

The role of mass coupling in binaries has been examined through a comparison between the outcomes relative to the random pairing procedure and those coming from the assumption of a power-law mass ratio distribution $f(q) \propto q^{-0.4}$.
Yet, throughout any discussion of $f(q)$ it is important to assess whether the distribution is effectively consistent with the two masses being chosen independently from the same MF, in such a way that the mass of neither component is influenced by its companion. To this end, Tout (1991) [100] studied the relation between the q-distribution in binary stars and the MF for single stars, founding that, if this is the case, the q-distribution is most sensitive to the low-mass behavior of the MF: since the true nature of the MF is uncertain at low masses, the analysis of the mass-ratio data is equally doubtful. He also argued that observations of spectroscopic binaries can easily adhere to the aforementioned hypothesis, provided that very simple selection effects are taken into account. Indeed, from the complete distance-limited investigation of G-dwarf stars, including both spectroscopic and visual binaries, in the solar neighborhood conducted by Duquennoy and Mayor (1991) [19] emerged that the derived q-distribution complies with a Kroupa IMF because it

shows no maximum toward values close to unity, but a continuous increase toward small secondary masses. Thereby the authors conjectured that binaries can form by random associations of stars from the same IMF, although this scenario, actually acceptable for long-period binaries, may seem surprising for tight ones. Such a result clearly disagrees with the bimodal distribution, presenting a peak near $q = 1$ and another near $q = 0.3$, detected by Trimble (1974) [102] for single-lined (SB1) and double-lined (SB2) spectroscopic binaries. On the other hand, by using a similar sample, Boffin (2015) [10] discovered the q-distribution to be not only a function of the spectral type of the primary, and thus of its mass, but also relatively flat, with K-stars lacking smaller companions and F-stars displaying an excess of twins.

While in low-mass binaries a flat q-distribution is generally the product of a bias, in massive ones it reflects their tendency to prefer stars of equal mass: as suggested by Sana et al. (2013) [84], effectively, the majority of massive stars have their evolution strongly affected by the interaction with a nearby companion, the nature of which is largely determined by the initial orbital period and mass ratio of the binary system they belong to. The fact that the q-distribution of O+OB binaries appears uniform in the range $0.2 < q < 1$ supports the formation of these binaries in early dynamical exchanges favoring the capture of more and more massive secondaries, rather than by random pairing from a Salpeter or Kroupa IMF (Sana and Evans, 2011 [85]).

However, such a dependence of the q-distribution on the mass range is not attested by Reggiani and Meyer (2013) [82], who claimed the companion mass ratio distribution (CMRD) to be universal over a wide range of q values and primary masses, and to follow a single-slope power-law $dN/dq \propto q^{\beta}$, with $\beta = -0.25 \pm 0.29$, over the separation range $1 - 2400$ AU and primary mass range $0.25 - 6.5$ $M_{\odot}$. Reggiani and Meyer (2013) [82] justified their conclusion by invoking different binary formation mechanisms: if tidal capture models predict that for each primary the mass of the secondary is chosen randomly from the single-star MF, so that the CMRD matches the IMF, in fragmentation scenarios the subsequent, continued accretion onto both objects from a common reservoir acts to equalize the masses, hence making the q-distribution peak toward unity. They also noted that, even though not most relevant in binary formation, tidal capture may still occur during the dissolution phase of star clusters: as a consequence, the shape of the CMRD should change as a function of orbital separation, but no such evidence was uncovered in their modelization.

Along this line, being a complete compatibility of a given MF with a given binary mass ratio distribution impossible, $f(q) \propto q^{-0.4}$ has been deliberately implemented for the mock dwarf galaxies by normalizing the (m_1, m_2) mass pairs to yield the same binary

total mass $m_1 + m_2$ of the random pairing case. At fixed a_{max} of the reference model and varying a_{min} in the usual range, the values of σ^2 computed in the case of power-law q-distribution differ from the ones of random pairing for $\sim \pm 20\%$. A similar variation range is obtained if a_{min} is kept fixed and a_{max} is varied. As a net result, the choice of a power-law functional form leads to an average underestimate of σ^2 of the order of 15%: so, despite all the measured q-distributions for field stars and clusters look fundamentally at odds with random draws of secondaries from the IMF (Milone et al., 2012 [66]), this has little effect on the conclusions of this study, which are in the direction of pointing out the importance of binaries in the dynamical mass estimate of a dwarf-galaxy-like stellar system.

5.2.3 Dependence of the results on the system mass and scale radius

In order to perform a more comprehensive investigation of the impact of the binary content in small size, low dense stellar systems, binary stars have been placed in ever-decreasing density dwarf galaxies by extending the scale radius from 25 to 250 pc, with steps of 25 pc, for the fixed total mass $M = 5 \times 10^4$ $M_\odot$ assumed to represent an UFD in the simulations.

Fig. 5.8 (upper panel) displays the decreasing trend of σ_{tot}/σ_0 as a function of the mean mass density of the system without taking account of RLOF. Interestingly, with regards to the reference model ($\rho \simeq 0.1$ $M_\odot$ pc^{-3}) a binary fraction of just 5% suffices to produce a significant enhancement of the dynamical mass (of a factor of ~ 25.8 for the above-mentioned instance).

Furthermore, the results of Minor et al. (2010) [67], who predicted that, in dSphs with $\sigma_{obs} > 4$ kms^{-1}, the inflation due to binary orbital motion would unlikely exceed the 30%, are essentially recovered. Now, $\sigma_{obs} = 4$ kms^{-1}is derived for a binary fraction $f_b = 0.03$ and, since the intrinsic velocity dispersion σ_0 goes from ~ 1.6 to ~ 0.5 kms^{-1}at increasing scale radius of the system, it follows that the overestimate of the observed velocity dispersion reaches at most the 8%. Inversely, in the case of higher binary fractions, for which σ_{obs} is larger than 4 kms^{-1}, such an inflation grows exactly up to $\sim 30\%$. These considerations hold if RLOF is accounted for (Fig. 5.8, lower panel), because σ_{tot} decreases of less than $\sim 1\%$ with respect to the corresponding values in the absence of RLOF.

Note that, being $f_b \leq 0.4$ in the present analysis, it can obviously be argued that the threshold suggested by Minor et al. (2010) [67] for the boost of the observed velocity dispersion may be overtaken if a more numerous binary population with the simulated characteristics is considered. Yet, particular caution must be exercised in this respect,

given the differences in the modeling approach, especially as far as the choice of the binary velocity and period distributions is concerned.
Moreover, the dependence of σ_{tot}/σ_0 on the mean mass density explains why in systems like GCs, which are small sized but also dense, there is no expectation for a relevant velocity dispersion inflation due to binaries. Incidentally, GCs are deemed to be totally deprived of DM.
Note in addition that, contrary to dwarf galaxies, where the intrinsic non-collisionality would lead to an almost constant in time f_b, GCs are presently supposed to contain only a limited fraction of binaries owing to their collisional nature (Milone et al., 2012 [66]). Thereby, being the destruction rate of binary stars through dynamical interactions higher than the formation one (Hut et al., 1992 [41]), detecting a significant enhancement of the observed velocity dispersion in these environments is certainly unlikely.
This conclusion is enforced by the calculation of the half-mass relaxation time according to Eq. 5.17 (Tab. 5.1).

5.2.4 Mass-to-light ratio

As said in Sect. 5.2.1, for a given set of binary characteristics the dynamical mass estimation, M_{dyn}, is a linear function of f_b:

$$M_{dyn} = A + B f_b \ . \tag{5.40}$$

In particular, for the simulated UFD, the values of the coefficients are $A = 5.55 \times 10^4$ $M_\odot$ and $B = 2.50 \times 10^7$ $M_\odot$ in the original set-up, whereas $A = -7.41 \times 10^5$ $M_\odot$ and $B = 2.53 \times 10^7$ $M_\odot$ when considering RLOF. For the simulated dSph, these coefficients are $A = 9.90 \times 10^6$ $M_\odot$ and $B = 1.50 \times 10^9$ $M_\odot$ when RLOF and the luminosity cut-off are not taken into account, while $A = -3.89 \times 10^7$ $M_\odot$ and $B = 9 \times 10^8$ $M_\odot$ when both of them are considered.
Then, both the mass-to-bolometric light ratio, and the mass-to-light ratio in the V and B bands have been computed for selected binary fractions relative to the reference model (Tab. 5.3 and Tab. 5.4). Most notably, with regards to the B and V bands, it emerges (Tab. 5.3) that, for small sized systems such as UFDs, high values of M/L arise even in the presence of a modest binary population, overpassing 100 for $f_b > 0.3$. Of course, performing the RLOF rejection causes M/L to diminish, being the total luminosity fixed. These findings are validated by a comparison with Fig. 5.9 (right panel) of Simon (2019) [89], which reports the trend of the mass-to-light ratio within the half-light radius for a

sample of UFDs as a function of the luminosity in the V band. Here it must be noted that, for a luminosity $L \sim 10^4$ $L_{V,\odot}$, relative to the simulated UFD, $(M/L)_V$ ranges from $\sim 10^2$ to $\sim 10^4$ $M_\odot/L_{V,\odot}$, in accordance with the predictions of the reference model for $f_b \geq 0.3$; this is true also in the event of RLOF, since the mass-to-light ratio is slightly reduced. Nevertheless, it is worth stressing, for the sake of clarity, that the mass-to-light ratio estimates associated to the UFDs for which velocity dispersion measurements are available, are affected by large uncertainties in the aforementioned luminosity regime, and that the dynamical mass has been calculated by following the prescription of Wolf et al. (2010) [109], which may be a possible source of discrepancy with the present results. In closing, the fact that, after the application of the cut procedure, the value of σ_{tot} for the actual binary fraction $f_b = 0.37$ in the reference model dSph is magnified by a factor of ~ 5.5 with respect to the intrinsic value $\sigma_0 \simeq 2$ kms^{-1}must be put into evidence; this is consistent with the observations made by Spencer et al. (2018) [93], who expected a non-negligible effect of Leo II-like binary fractions in galaxies having $\sigma_0 \simeq 0.5 - 2$ kms^{-1}. Even so, as highlighted by Dabringhausen et al. (2016) [15], such an influence is tightly related to the total luminosity of the system, provided that virial equilibrium is assumed, and becomes much more pronounced when $L \leq 10^6$ $L_{V,\odot}$. This is a natural outcome of a velocity dispersion inflation as due to a given binary population, which is, of course, fractionally more important in lighter systems than in larger. Therefore, according to Dabringhausen et al. (2016) [15], for the considered dSph's total luminosity $L \simeq 10^7$ $L_{V,\odot}$, binaries alone would not be able to boost the observed velocity dispersion to the extent that the presence of DM may be totally ruled out. Indeed, $(M/L)_V$ corresponding to $f_b = 0.33$ for the simulated dSph (Tab. 5.4) undergoes a minor enhancement owing to the sole action of binaries, if compared to the UFD case, where the total luminosity is set at $L \simeq 10^4$ $L_{V,\odot}$. Consequently, confirmation is found that binary stars affect the internal dynamics of UFDs to a greater degree than dSphs, which may be unlikely regarded as utterly composed of baryonic matter.

Object	f_b	$(M_{dyn}/L)_{bol}$ $(M_\odot/L_\odot)$	$(M_{dyn}/L)_V$ $(M_\odot/L_{V,\odot})$	$(M_{dyn}/L)_B$ $(M_\odot/L_{B,\odot})$
dSph	0	0.07	0.73	0.60
	0.05	0.63	6.15	5.06
	0.15	1.75	17.07	14.03
	0.30	3.41	33.38	27.44
	0.40	4.53	44.29	36.40
UFD	0	0.07	0.73	0.60
	0.05	1.95	19.04	15.65
	0.15	5.64	55.16	45.34
	0.30	11.26	110.13	90.53
	0.40	14.92	145.88	119.95

Table 5.3: Values of the mass-to-light ratio in the bolometric and V and B photometric bands for various binary fractions, in the case of our reference model.

Object	f_b	$(M_{dyn}/L)_{bol}$ $(M_\odot/L_\odot)$	$(M_{dyn}/L)_V$ $(M_\odot/L_{V,\odot})$	$(M_{dyn}/L)_B$ $(M_\odot/L_{B,\odot})$
dSph	0	0.07	0.73	0.60
	0.09	0.44	4.33	3.56
	0.23	1.13	11.07	9.10
	0.37	2.19	21.46	17.64
	0.44	2.68	27.27	22.41
UFD	0	0.07	0.73	0.60
	0.05	1.36	13.34	10.96
	0.15	4.31	42.12	34.63
	0.30	9.88	96.65	79.45
	0.40	14.69	142.63	117.27

Table 5.4: As Tab. 5.3, but accounting for both RLOF and the luminosity cut-off (dSph case) and RLOF only for the UFD case. For the dSph, f_b refers to the actual binary fraction obtained after the luminosity cut procedure.

5.3 Summary and conclusions

The role of unresolved binary stars in inflating the observed velocity dispersion of dwarf galaxies has been examined by realizing a set of non-dynamical simulations in dependence on various binary system parameters.
At odds with previous investigations where sophisticated statistical analyses were performed (Minor et al., 2010 [67]; Spencer et al., 2018 [93]), in this first application of the model the explicit influence of each orbital element has been taken into account, and conservative regions of the parameter space have been carefully explored. Two distinct spherical systems, aiming at representing a typical dSph and UFD galaxy, have been considered, and attention has been paid to the effects of the variation of binary orbital parameters, obtaining, as principal result, that the dominant impact on the estimate of the system velocity dispersion, in the hypothesis of an unresolved binary population, is given by the semi-major axis (and so by the orbital period) distribution.

The main outcomes of this study can be summarized as follows:

- the presence of an abundant quantity of unresolved binaries with relatively low periods (Tab. 5.2) leads to a significant enhancement of the observed velocity dispersion, and, consequently, of the dynamical mass evaluated through the virial theorem upon assumption of stationary systems. This result differs from the findings of Minor et al. (2019) [68], who assert, referring to the galaxy Ret II, that a high fraction of close binaries in low-metallicity environments, such as UFDs, is unable to give an appreciable input to the observed velocity dispersion;
- the observed squared velocity dispersion is a linear function of the binary fraction, as outlined, e.g., by Minor et al. (2010) [67];
- the corresponding mass estimate is inflated with respect to the real mass of the system, and increases with both the binary fraction and the shrinking of the binary semi-major axis (i.e., by diminishing the binary orbital period);
- low-mass systems (UFDs) suffer more from the contribution of a given binary population due to their smaller intrinsic velocity dispersion ($\sigma \propto \sqrt{M}$);
- the action of RLOF translates into a moderate reduction of the observed velocity dispersion in both the simulated galaxies. However, its decline is more prominent in the model dSph, given the additional luminosity cut-off, which involves single and binary stars differently;

- the introduction of a power-law mass ratio distribution $f(q) \propto q^{-0.4}$ for the binary mass coupling causes σ^2 to be underestimated of $\sim 15\%$ with respect to the random pairing case, hence affecting in a modest way the evaluation of the dynamical mass;
- the boost of the observed velocity dispersion by binary stars is a steeply decreasing function of the mean mass density of the system. In particular, for low-density galactic hosts, even a small fraction (5%) of binaries with the selected standard characteristics produces a non-negligible inflation of the dynamical mass (i.e., by a factor of ~ 25.8 in the reference model instance, without accounting for RLOF);
- the obtained values of the mass-to-light ratio are large and look compatible with those estimated observationally for UFDs and dSphs, offering, in the case of UFDs, an interpretation based on unresolved binaries as alternative or, at least, complementary to that of an overabundance of non-baryonic dark matter in such low density systems.

In conclusion, this model provides a realistic and physically consistent explanation of the role of binary stars in the dynamical mass estimate of stellar systems, with the ultimate purpose of challenging the claim that only the presence of vast amounts of DM is of primary importance in this context.
However, more robust and precise results would require several improvements in both theoretical modelization and spectroscopic data availability, especially related to UFDs: thus, while waiting for future observational facilities, the model might be upgraded by accounting for the effects not only of stellar evolution (i.e., mass loss) and dynamics, but also of close interactions between binary components, in order to give a full-time picture of the mock galaxies.

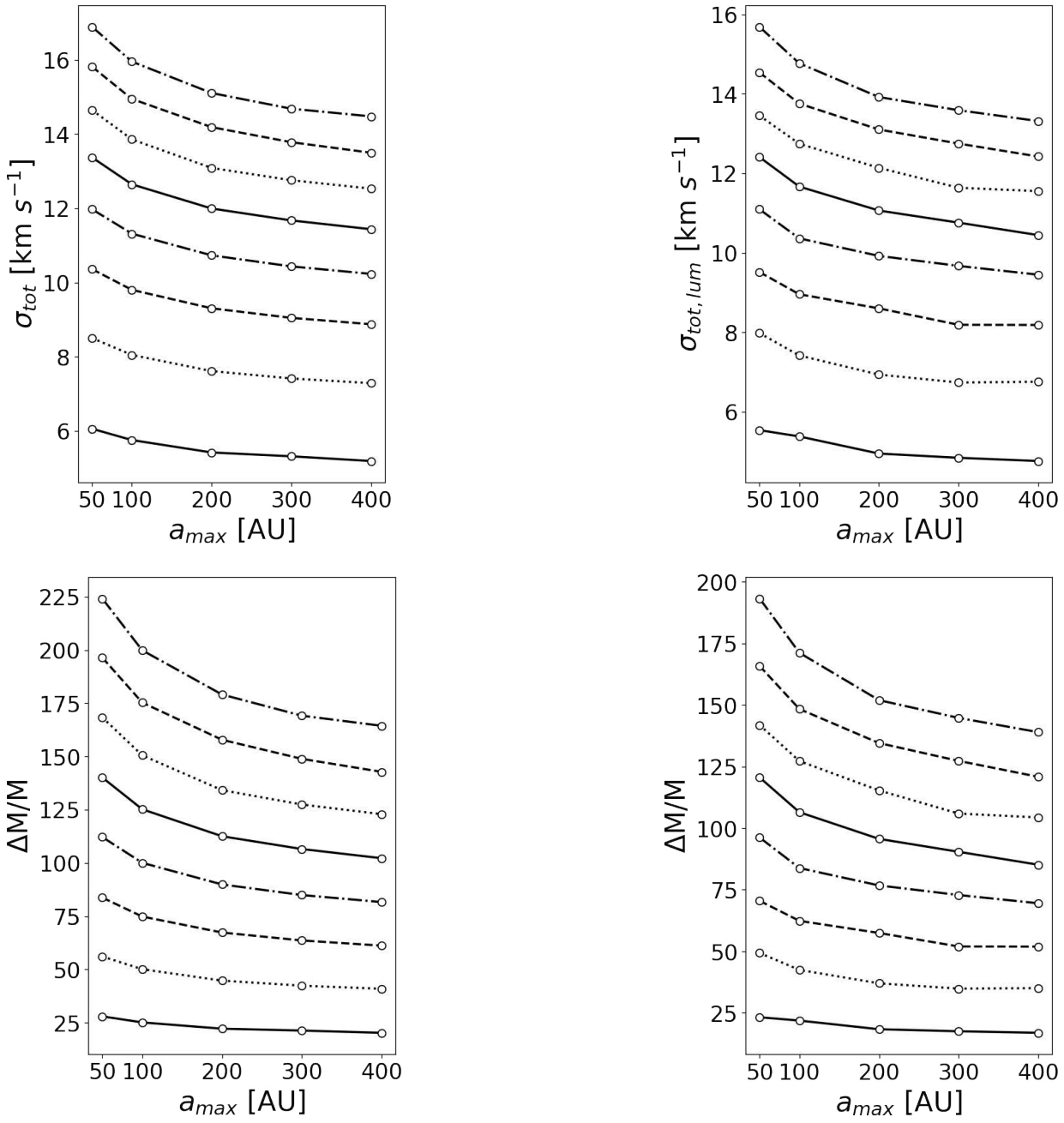

Figure 5.1: For the simulated UFD: upper panels illustrate the dependence of the velocity dispersion σ_{tot} (top-left panel) and of the luminosity averaged velocity dispersion $\sigma_{tot,lum}$ (top-right panel) on the variation of the upper boundary a_{max} of the binary semi-major axis distribution at fixed lower boundary $a_{min} = 0.2$ AU. Lower panels show the corresponding relative mass difference $\Delta M/M$. Each curve refers to a different value of f_b going bottom-up from 0.05 to 0.4 in steps of 0.05.

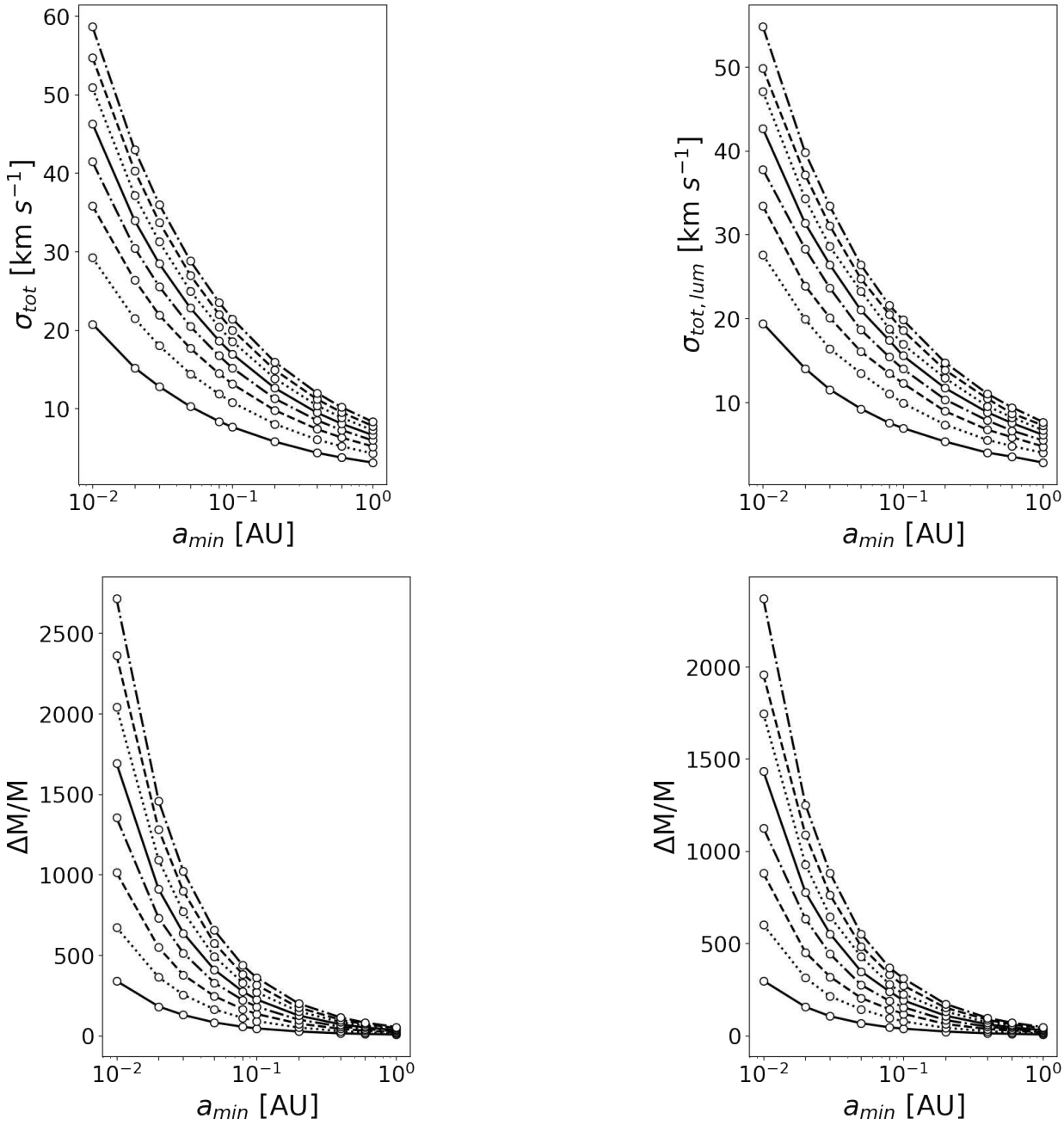

Figure 5.2: As in Fig. 5.1, but for the variation of a_{min} at fixed value of $a_{max} = 100$ AU.

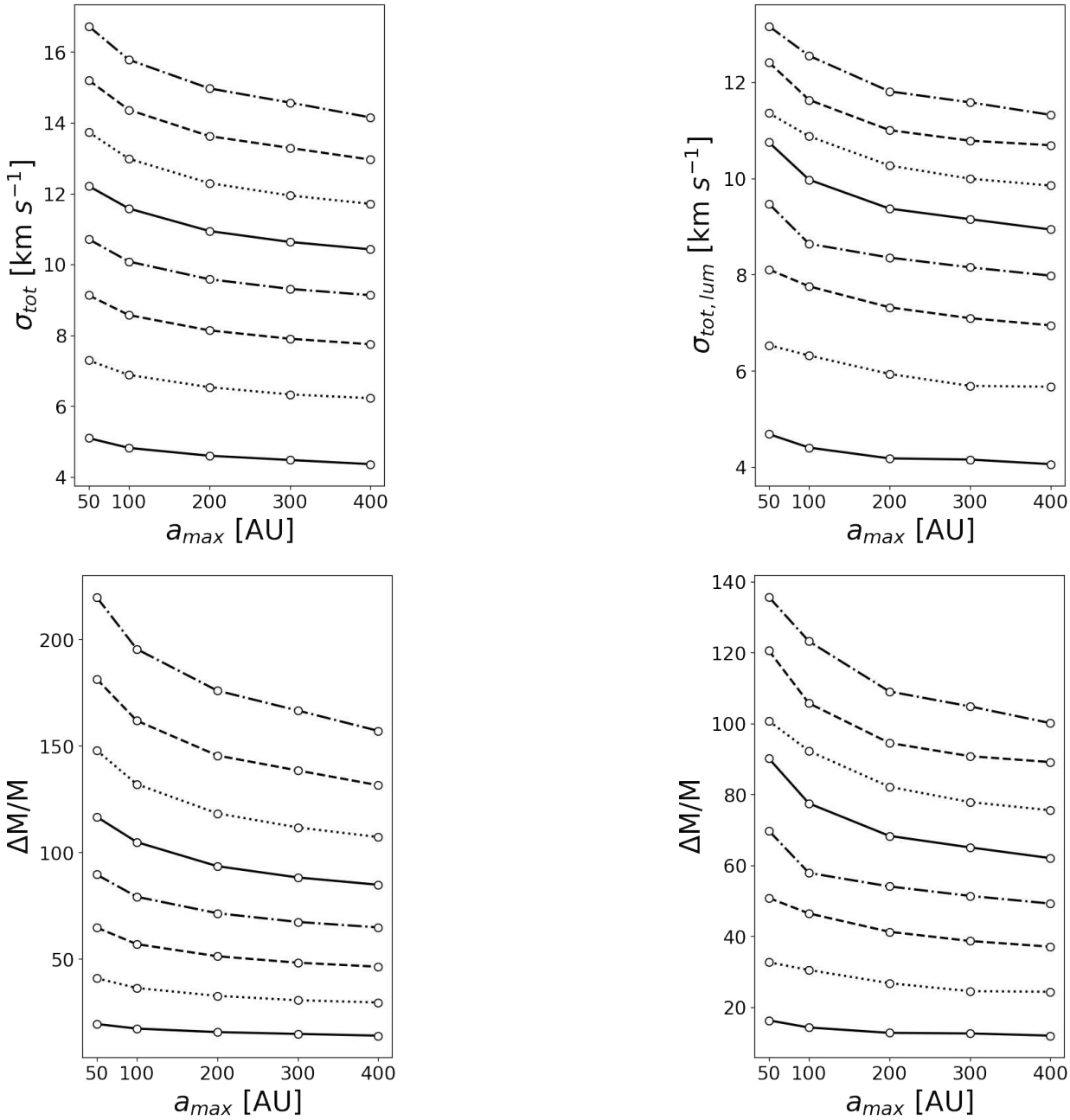

Figure 5.3: As in Fig. 5.1, but accounting for RLOF.

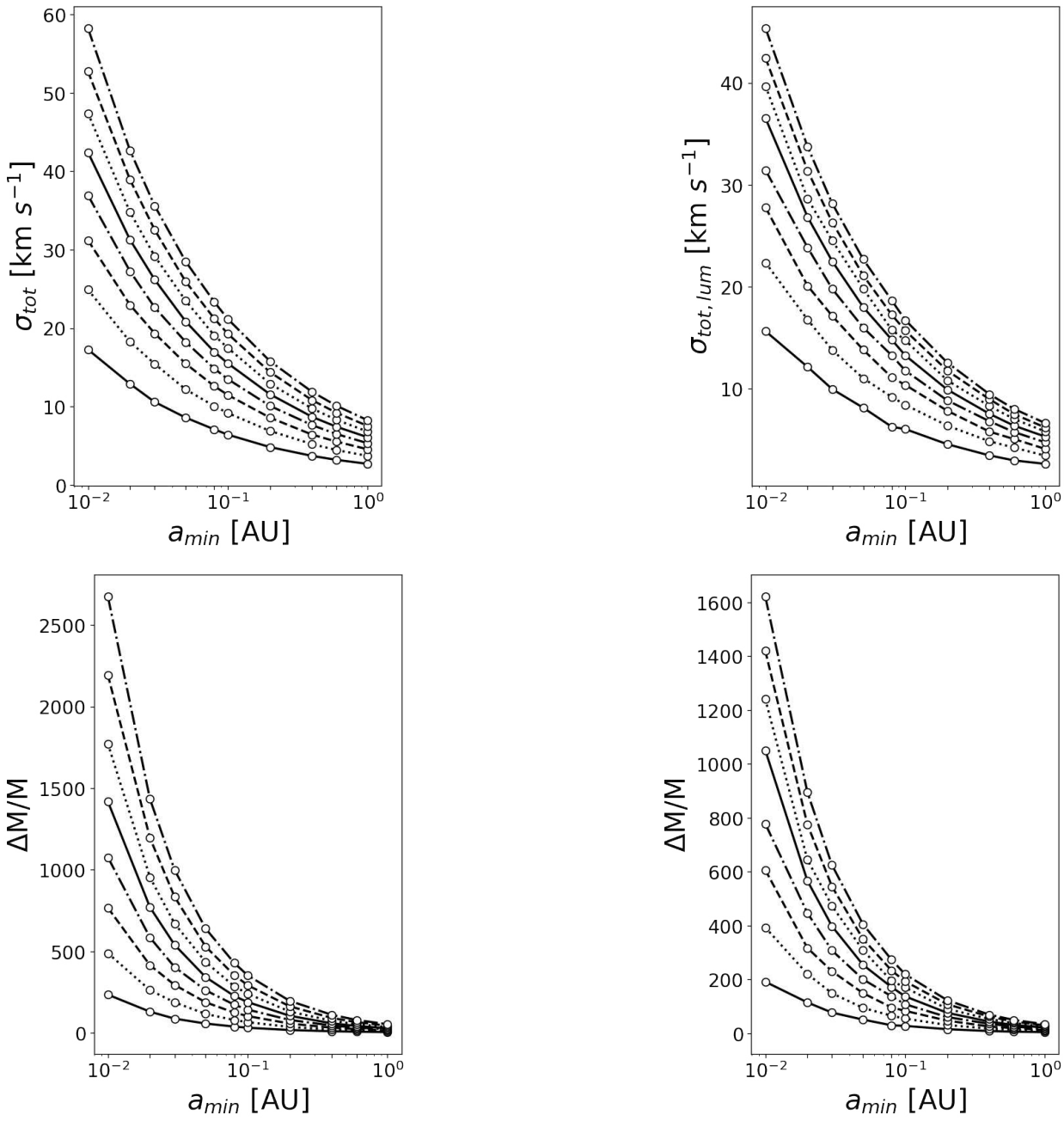

Figure 5.4: As in Fig. 5.2, but accounting for RLOF.

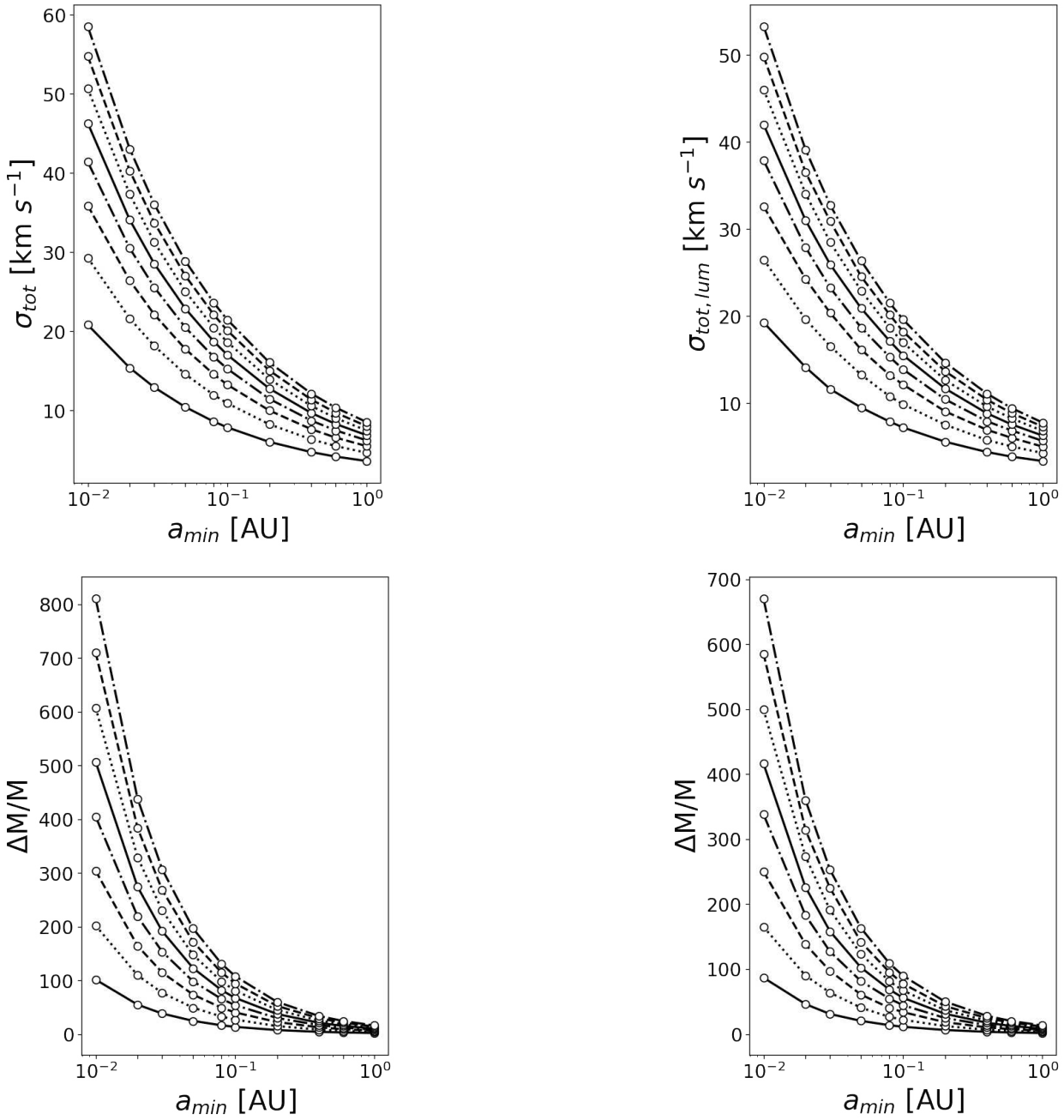

Figure 5.5: For the simulated dSph: upper panels illustrate the dependence of the velocity dispersion σ_{tot} (top-left panel) and of the luminosity averaged velocity dispersion $\sigma_{tot,lum}$ (top-right panel) on the variation of the lower boundary a_{min} of the binary semi-major axis distribution at fixed upper boundary $a_{max} = 100$ AU. Lower panels show the corresponding relative mass difference $\Delta M/M$. Each curve refers to a different value of f_b going bottom-up from 0.05 to 0.4 in steps of 0.05.

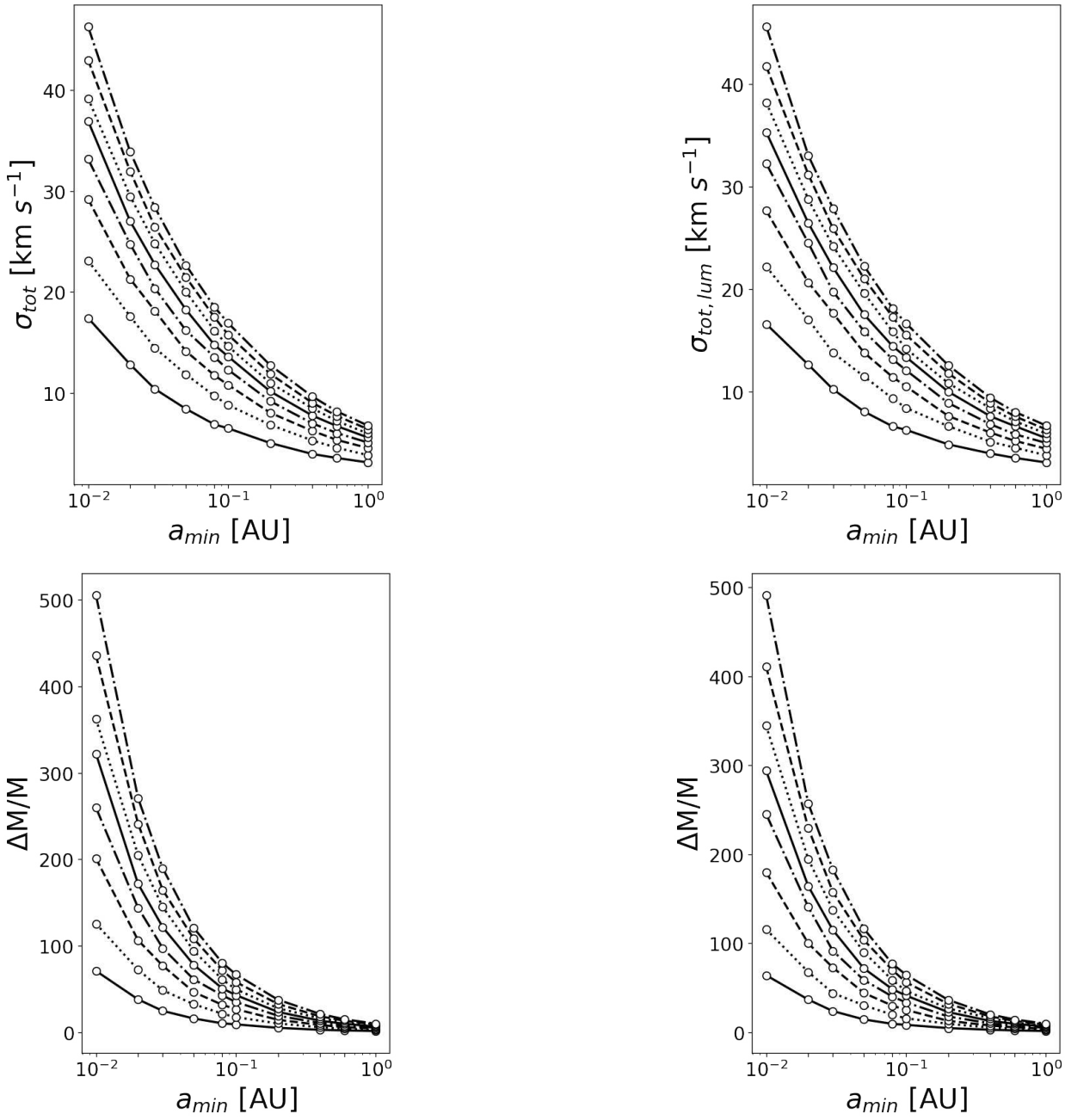

Figure 5.6: As Fig. 5.5, but accounting for both RLOF and the luminosity cut-off.

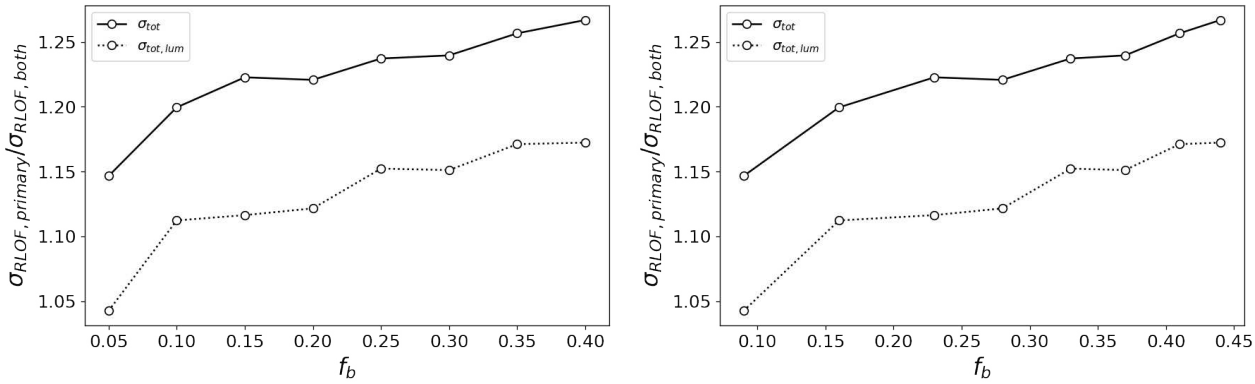

Figure 5.7: Ratio between the velocity dispersion for RLOF of only primaries to that for RLOF of both binary components in the case of the reference model UFD (left panel) and dSph (right panel). In particular, the solid line refers to σ_{tot}, whereas the dotted line to $\sigma_{tot,lum}$.

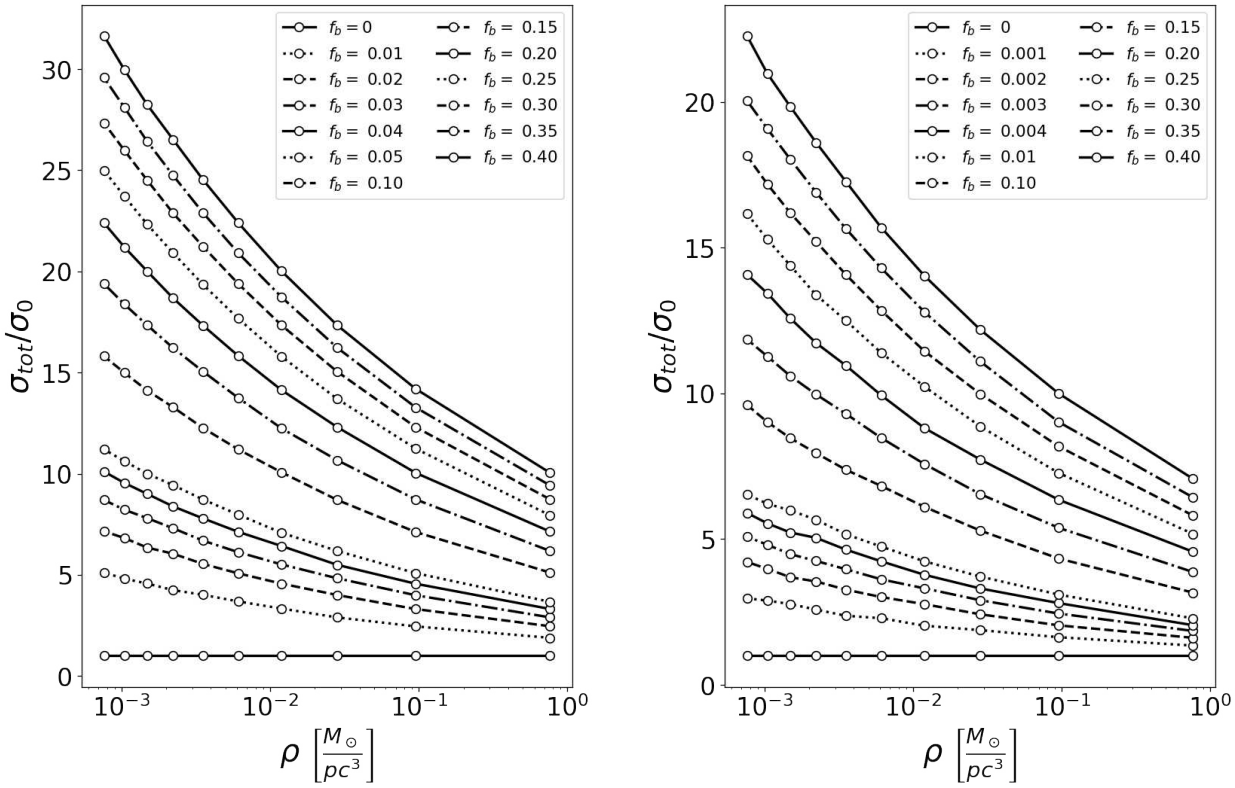

Figure 5.8: Dependence of the ratio σ_{tot}/σ_0 on the mean mass density of the system obtained by varying the scale radius R from 25 to 250 pc with steps of 25 at fixed total mass $M = 5 \times 10^4$ $M_\odot$. The values of f_b label each curve going bottom-up, according to the legend, and differ depending on whether RLOF is taken into account (right panel) or not (left panel) in the calculation of σ_{tot}.

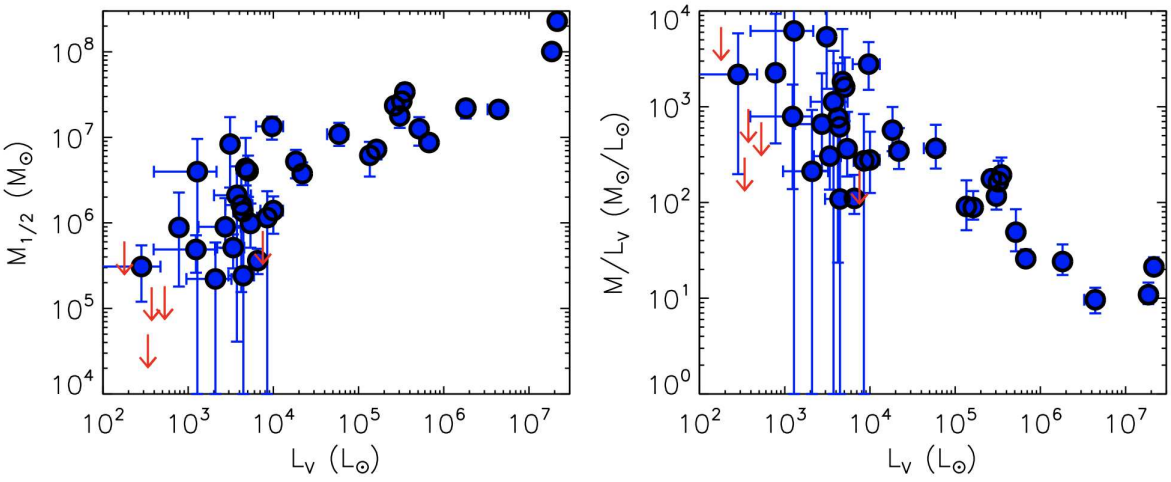

Figure 5.9: Dynamical masses (left panel) associated mass-to-light ratios within the half-light radius (right panel) for a sample of ultra-faint MW satellites as a function of luminosity in the V band. Measurements and uncertainties are shown as the blue points with error bars, and mass limits determined from the 90% confidence upper limits on the dispersion are displayed as red arrows for systems without resolved velocity dispersions.

Chapter VI

Conclusions

The role of binaries in the structural evolution of star clusters and dwarf galaxies has been deeply analyzed by both referencing previous astrophysical works on the subject and performing computational simulations to provide new perspectives and issues to discuss. After a detailed description of the various processes connected to energy equipartition (i.e., evaporation, mass segregation and core collapse) in Chap. II, the differences not only between primordial and dynamically formed, but also between soft and hard binaries have been introduced with the aim of understanding to which extent they may affect stellar dynamics. In particular, it turned out that the harder a binary, the more unlikely for it to be destroyed in encounters with other stars: thereby, under specific conditions depending on the environment they are part of, close binary systems act as an internal energy source able to halt, or at least delay, the core collapse phase in star clusters.
By implication, Chap. III has been mainly devoted to sort through the mechanisms leading to cluster dissolution. Starting from early life stages, mass loss due first to residual gas expulsion and then to stellar evolution has been taken into consideration to explain violent relaxation and the eventual infant mortality of star clusters in the MW. If, however, a novel equilibrium state is reached, subsequent encounters with GMCs, periodic disk shocks and, ultimately, the presence of an external tidal field may alter such a condition in a dramatic fashion: stellar systems must be either very dense and compact, such a GCs, or located far from the Galactic plane, such as old OCs, in order to survive longer and avoid rapid disruption, which clearly accounts for the scarcity of young OCs close to the Galaxy center. Nevertheless, given the shorter timescale for tidal dissolution compared to that for utter suppression of a primordial binary population, the overall system dynamical

configuration should change similarly to the isolated case exactly thanks to the presence of binaries. As a result, the evolution of the binary fraction in star clusters is a crucial study matter, even though a general consensus on this topic has not yet been achieved, so that a definite, reliable picture still lacks. Contrariwise, the impact of binary stars on inflating the cluster velocity dispersion has been recognized as a valuable explanation for the discrepancy between the dynamical and photometric mass of OCs, which are able to retain a high binary fraction throughout their whole life.
To this regard, simulating an old OC like M67 via the state-of-the-art *N*-body code *PeTar* might be worthwhile not only to fully investigate both the stellar and the dynamical evolution of a typical OC binary population, but also to determine its effects on the system velocity dispersion, without neglecting the existence of the Galactic tidal field and compromising cluster survivability as well. In particular, the possible development of a Python program for initial conditions generation and simulations' output data analysis may serve as a flexible tool to interact with *PeTar* and test the validity of the theories, involving binaries in star clusters, so far presented.
Chap. IV is instead concerned with a comprehensive treatise of dwarf galaxy formation inside the cosmological ΛCDM model, whose predictions are actually altered by the inclusion of baryonic feedback in pure DM simulations. In fact, feedback processes must have been considerably efficient in suppressing SF during the pre-reionization era, given the lower number of observed luminous MW satellites with respect to the forecast number of DM halos. Hereby the classification of dwarf galaxies based on their mass and gas content: bright dwarfs, classical dwarfs and UFDs. Among them, UFDs are notoriously deemed as pristine relics of the early universe since they ceased to evolve after reionization, when SF had already been quenched: for this reason, they should represent the most DM-dominated systems to date known. Consequently, dwarf galaxies, UFDs in the specific, result valuable laboratories to try and constrain the nature of DM. The possible over-abundance of DM in dwarf galaxies is typically inferred from their notably large velocity dispersion, responsible for the huge enhancement of their dynamical mass and mass-to-light ratio, but alternative scenarios to interpret this phenomenon have been put forward: if, on the one hand, the tidal stripping hypothesis has been ruled out in favor of DM, on the other hand the presence of a non-negligible number of unresolved binaries is still a matter of debate.
To this end, in Chap. V a parametric study has been proposed as a new method to gauge the relevance of binary stars in the dynamical mass determination of the faintest MW satellites. Such a theoretical model consists in an exploration of the effects that selecting binary orbital parameters may have on the observed velocity dispersion of two

mock dwarf galaxies, namely a dSph and an UFD, at varying binary fraction. Assuming an unresolved binary population, then, the major inflation of the dynamical mass with respect to its true value is obtained by either shrinking the binary semi-major axis or increasing the binary fraction, and is evident especially in the simulated UFD due to its smaller intrinsic velocity dispersion. Coherently, the mass-to-light ratio derived from this mass estimate, being it compatible with observations, seems to confirm that only in the case of UFDs unresolved binaries may constitute an alternative or, at least, complementary scenario to the most accredited predominance of dark matter.

A possible limitation of this analysis may reside in the absence of both stellar and dynamical evolution in the simulations, since the realized parametric study is intended to portray the systems at a particular life stage, without following their temporal development; nonetheless, the inclusion of a conservative treatment for RLOF may offer preliminary considerations about the importance of binary interactions in the modelization.

In conclusion, further work certainly needs to be done in order to give a full picture of the role of binaries in the structural evolution of star clusters and dwarf galaxies, but, as Stephen Hawking said, to confine our attention to terrestrial matters would be to limit the human spirit, so that we should try to find meaning to what we see and always ask ourselves why everything exists. Being curious is the prime mover of any discovery.

Bibliography

[1] S. J. Aarseth, M. Henon, and R. Wielen. "A comparison of numerical methods for the study of star cluster dynamics". In: *A&A* 37.1 (Dec. 1974), pp. 183–187.

[2] N. C. Amorisco and N. W. Evans. "Phase-space models of the dwarf spheroidals". In: *MNRAS* 411.4 (Mar. 2011), pp. 2118–2136.

[3] Carles Badenes et al. "Stellar multiplicity meets stellar evolution and metallicity: the APOGEE view". In: *ApJ* 854.2 (2018), p. 147.

[4] H. Baumgardt and P. Kroupa. "A comprehensive set of simulations studying the influence of gas expulsion on star cluster evolution". In: *MNRAS* 380.4 (Oct. 2007), pp. 1589–1598.

[5] Holger Baumgardt, Piet Hut, and Douglas C. Heggie. "Long-term evolution of isolated N-body systems". In: *MNRAS* 336.4 (Nov. 2002), pp. 1069–1081.

[6] V. Belokurov et al. "Cats and dogs, hair and a hero: a quintet of new Milky Way companions". In: *ApJ* 654.2 (Jan. 2007), pp. 897–906.

[7] V. Belokurov et al. "The discovery of Segue 2: a prototype of the population of satellites of satellites". In: *MNRAS* 397.4 (Aug. 2009), pp. 1748–1755.

[8] A. Benıtez-Llambay et al. "The imprint of reionization on the star formation histories of dwarf galaxies". In: *MNRAS* 450.4 (July 2015), pp. 4207–4220.

[9] G. Bergond, S. Leon, and J. Guibert. "Gravitational tidal effects on galactic open clusters". In: *A&A* 377 (Oct. 2001), pp. 462–472.

[10] Henri M. J. Boffin. "Mass-ratio distribution of extremely low-mass white dwarf binaries". In: *A&A* 575 (Mar. 2015), p. L13.

[11] Mia S. Bovill and Massimo Ricotti. "Pre-reionization fossils, ultra-faint dwarfs, and the missing Galactic satellite problem". In: *ApJ* 693.2 (Mar. 2009), pp. 1859–1870.

[12] Jo Bovy. "Galpy: a Python library for Galactic dynamics". In: *ApJS* 216.2, 29 (Feb. 2015), p. 29.

[13] Michael Boylan-Kolchin et al. "The Local Group as a time machine: studying the high-redshift Universe with nearby galaxies". In: *MNRAS* 453.2 (Oct. 2015), pp. 1503–1512.

[14] James S. Bullock and Michael Boylan-Kolchin. "Small-scale challenges to the ΛCDM paradigm". In: *Annual Review of Astronomy and Astrophysics* 55.1 (Aug. 2017), pp. 343–387.

[15] J. Dabringhausen et al. "Understanding the internal dynamics of elliptical galaxies without non-baryonic dark matter". In: *MNRAS* 463.2 (Dec. 2016), pp. 1865–1880.

[16] R. de Grijs et al. "Open cluster stability and the effects of binary stars". In: *A&A* 492.3 (Dec. 2008), pp. 685–693.

[17] R.A.C. Dolcetta. *Classical Newtonian gravity: a comprehensive introduction, with examples and exercises*. Springer International Publishing, 2019.

[18] A. Duquennoy and M. Mayor. "Duplicity of solar-like stars in the solar neighbourhood". In: *New windows to the Universe*. 1990, p. 253.

[19] A. Duquennoy and M. Mayor. "Multiplicity among solar-type stars in the solar neighbourhood. II. Distribution of the orbital elements in an unbiased sample." In: *A&A* 500 (Aug. 1991), pp. 337–376.

[20] P. P. Eggleton. "Approximations to the radii of Roche lobes". In: *ApJ* 268 (May 1983), pp. 368–369.

[21] M. Fellhauer, M. I. Wilkinson, and P. Kroupa. "Merging time-scales of stellar subclumps in young star-forming regions". In: *MNRAS* 397.2 (Aug. 2009), pp. 954–962.

[22] J. M. Fregeau et al. "Monte Carlo simulations of globular cluster evolution. III. Primordial binary interactions". In: *ApJ* 593.2 (Aug. 2003), pp. 772–787.

[23] John M. Fregeau. "Dynamics and evolution of dense stellar systems". PhD thesis. Massachusetts Institute of Technology, Oct. 2004.

[24] John M. Fregeau, Natalia Ivanova, and Frederic A. Rasio. "Evolution of the binary fraction in dense stellar systems". In: *ApJ* 707.2 (Dec. 2009), pp. 1533–1540.

[25] Eileen D. Friel. "The old open clusters of the Milky Way". In: *The globular cluster-Galaxy connection*. Ed. by Graeme H. Smith and Jean P. Brodie. Vol. 48. Astronomical Society of the Pacific Conference Series. Jan. 1993, p. 273.

[26] Marla Geha et al. "The least-luminous galaxy: spectroscopy of the Milky Way satellite Segue 1". In: *ApJ* 692.2 (Feb. 2009), pp. 1464–1475.

[27] Aaron M. Geller and Robert D. Mathieu. "WIYN open cluster study. XLVIII. The hard-binary population of NGC 188". In: *AJ* 144.2 (Aug. 2012), p. 54.

[28] Mark Gieles. "Star cluster disruption". In: *Star clusters: basic Galactic building blocks throughout time and space*. Ed. by Richard de Grijs and Jacques R. D. Lépine. Vol. 266. Jan. 2010, pp. 69–80.

[29] L. Girardi et al. "Theoretical isochrones in several photometric systems. I. Johnson-Cousins-Glass, HST/WFPC2, HST/NICMOS, Washington, and ESO Imaging Survey filter sets". In: *A&A* 391 (Aug. 2002), pp. 195–212.

[30] M. Ángeles Gómez-Flechoso and D. Martınez-Delgado. "A new method of estimating the mass-to-light ratio of the Ursa Minor dwarf spheroidal galaxy". In: *ApJ* 586.2 (Apr. 2003), pp. L123–L126.

[31] Simon P. Goodwin and Nate Bastian. "Gas expulsion and the destruction of massive young clusters". In: *MNRAS* 373.2 (Dec. 2006), pp. 752–758.

[32] D. C. Heggie. "Binary evolution in stellar dynamics." In: *MNRAS* 173 (Dec. 1975), pp. 729–787.

[33] Douglas C. Heggie. "The N-body problem in stellar dynamics". In: *Long-term dynamical behaviour of natural and artificial N-body systems*. Ed. by Archie E. Roy. Springer Netherlands, 1988, pp. 329–347.

[34] X Hernandez and William H Lee. "The tightening of wide binaries in dwarf spheroidal galaxies through dynamical friction as a test of the dark matter hypothesis". In: *MNRAS* 387.4 (2008), pp. 1727–1734.

[35] J. G. Hills. "Collisional coalescence of binaries in globular clusters". In: *Bulletin of the American Astronomical Society*. Vol. 16. Sept. 1984, p. 946.

[36] J. G. Hills. "Effect of binary stars on the dynamical evolution of stellar clusters. II. Analytic evolutionary models." In: *AJ* 80 (Dec. 1975), pp. 1075–1080.

[37] J. G. Hills. "The effect of mass loss on the dynamical evolution of a stellar system - Analytic approximations". In: *ApJ* 235 (Feb. 1980), pp. 986–991.

[38] J. R. Hurley et al. "Dynamical models with stellar evolution and binaries". In: *New horizons in globular cluster astronomy*. Ed. by Giampaolo Piotto et al. Vol. 296. Astronomical Society of the Pacific Conference Series. Jan. 2003, p. 69.

[39] Jarrod R. Hurley, Sverre J. Aarseth, and Michael M. Shara. "The core binary fractions of star clusters from realistic simulations". In: *ApJ* 665.1 (Aug. 2007), pp. 707–718.

[40] Jarrod R. Hurley et al. "A complete N-body model of the old open cluster M67". In: *MNRAS* 363.1 (Oct. 2005), pp. 293–314.

[41] Piet Hut et al. "Binaries in globular clusters". In: *Astronomical Society of the Pacific* 104 (Nov. 1992), p. 981.

[42] N. Ivanova et al. “The evolution of binary fractions in globular clusters”. In: *MNRAS* 358.2 (Apr. 2005), pp. 572–584.
[43] K. A. Janes and R. L. Phelps. “The Galactic System of Old Star Clusters: The Development of the Galactic Disk”. In: *AJ* 108 (Nov. 1994), p. 1773.
[44] J. H. Jeans. “The origin of binary systems”. In: *MNRAS* 79 (Apr. 1919), p. 408.
[45] Ivan King. “Density law in spherical stellar systems.” In: *AJ* 67 (June 1962), pp. 274–275.
[46] Ivan R. King. “Stellar Dynamics”. In: *Celestial Mechanics* 9.3 (May 1974), pp. 349–357.
[47] Evan N. Kirby et al. “Segue 2: the least massive galaxy”. In: *ApJ* 770.1 (June 2013), p. 16.
[48] M. B. N. Kouwenhoven and R. de Grijs. “How do binaries affect the derived dynamical mass of a star cluster?” In: *Ap&SS* 324.2-4 (Dec. 2009), pp. 171–176.
[49] M. B. N. Kouwenhoven and R. de Grijs. “The effect of binaries on the dynamical mass determination of star clusters”. In: *A&A* 480.1 (Mar. 2008), pp. 103–114.
[50] M. B. N. Kouwenhoven et al. “Pairing mechanisms for binary stars”. In: *Astronomische Nachrichten* 329 (Dec. 2008), pp. 984–987.
[51] P. Kroupa and A. Burkert. “On the origin of the distribution of binary star periods”. In: *ApJ* 555.2 (July 2001), p. 945.
[52] Pavel Kroupa. “On the variation of the initial mass function”. In: *MNRAS* 322.2 (Apr. 2001), pp. 231–246.
[53] Pavel Kroupa. “The dynamical properties of stellar systems in the Galactic disc”. In: *MNRAS* 277 (Dec. 1995), p. 1507.
[54] Pavel Kroupa and Andreas Burkert. “On the origin of the distribution of binary star periods”. In: *ApJ* 555.2 (July 2001), pp. 945–949.
[55] Zhongmu Li and Caiyan Mao. “Evolution of optical binary fraction in sparse stellar systems”. In: *ApJ* 859.1 (May 2018), p. 36.
[56] D. Lynden-Bell. “Statistical mechanics of violent relaxation in stellar systems”. In: *MNRAS* 136 (Jan. 1967), p. 101.
[57] Piero Madau, Sijing Shen, and Fabio Governato. “Dark matter heating and early core formation in dwarf galaxies”. In: *ApJ* 789.1 (July 2014), p. L17.
[58] Gregory D. Martinez et al. “A complete spectroscopic survey of the Milky Way satellite Segue 1: dark matter content, stellar membership, and binary properties from a Bayesian analysis”. In: *ApJ* 738.1 (Sept. 2011), p. 55.
[59] Sergey Mashchenko, James Wadsley, and H. M. P. Couchman. “Stellar feedback in dwarf galaxy formation”. In: *Science* 319.5860 (Jan. 2008), p. 174.

[60] D. Massari and A. Helmi. "With and without spectroscopy: Gaia DR2 proper motions of seven ultra-faint dwarf galaxies". In: *A&A* 620 (Dec. 2018), A155.

[61] Mario Mateo. "The kinematics of dwarf spheroidal galaxies". In: *The nature of elliptical galaxies*. Vol. 116. Astronomical Society of the Pacific Conference Series. Jan. 1997, p. 259.

[62] Mario Mateo et al. "The Carina dwarf spheroidal galaxy: how dark is it?" In: *AJ* 105 (Feb. 1993), p. 510.

[63] Alan W. McConnachie and Patrick Côté. "Revisiting the influence of unidentified binaries on velocity dispersion measurements in ultra-faint stellar systems". In: *ApJ* 722.2 (Oct. 2010), pp. L209–L214.

[64] Stephen L. W. McMillan. "The role of binaries in cluster dynamical evolution". In: *The formation and evolution of star clusters*. Vol. 13. Astronomical Society of the Pacific Conference Series. Jan. 1991, pp. 324–338.

[65] S. Mikkola. "Heating of stellar systems by binary collisions". In: *MNRAS* 205 (Nov. 1983), pp. 733–745.

[66] A. P. Milone et al. "The ACS survey of Galactic globular clusters. XII. Photometric binaries along the main sequence". In: *A&A* 540 (Apr. 2012), A16.

[67] Quinn E. Minor et al. "Correcting velocity dispersions of dwarf spheroidal galaxies for binary orbital motion". In: *ApJ* 721.2 (Oct. 2010), pp. 1142–1157.

[68] Quinn E. Minor et al. "Robust velocity dispersion and binary population modelling of the ultra-faint dwarf galaxy Reticulum II". In: *MNRAS* 487.2 (Aug. 2019), pp. 2961–2968.

[69] Edward W. Olszewski, Carlton Pryor, and Taft E. Armandroff. "The mass-to-light ratios of the Draco and Ursa Minor dwarf spheroidal galaxies. II. The binary population and its effects on the measured velocity dispersions of dwarf spheroidals". In: *AJ* 111 (Feb. 1996), p. 750.

[70] J. H. Oort. "Survey of some general properties of the Galactic system". In: *4th International Cosmic Ray Conference (ICRC4)*. Vol. 4. International Cosmic Ray Conference. Jan. 1958, pp. 491–496.

[71] Jeremiah P. Ostriker, Jr. Spitzer Lyman, and Roger A. Chevalier. "On the evolution of globular clusters". In: *ApJ* 176 (Sept. 1972), p. L51.

[72] Jorge Peñarrubia et al. "Wide binaries in ultra-faint galaxies: a window onto dark matter on the smallest scales". In: *Monthly Notices of the Royal Astronomical Society: Letters* 461.1 (2016), pp. L72–L76.

[73] Slawomir Piatek and Carlton Pryor. "The effect of Galactic tides on the apparent mass-to-light ratios in dwarf spheroidal galaxies". In: *AJ* 109 (Mar. 1995), p. 1071.

[74] H. C. Plummer. "On the problem of distribution in globular star clusters". In: *MNRAS* 71 (Mar. 1911), pp. 460–470.

[75] Philipp Podsiadlowski. "The evolution of massive binaries". In: *Binary systems, their evolution and environments*. Sept. 2014, p. 13.

[76] Simon F. Portegies Zwart et al. "Star cluster ecology - IV. Dissection of an open star cluster: photometry". In: *MNRAS* 321.2 (Feb. 2001), pp. 199–226.

[77] C. Pryor. "Models of dwarf galaxy destruction". In: *Formation of the Galactic halo...inside and out*. Vol. 92. Astronomical Society of the Pacific Conference Series. Apr. 1996, p. 424.

[78] C. Pryor, E. W. Olszewski, and T. E. Armandroff. "The velocity dispersions of the Draco and Ursa Minor dwarf spheroidal galaxies". In: *Stellar populations*. Vol. 164. Jan. 1995, p. 418.

[79] Deepak Raghavan et al. "A survey of stellar families: multiplicity of Solar-type stars". In: *ApJS* 190.1 (Sept. 2010), pp. 1–42.

[80] Saul Rappaport et al. "Formation of compact binaries in globular clusters". In: *Evolution of binary and multiple star systems*. Ed. by Ph. Podsiadlowski et al. Vol. 229. Astronomical Society of the Pacific Conference Series. Jan. 2001, p. 409.

[81] Sara Rastello, Giovanni Carraro, and Roberto Capuzzo-Dolcetta. "Effect of binarity in star cluster dynamical mass determination". In: *ApJ* 896.2 (June 2020), p. 152.

[82] M. Reggiani and M. R. Meyer. "Universality of the companion mass-ratio distribution". In: *A&A* 553 (May 2013), A124.

[83] Massimo Ricotti and Nickolay Y. Gnedin. "Formation histories of dwarf galaxies in the Local Group". In: *ApJ* 629.1 (Aug. 2005), pp. 259–267.

[84] H. Sana et al. "Multiplicity of massive O stars and evolutionary implications". In: ed. by G. Pugliese, A. de Koter, and M. Wijburg. Vol. 470. Astronomical Society of the Pacific Conference Series. Jan. 2013, p. 141.

[85] Hugues Sana and Christopher J. Evans. "The multiplicity of massive stars". In: *Active OB stars: structure, evolution, mass loss, and critical limits*. Ed. by Coralie Neiner et al. Vol. 272. July 2011, pp. 474–485.

[86] J. F. Sepinsky, B. Willems, and V. Kalogera. "Equipotential surfaces and Lagrangian points in non-synchronous, eccentric binary and planetary systems". In: *ApJ* 660.2 (May 2007), pp. 1624–1635.

[87] B. Shukirgaliyev et al. "The star cluster survivability after gas expulsion is independent of the impact of the Galactic tidal field". In: *MNRAS* 486.1 (June 2019), pp. 1045–1052.

[88] Bekdaulet Shukirgaliyev et al. "Impact of a star formation efficiency profile on the evolution of open clusters". In: *Astronomy & Astrophysics* 605 (2017), A119.
[89] Joshua D. Simon. "The faintest dwarf galaxies". In: *Annual Review of Astronomy and Astrophysics* 57 (Aug. 2019), pp. 375–415.
[90] Joshua D. Simon and Marla Geha. "The kinematics of the ultra-faint Milky Way satellites: solving the missing satellite problem". In: *ApJ* 670.1 (Nov. 2007), pp. 313–331.
[91] A. Sollima. "The evolution of the binary population in globular clusters: a full analytical computation". In: *MNRAS* 388.1 (July 2008), pp. 307–322.
[92] Meghin E. Spencer et al. "The binary fraction of stars in dwarf galaxies: the case of Leo II". In: *AJ* 153.6 (June 2017), p. 254.
[93] Meghin E. Spencer et al. "The binary fraction of stars in dwarf galaxies: the cases of Draco and Ursa Minor". In: *AJ* 156.6 (Dec. 2018), p. 257.
[94] Jr. Spitzer Lyman. "Disruption of Galactic clusters". In: *ApJ* 127 (Jan. 1958), p. 17.
[95] Jr. Spitzer Lyman. "Equipartition and the formation of compact nuclei in spherical stellar systems". In: *ApJ* 158 (Dec. 1969), p. L139.
[96] Jr. Spitzer Lyman and Martin Schwarzschild. "The possible influence of interstellar clouds on stellar velocities". In: *ApJ* 114 (Nov. 1951), p. 385.
[97] L. Spitzer. "Dynamical evolution of dense spherical star systems". In: *Study week on nuclei of galaxies*. Jan. 1971, p. 443.
[98] Lyman Spitzer. *Dynamical evolution of globular clusters*. 1987.
[99] Louis E. Strigari et al. "A common mass scale for satellite galaxies of the Milky Way". In: 454.7208 (Aug. 2008), pp. 1096–1097.
[100] Christopher A. Tout. "On the relation between the mass-ratio distribution in binary stars and the mass function for single stars." In: *MNRAS* 250 (June 1991), pp. 701–706.
[101] Michele Trenti, Douglas C. Heggie, and Piet Hut. "Star clusters with primordial binaries - II. Dynamical evolution of models in a tidal field". In: *MNRAS* 374.1 (Jan. 2007), pp. 344–356.
[102] Virginia Trimble. "On the distribution of binary system mass ratios". In: *AJ* 79 (Sept. 1974), p. 967.
[103] F. Verbunt and P. Hut. "Magnetic braking and tidal energy dissipation in close binaries". In: *A&A* 127.1 (Oct. 1983), pp. 161–163.
[104] E. Vesperini. "Star cluster dynamics". In: *Philosophical Transactions of the Royal Society of London Series A* 368.1913 (Jan. 2010), pp. 829–849.

[105] Enrico Vesperini, Stephen L. W. McMillan, and Simon Portegies Zwart. "Effects of primordial mass segregation on the dynamical evolution of star clusters". In: *ApJ* 698.1 (June 2009), pp. 615–622.

[106] Ted von Hippel. "Galactic open clusters". In: *arXiv e-prints* (Sept. 2005), astro–ph/0509152.

[107] Long Wang et al. "PETAR: a high-performance N-body code for modelling massive collisional stellar systems". In: *MNRAS* 497.1 (Sept. 2020), pp. 536–555.

[108] R. Wielen. "Dynamics of star clusters: comparison of theory with observations and simulations". In: *Dynamics of the solar systems*. Ed. by Avram Hayli. Vol. 69. Jan. 1975, pp. 119–131.

[109] Joe Wolf et al. "Accurate masses for dispersion-supported galaxies". In: *MNRAS* 406.2 (Aug. 2010), pp. 1220–1237.

[110] Xiaoan Wu. "The mass distribution of dwarf spheroidal galaxies from stellar kinematics: Draco, Ursa Minor and Fornax". In: *arXiv e-prints* (Feb. 2007).

[111] Rosemary F. G. Wyse and Gerard Gilmore. "Observed properties of dark matter on small spatial scales". In: *Dark galaxies and lost baryons*. Vol. 244. May 2008, pp. 44–52.